Ollscoil na hÉireann

THE NATIONAL UNIVERSITY OF IRELAND

Coláiste na hOllscoile, Corcaigh

UNIVERSITY COLLEGE, CORK

SCHOOL OF FOOD AND NUTRITIONAL SCIENCES

STRENGTH ANALYSIS FOR UNDERSTANDING STRUCTURAL RELAXATIONS IN FOOD MATERIALS

Thesis presented by

VALENTYN MAIDANNYK

M.Sc. Chemistry (Lomonosov Moscow State University, Russian Federation)

For the degree of

Doctor of Philosophy

(PhD in Food Science and Technology)

Under the supervision of

Professor Yrjö H. Roos

September 2017

DECLARATION

This thesis has not been submitted in whole or part to this or any other university for any degree, and is, unless stated, the original work of the author.

Valentyn Maidannyk September 2017

DEDICATION

To My Family

with Love, Respect and Gratitude

ACKNOWLEDGEMENT

I would like to say deepest thanks to my supervisor prof. Y.H. Roos, for his support, help, patience and guidance during my study in the School of Food and Nutritional Science, UCC. It was a great honour to be his student and study in his lab. Thank you very much for introducing me to the world of food material science.

I would like to thank my examiners Dr. D. Champion and Dr. J. Oliveira for valuable discussion and support during my viva. Their comments and suggestions were important for my furure research. It was a pleasure for me to have such a wonderful time during the scientific discussion.

I appreciate the Food Institutional Research Measure (FIRM) of the Department of Agriculture, food and Marine of Republic of Ireland for financial support in the project "Formulation and Design for Food Structure and Stability" (11-F-001).

Big thanks to all technical and administrative staff in particular Mr. James McNamara, Mr. Donal Humphreys, Mr. Maurice Conway, Mr. David Waldron, Ms. Avril McCord, Ms. Anne Cahalane and Dr. Therese Uniacke-Lowe in School of Food and Nutritional Science for their kind help and guidance.

Millions of thanks and deepest gratitude for all my friends in 322A lab. You did my PhD study pleasurable and unforgettable. Dr. Naritchaya Potes, Dr. Bambang Nurhadi, Dr. Aaron Lim, Dr. Fannghui Fan, Ms. Sarah Al-Jassar, Ms. Qiao Ma, Mr. Pieter Dekker, Mr. Cristian Flaker, Ms. Sandy Abidh, Mr. Cesar Palomino, Dr. Jituska Langova, Dr. Mingquan Huang, Dr. Gulsan Caliskan and Dr. Suwanoot Tuntragul thank you very much for all the help, happiness and friendship during my PhD.

The completion of my study would not have been achieved without the support of my wife (Dr. Alina Kondrashina), daughter (little Anne-Michelle), mother (Mrs. Larysa Bochovchuk), brother (Dr. Fedir Bochovchuk), aunt (Dr. Vera Zimina) and the whole our family and my friends in Ukraine, Ireland and Russian Federation. Thank you for great support, warm hugs and cheerful worlds during my study.

Once again, a millions thanks to everyone that was a part of this journey!

Valentyn Maidannyk

September 2017.

ABSTRACT

Fundamental understanding of structural relaxation time is important in characterization of food materials. Various relationships, such as Arrhenius, Vogel-Tammann-Fulcher (VTF), Williams-Landel-Ferry (WLF) and Angell's fragility have been used to model the temperature dependence of structural relaxation times of amorphous materials. However, the complexity of real systems reduces the validity of such models, although a simple approach to describe material characteristics is often required. A new approach uses a simple structural "strength" concept. Strength uses modeling of structural relaxation times for single and multicomponent amorphous solid systems around measured glass transition to translate experimental relaxation times data to a practically meaningful critical temperature difference value of food and pharmaceutical materials where liquid properties are exceeded for successful processing and storage performance.

The present study focused on systems with various ratios (0-100% at 20% intervals) of trehalose-whey protein isolate (WPI) and lactose-WPI as carbohydrate-protein model; trehalose-maltodextrin represented miscible carbohydrates and partially crystalline with trehalose was a pre-crystallised system.

The experimental part of structural strength analysis involved two main sections:

(I) sample preparation and preliminary analyses (initial water content, water sorption, freeze-drying);
(II) thermal (DSC), mechanical (DMA), dielectric (DEA) analyses and volume rheology of high water content systems (60%, 70%, 80% and 90% of water).

The Guggenheim-Anderson-de Boer (GAB) equation was used as a tool to model water sorption isotherms including high water activities (0 - 0.85 a_w) for all systems. The calorimetric onset glass transition temperature (T_g) was detected by differential scanning calorimeter (DSC). The Gordon-Taylor (GT) equation was fitted to experimental T_g data and used for extrapolation of T_g values of high water content systems. Dynamic mechanical (DMA) and dielectric (DEA) analyses in multi-frequency mode allowed determination of α-relaxation temperatures (T_α) over a wide range of structural relaxation times. Volume rheology provided structural relaxation time – temperature dependence for high water content systems. The presence of water significantly decreased T_g and T_α in all systems.

In the present study, the structural strength was defined and established using trehalose-WPI systems as a basic carbohydrate-protein model. Lactose-WPI systems were used to create a relationship, which allowed determination of strength values over a range of water contents. Structural strength of pure water (6.0°C) and WPI at different water contents were also obtained. Trehalose-maltodextrin systems showed that new strength concept can explain and predict variation of structural relaxation times at different ratios of miscible components. Moreover, structural strength analysis showed good consistency in measuring the amorphous or crystalline content in partially crystalline systems. A known strength value for pure substances allows calculation of a strength estimate for mixtures of such components at various ratios.

The structural strength approach was proposed and validated in a wide area of practical applications for adaptation to processing characterisation of food materials as well as for quality and stability control during production and storage.

TABLE OF CONTENTS

INTRODUCTION

Physical state of material components often determines functional properties of food systems. Equilibrium crystalline, liquid and gaseous states of materials can be controlled by pressure and temperature. A detailed study of materials nature allowed an early proposal of the glassy state being the fourth state of matter (Parks and Huffman 1927). Nevertheless, at certain conditions, any material can exist in a non-equilibrium glassy state. Despite the fact that glassy state is unstable and time-dependent it is common in foods and known to preserve the taste, flavour and colour of food materials (Roos and Drusch 2015).

The calorimetric glass transition temperature (T_g) is usually determined by differential scanning calorimetry (DSC) for numerous food components, primarily carbohydrates (Roos 1993) and proteins (Jouppila et al. 1997), as well as for systems including lipids (Vega et al. 2005). Glass transition of amorphous solids (mono- and disaccharides) occurs at about 100 - 150°C below the equilibrium melting temperature. Despite the fact, that T_g gives information on the temperature range over which dramatic changes in material properties may occur it does not provide information on the kinetics of the transition (Roos 2013).

The T_g of food materials (carbohydrates and proteins) highly depends on the water content of the systems as water in foods exhibit strong plasticization properties (Slade and Levine 1995, Roos 2008). Water sorption isotherms provide a quantitative tool for water content estimation in many systems, which is essential to control processing, storage and handling of food materials (Slade, et al. 1991; Okos et al. 2006; Chirife and Fontana 2007).

During heating at temperatures close to T_g, amorphous solids (e. g. glass) are converting to supercooled liquids (e. g. rubber) with a significant difference in physical properties (decreased viscosity, increased molecular mobility, rapid decrease in structural relaxation times, etc.) and liquid-like viscous flow (Williams et al. 1955; Levine and Slade 1986; Angell et al. 2000; Roos 2008). Changes in molecular mobility appear in mechanical and dielectrical properties below and close to T_g and result in α-, β- γ- relaxations, which occur due to increase of molecular mobility. Such structural relaxations can be analysed by dynamic mechanical (DMA) and dielectrical (DEA) analyses in multi-frequency mode and detected from changes in loss modulus (E'' – mechanical energy dissipation), storage

modulus (E' – mechanical energy storage) and tan δ (tanδ = E''/E') for DMA and from the peak temperature of dielectric loss (ε'') for DEA (Moateset al. 2001; Ermolina et al. 2007; Silalai and Roos 2011; Potes et al. 2012). For systems with high water contents, values of structural relaxation times may be obtained from volume rheology (Angell 2002). Thereby, establishing the time-dependent parameter of thermal, electric and mechanical changes, which is a practically important task.

Many traditional kinetic models, such as Arrhenius (Peleget al. 2002), Vogal-Tammar-Fultcher (VTF) (Rault 2000), Williams-Landel-Ferry (WLF) (Williams et al. 1955) and Angell (Angell 2002) relationships have been used to model temperature dependence of structural relaxation times. Structural relaxation times are characteristic of mechanical properties, which control stability and quality of food upon storage (viscosity, flow characteristics, stickiness, collapse, particle structure). However, real food systems have a very complex structure, although a simple kinetic model is often required. Comparison of existing kinetics models shows that modified (with unfixed C_1 and C_2 constants) WLF relationship, which is often used to define mobility in terms of the non-Arrhenius temperature behaviour of structural relaxation processes, has the best fit to experimental data (Peleg 1992, Slade and Levine 1995, Peleg and Chinachoti 1996, Roos and Drusch 2015). However, the extrapolation of the WLF equation to the range around T_g, gives non-realistic fit for systems (Peleget al. 2002), hence, WLF does not predict system behaviour under changing conditions (composition, water content, etc.).

The studies included in the present thesis investigated structural relaxation phenomena over a wide temperature range (including T_g) of various food model systems. These systems covered investigations of structural relaxations in carbohydrate-protein (trehalose-whey protein isolate (WPI); lactose-WPI); miscible carbohydrate-carbohydrate (trehalose-maltodextrin) and partially crystalline carbohydrates (trehalose), which are simple but typical models of formulated foods.

The main hypotheses of the present study were the following:

(i) The use of the WLF equation in a simple and convenient form allows describing relaxation time – temperature relationship over a wide temperature range, including region around T_g.

(ii) A kinetic concept in terms of component and water contents can be analysed using a simple single parameter.

(iii) Practical applications benefit from a simple concept in various food systems (carbohydrate-protein; miscible; partially crystalline).

The above hypotheses were tested using a series of experiments with the objectives:

(i) To carry out water sorption analysis for amorphous and partially crystalline systems: control water content and crystallization at different water activities (up to 0.85 a_w) and ratios of components.

(ii) Use DSC, DMA, DEA, Rheology: investigation of the effect of water and components contents on glass transition and α-relaxation temperatures as well as on new kinetic parameter.

(iii) To develop and experimentally verify a model, which allows predicting structural relaxation times for pure components and their mixtures at various water contents.

(iv) To investigate effects of miscibility on structural relaxation times and their modeling.

(v) To investigate the effect of crystalline structure on structural relaxation times and modeling.

CHAPTER I

LITERATURE REVIEW

1 Literature review

1.1 Glass transition

1.1.1 The glassy state

Physical state of a material can be controlled by surrounding conditions (temperature, pressure, etc.) according to its thermodynamic properties. Simple one-component systems may exist as crystalline solids, liquid and gas. The deep comprehensive studies of material properties (thermal conductivity, apparent viscosity, heat capacity etc.) proposed the glassy state of materials as the fourth state of matter, distinct from the liquid and crystalline states (Parks and Huffman 1927). Although such definition is not valid, any material under certain conditions (rapid condensation of vapour; quench cooling of a liquid (melt); rapid removal of solvent from solution; removal of crystallized solvent) may enter a nonequilibrium solid in the glassy state (Roos and Karel 1991; Slade et al. 1991; Sperling 2005; Roos 2008).

Inorganic glasses (Sakka and Mackenzie 1971), synthetic noncrystalline polymers (Gordon and Taylor 1952; Sperling 2005) as well as many food components typically exist in a glassy state. At such state, materials show transparency, solid appearance and brittleness (White and Cakebread 1966; Sperling 2005) due to disordered molecular structure (short range molecular alignment). These amorphous (e.g., glass) and supercooled liquid (e.g., rubber) materials exhibit a larger volume than the same material in equilibrium crystalline state (Slade and Levine 1995; Roos 2008).

Dairy powders (Supplee 1926) and glucose (Parks et al. 1928; Parks and Thomas 1934) were among the first food materials, studied for glass formation. These and later studies showed that dehydrated food systems (i.e. amorphous) and their physical state control product stability (preserve taste, flavor, color, etc.) (Roos 2008). Many food processing operations, such as extrusion, baking, freezing and dehydration, result in removal of water and a non-crystalline amorphous or partially crystalline state (Roos and Drusch 2015). Different rates of water removal lead to a variety of glass properties. Carbohydrates and proteins are typical food components, which tend to form amorphous, non-crystalline structures at low water contents (White and Cakebread 1966; Slade et al. 1991; Roos 2008, Roos and Drusch 2015).

Several glass transition-related changes, such as stickiness, caking, collapse, crispness, enzymatic reactions, crystallization and recrystallization significantly affect the stability and properties of food products (Slade and Levine 1995; Roudaut et al. 2004; Roos 2008; Roos and Drusch 2015).

1.1.2 The glass transition

Thermodynamic considerations

Despite the fact that definition of glass transition is not clear and its characteristics are continuously discussed (Angell 2002), it is well known that at the glassy state materials have higher thermodynamic parameters (viscosity, entropy, enthalpy, free volume etc.) than at their equilibrium state in the same conditions. During heating to above the temperature, named the glass transition temperature (T_g), materials soften over the transition region from amorphous solids (e.g., glass) to supercooled liquid (e.g., rubber) and display dramatic physical change (decrease of viscosity; increase of molecular mobility, rapid decrease in structural relaxation time) (Williams et al. 1955; Levine and Slade 1986; Angellet al. 2000). However, these changes are not obvious at the molecular level and materials stay topologically disordered both in the liquid and glassy state (Casalini and Roland 2007). The glass transition usually occurs at about 100-150ºC below equilibrium melting temperature (T_m) of a material (Figure 1.1) (Roos 2008). It is generally considered that liquid during cooling becomes a glass at a viscosity value 10^{12} Pa s (10^{13} poise) or where relaxation time is 10^2 s (Kittel and Holcomb 1967; Ojovan and Lee 2006).

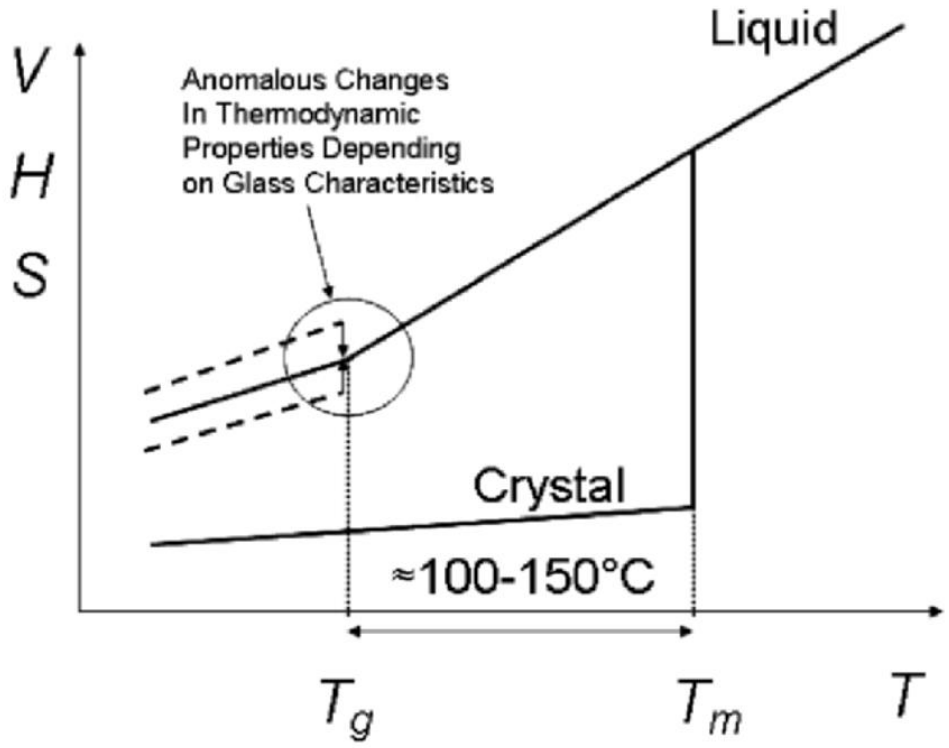

Figure 1.1 Changes in physical properties (V - specific volume, H - enthalpy, and S - entropy) around glass transition and melting (Source: Roos, 2008).

At the liquid-glass transition (e. g. glass transition) the first derivatives of the free energy as volume, enthalpy, and entropy are continuous quantities, but the second derivatives as specific heat, compressibility, and thermal expansion coefficient manifest anomalous jumps. That means that glass transitions do not involve change in the phase but involve a change in the state of amorphous material (Roos 2008). According to Ehrenfest et al. *glass transitions are reversible second-order (e.g. continuous) phase transitions* (Ehrenfest 1933). Mathematically, the second order phase transition can describe the temperature behaviour of the specific heat (e. g. heat capacity) (C_p) near the T_g by Landau equation (Eq. 1) in a simple form (Landau and Lifshitz 1984; Ojovan and Lee 2006; Landau and Lifshitz 2013):

$$C_p(T) \propto \frac{1}{|T-T_g|^{\alpha}} \quad (1)$$

where α is the universal critical exponent.

If materials exist in nonequilibrium glassy state they exhibit thermodynamically driving force towards the equilibrium crystalline state. Materials in glassy state have time-

dependent properties, thereby they cannot be described only in thermodynamic terms (Roos 2008). The glass transition is a kinetically-controlled transformation and exhibits a range of T_g, which depends on the cooling rate (maximal T_g at the highest rates of cooling) (Zarzycki 1991; Ojovan and Lee 2006). Thereby, the glass transition has features both in common with second order thermodynamic phase transition and of kinetic origin (Ojovan and Lee 2006).

1.1.3 Water plasticization

The glass transition is a property of nonequilibrium, amorphous solids which can exist in dehydrated, low-moisture or frozen materials with noncrystalline concentrated solute phase. *Water plasticization* refers to the presence and interaction of water molecules within solid materials, resulting in changes of amorphous structure and significant decrease of T_g (Roos 2008).

Water sorption isotherm is a powerful tool to monitor water content in the system during storage at various water activities (a_w) (Blahovec and Yanniotis 2009; Potes et al. 2012; Roos and Drusch 2015). The Guggenheim-Anderson-de Boer (GAB) relationship (Equation 2) is a model of water sorption isotherm, which covers a wide range of a_w (from 0 to 0.9 a_w) (Rizvi 2005; Nurhadi 2016)

$$\frac{m}{m_0} = \frac{Cka_w}{(1-ka_w)(1-ka_w+Cka_w)} \quad (2)$$

where m is the water content (g of water/100 g of dry solids), m_0 - the monolayer value of water content, C, k - constants related to energy constant, which can be calculated from m_0 respectively.

The GAB model was chosen by European Project COST 90 on physical properties of food as the standard water sorption isotherm method (Wolf and Spiess, 1985; Rizvi 2005). In theory, water content above m_0 attaches as multi-layer, whose heat of sorption is higher than the evaporative latent heat of pure water and at higher water activities, water would act as pure water (Rizvi 2005; Nurhadi 2016). The constants C and k correspond to energy difference between water molecule in upper layer and in the monolayer (Timmermann et al. 2001; Nurhadi 2016). The fractional water sorption method shown by Potes et al. (2012) allows calculation of fractional water content of material stored at high water activities (Equation 3):

$$W_t = n_1 W_1 + n_2 W_2 \quad (3)$$

where, W_t is the total equilibrium water content in the system, n_1 and n_2 - multipliers of each component in the system ($n_1 + n_2 = 1$), W_1 and W_2 - water contents in each non-crystallized component (Potes 2014).

Water shows a primary interaction with proteins and carbohydrates. In fully amorphous carbohydrates and proteins, *water acts as a plasticizer and solvent*. The free volume of material increases with increasing water content because of enhanced molecular mobility and a concomitant decrease in the glass transition temperature (Slade et al. 1991; Roos 2008; Meinders and van Vliet 2009). The relationship between water plasticization properties and water sorption is used to determine critical water activity and critical water content (Roos and Drusch 2015; Nurhadi 2016). Measurement of T_g at very high water content in the system is practically complicated. For such systems Gordon-Taylor equation (Equation 4) shows the relationship between water content and T_g:

$$T_g = \frac{w_1 T_{g1} + k w_2 T_{g2}}{w_1 + k w_2} \quad (4)$$

where, w_1 and w_2 are the mass fraction of amorphous material and water, T_{g1} and T_{g2} - glass transition temperatures, respectively, and k is a constant, T_{g2} = -135°C (Angell 2002) - the glass transition of water.

The assumption of Gordon-Taylor equation is ideal volume mixing, where two components are miscible and their volumes are additive (Liu et al. 2006; Nurhadi 2016). The value of k is valid for the temperature range used and should not be extrapolated to the wider range (Ruiz-Cabrera and Schmidt 2015; Nurhadi 2016).

1.1.4 Methodology

The calorimetric glass transition temperature (T_g) may be observed from changes in thermodynamic quantities, which usually are detected by calorimetric techniques, dilatometry and thermal analysis. Upon heating, these techniques can determine changes in heat capacity, which are characteristic for glass transition. The T_g may be taken from the onset temperature of the glass transition temperature range (onset T_g) or as a temperature corresponding to 50% change in heat capacity occurring over the transition (midpoint T_g) in the *differential scanning calorimetry* (DSC) (Figure 1.2) (Roos 2008).

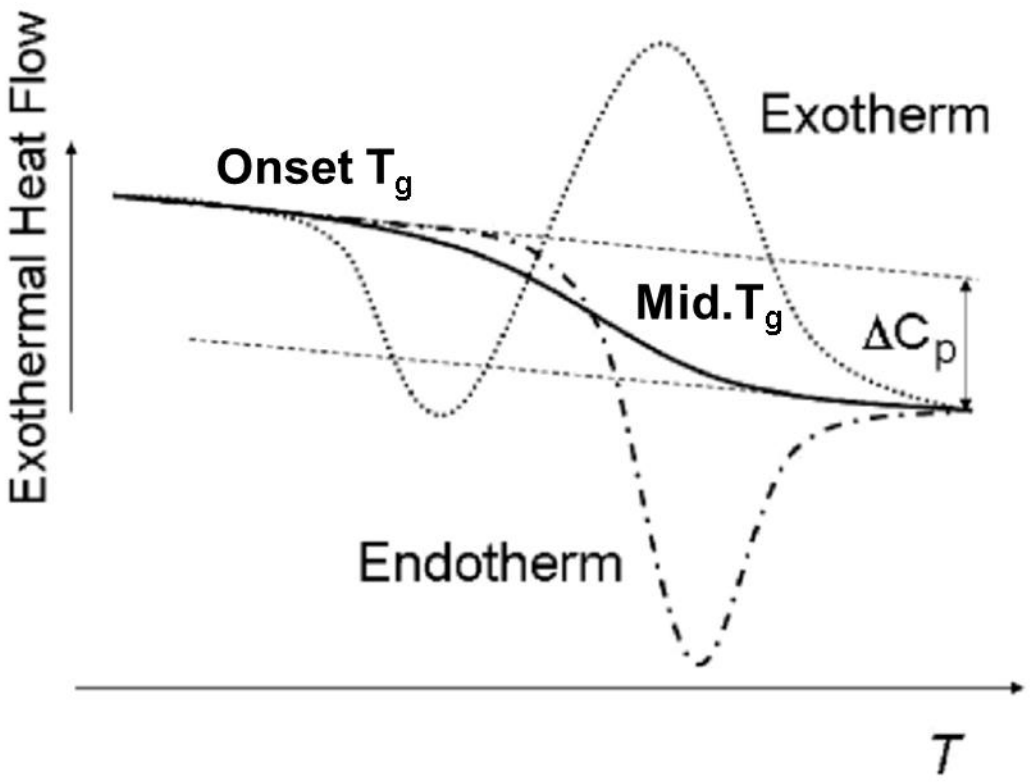

Figure 1.2. The schematic differential scanning calorimetry curves. Onset T_g, midpoint T_g and possible exothermal and endothermal relaxations (Source: Roos, 2008).

DSC and *differential thermal analysis* (DTA) are traditional and most common techniques for T_g determination in inorganic, organic, polymeric and food material systems (Roos 1993; Roos 2008; Roos and Drusch 2015). DTA measures the temperature of a sample in the dynamic heating or cooling process, while DSC detects the temperature difference between sample and the reference, which allows deriving the difference in the energy supplied. First-order phase transition produces peaks and second-order phase transition shows a step change in the heat flow (Roos 2008).

Many authors report that changes in mechanical and dielectric properties, which occur during glass transition, can be detected by dynamic mechanical thermal analysis (DMA/DMTA) and dielectric analysis (DEA/DETA) (Kalichevsky et al. 1992; Slade and Levine 1995; Cruz et al. 2001; Roudaut et al. 2004; Boonyai et al. 2005; Sperling 2005, Thuc et al. 2010; Rahman et al. 2011). However, these techniques usually detected a change in complex moduli (DMA) and dielectric properties of materials, which are referred to the structural α-relaxations. Structural relaxations occur in a system during liquid-glass transition

and show higher temperature in comparision to the calorimetric glass transition temperature. Thereby these analyses are very suitable to determine relaxation phenomena in amorphous materials.

Spectroscopic methods, such as FT-infrared (FTIR) and Raman spectroscopy are also available to determine changes in molecular mobility around transition temperatures. Various electron spin resonance (ESR) spectroscopy and nuclear magnetic resonance (NMR), however, are used more common for detection of transition-related changes in molecular rotation and diffusion (Roudaut et al. 2004; Roos 2008).

Unfortunately, calorimetric glass transition temperature of materials alone does not provide sufficient information about kinetics of the transition process. Hence, determination and prediction of the time-dependent parameters of dielectric, thermal and mechanical changes is a very important practical task.

1.2. Motions in a glass

1.2.1 Structural relaxation phenomena

Localised motions in amorphous non-crystalline structures occur during liquid-glass transition. The nature of such processes can be distinguished from density fluctuations (Stillinger and Hodgdon 1994), reorientations in structure (Ediger et al. 1996) and quasi-punctual defects (dense and less dense regions in the glassy state) (Perez 1990), where localised motions remain possible (Roudaut et al. 2004). The glass transition from glass to rubber results in significant rapid change of structural relaxation times (Angell et al. 2000).

Study of relaxation is a classic approach to explain molecular motions in the noncrystalline state. Sub-T_g relaxations are named according to their position relative to the main α-relaxation and have been detected in many biological and food systems (Perez 1994). However, the origin of sub-T_g (β, γ, …) relaxations is not clearly understood and is still a matter of debate (Roudaut et al. 2004).

Dynamic mechanical thermal analysis (DMA) and dielectric analysis (DEA) are powerful methods to observe changes in mechanical and dielectric properties of materials. Figure 1.3 shows the typical DMA and DEA plots in multi-frequency modes.

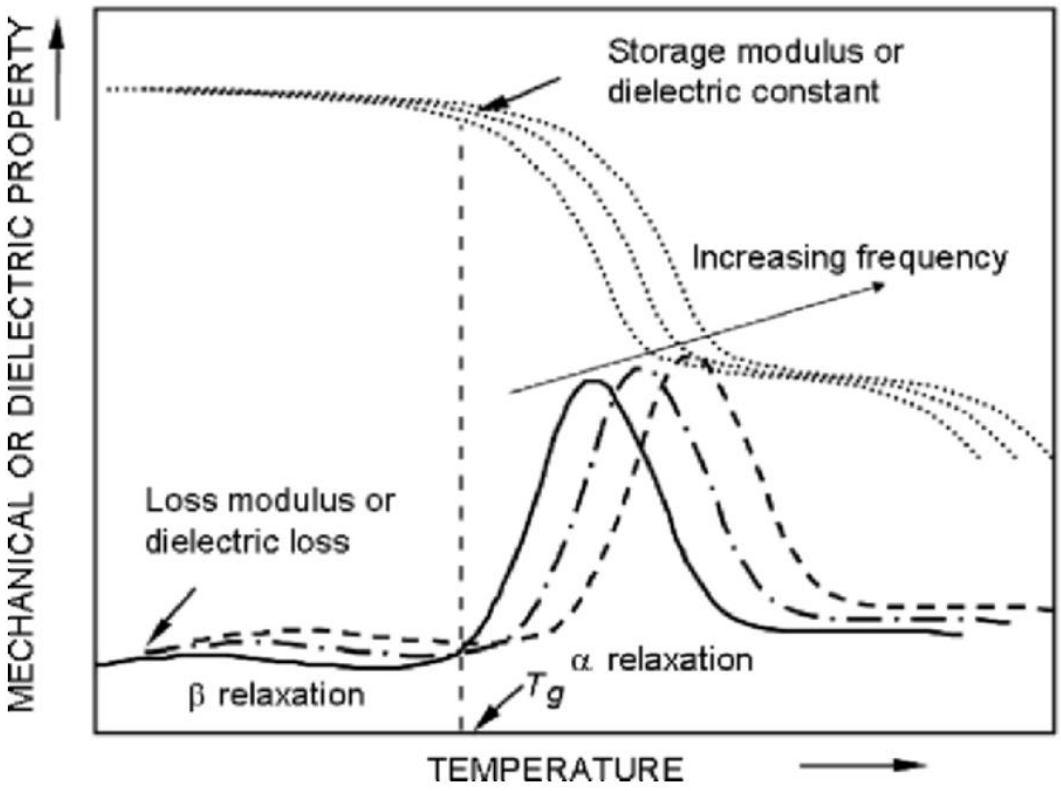

Figure 1.3. A schematic representation of typical alpha and beta relaxations obtained from DMA and DEA. The observed relaxation temperatures increase with increasing frequency (Source: Roos 2008).

DMA detects mechanical properties of materials continuously upon heating or cooling by dynamic scans. The measurements are typically made by compression or bending tests, which quantify the modulus of elasticity by detecting the stress caused by a given input strain (Luyben 1989; Cruz et al. 2001). According to the theory in the linear viscoelastic range the response of any stable system will tend to an output sinusoidal stress that has the same frequency as the input strain (Luyben 1989), although with a phase angle it may vary from 0° to 90° for an ideal liquid (Darby 1976; Cruz et al. 2001). It was also shown that in the linear viscoelastic range, the phase angle (δ) and the ratio of the amplitudes of the output and input sinusoidal waves allows quantification of the fraction of mechanical energy input which is stored (*elastic behaviour*) and the fraction which is dissipated (*plastic behaviour*) (Cruzet al. 2001).The following equations show relationships between the settings and system variables:

Input strain wave: $$\varepsilon = \varepsilon_0 \sin(\omega t)$$

Output stress wave: $$\sigma = \sigma_0 \sin(\omega t + \delta)$$

Complex elastic modulus: $E^* = E' + iE''$; $|E^*| = \frac{\sigma_0}{\varepsilon_0} = (E'^2 + E''^2)^{\frac{1}{2}}$

Storage modulus: $E' = |E^*| cos\delta$

Loss modulus: $E'' = |E^*| sin\delta$

Phase angle: $tan\delta = \frac{E''}{E'}$

where ε is a strain at time t, ε_0 - strain amplitude, σ - stress at time t, σ_0 - stress amplitude, ω - frequency, δ - phase angle (tanδ is the visco-elastic ratio), E* - complex elastic modulus, E' - storage elastic modulus (mechanical energy storage), E'' - loss elastic modulus (mechanical energy dissipation) and i - imaginary unit ($i^2 = -1$) (Luyben 1989; Cruz et al. 2001).

DEA is a materials science technique similar to DMA except that an oscillating electrical field is used instead of the mechanical force (Gaisfordet al. 2016). In DEA measurements, dielectric constant, ε', dielectric loss constant, ε'', and tanδ can be detected by placing a sample between parallel capacitors and alternating the electrical field. Polar groups in the sample respond to the alternating electrical field, which provides an absorption maximum correlated with molecular motions (Roos 2008).

DMA and DEA measurements show that the observed relaxation temperature is highly dependent on the device frequency of the applied mechanical stress or voltage (Figure 3). Hence the character of material response to disturbance is time-dependent. At temperature around T_g, DMA and DEA demonstrate significant decrease in structural relaxation times (Roos 2013). The equation 5 allows determination of structural relaxation times (τ), measured by DMA and DEA at various frequencies (*f*) (Noel et al., 2000; Potes et al., 2012):

$$\tau = \frac{1}{2\pi f} \quad (5)$$

1.3 Existing kinetic models

Traditionally, Arrhenius, Vogal-Tammar-Fultcher (VTF), Williams-Landel-Ferry (WLF) and Angell "fragility" models have been used to model temperature dependence of structural relaxation times.

1.3.1 Arrhenius model

The Arrhenius equation is the oldest and most common mathematical model, which describes the effect of temperature on the rate of chemical reactions (Peleg et al. 2002). Its application has been extended to the effect of temperature on viscosity and structural relaxation times (Peleg et al. 2002; Rizvi 2005; Jay 2012). Typically, Arrhenius equation is expressed in a form (Equation 6):

$$k = k_0 exp\left[\pm\frac{E}{R}\left(\frac{1}{T} - \frac{1}{T_0}\right)\right] \quad (6)$$

or in the logarithmic form (Equation 7):

$$ln\left(\frac{k}{k_0}\right) = \pm\frac{E}{R}\left(\frac{1}{T} - \frac{1}{T_0}\right) \quad (7)$$

where k is reaction rate at temperature T (in Kelvin), k_0 - the rate constant at a reference temperature T_0, E - the energy of activation in J mol^{-1} and R - the gas constant ($R = 8.31$ J/(mole*K)) (Figure 1.4).

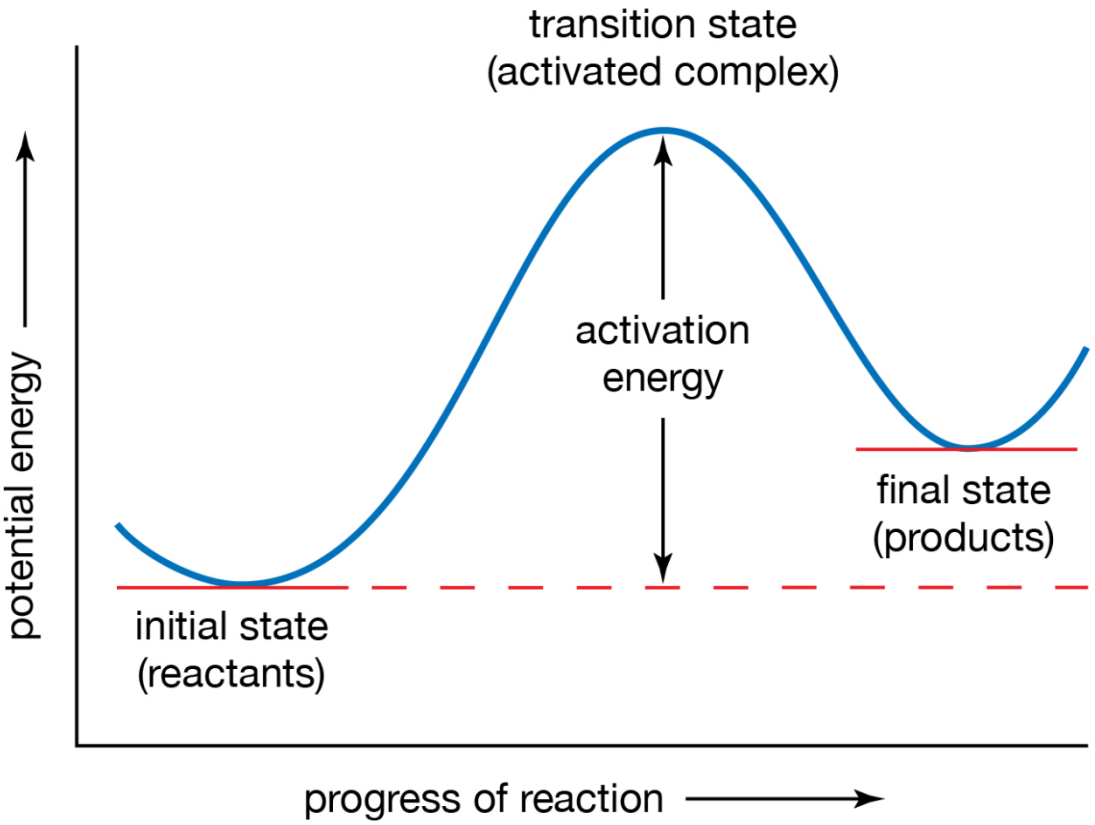

Figure 1.4. Potential-energy curve for an endothermic reaction. The activation energy represents the minimum amount of energy required to transform reactants into products in a chemical reaction. The activation energy can be visualized as a barrier that must be overcome by reactants before products can be formed (Source: (Britannica 2015)).

Newtonian viscosity η or apparent viscosity η_a (τ and τ_s for structural relaxation times) can replace the rate constants k and k_0 (Peleg et al. 2002). The obvious advantage of Arrhenius model is that the values of k at any two temperatures are sufficient to calculate the energy of activation. Then this energy can be used to estimate the magnitude of k at any other temperature in the pertinent range (Peleg et al. 2002).

The Arrhenius model shows that the plot of *ln k versus 1/T* is a straight line with the slope *E/R*, from which energy of activation can be obtained. This approach is used for simple chemical reactions where the rate constant *k* is clearly defined. However, at very complex systems, the Arrhenius model is clearly inadequate (Peleg et al. 2002), which is revealed by *ln k versus 1/T* plots.

1.3.2 Vogel-Tammann-Fulcher model

Another popular kinetic model, which has been given much attention, is that first proposed for viscosity by Vogel (Vogel 1921), later was applied to various liquids by Tammann (Tammann and Hesse 1926) and independently to molten oxides by Fulcher (Fulcher 1925) (Angell and Smith 1982). In a simple form, the Vogel-Tammann-Fulcher (VTF) equation is (Equation 8):

$$\tau = \tau_0 exp \frac{B}{T - T_0} \quad (8)$$

where τ is structural relaxation times; τ_0, B – constant; T_0 – reference temperature; T – temperature.

The entropy theories of Gibbs and di Marzio (Gibbs and DiMarzio 1958) and Adam and Gibbs (AG) (Adam and Gibbs 1965) state that (Equation 9):

$$\tau \approx exp \frac{A}{T S_c(T)} \quad (9)$$

where A is constant; $S_c(T) = \int_{T_0}^{T} \Delta C_p(T')/T' dT'$, - configurational entropy, T – temperature, τ – structural relaxation times. At $T = T_0$, $S_c = 0$. This AG equation leads to the VTF equation if one assumes that the jump of the heat capacity ΔC_p (liquid-solid) varies as 1/T, this is difficult to verify and moreover these theories do not give exact interpretation of the constants τ_0 and B (Rault 2000).

Below T_g, the materials are not in equilibrium; then often the factor $(T-T_0)$ in the VTF law is replaced by $T(1 - T_0/T_f)$, where T_f is a fictive temperature, which depends on the time of annealing and of experiment; the VTF and AG equations are then replaced by a non-linear equation (Matsuoka 1992; Rault 2000).

It is clear that all the glass-forming materials have an Arrhenius behaviour above a temperature T* and a VTF-like behaviour below this temperature (Figure 1.5). This crossover temperature T* is characterizing the α, β – bifurcation, which can be analysing by DEA and DMA (Rault 2000).

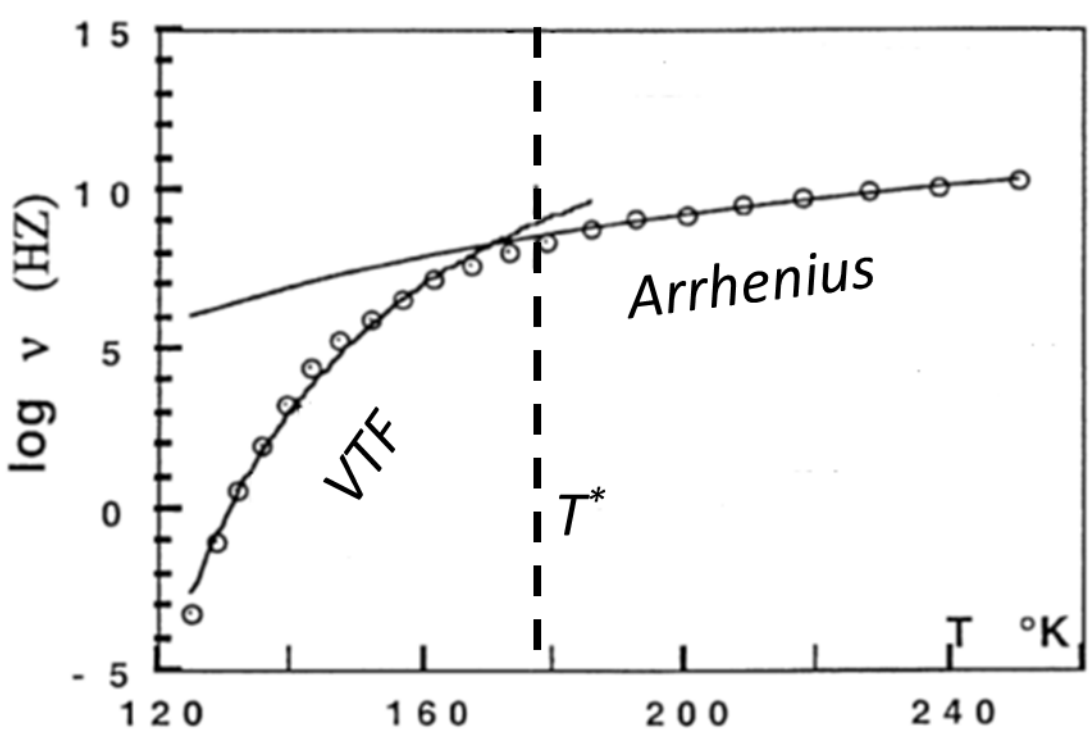

Figure 1.5. Log relaxation times versus temperature. VTF and Arrhenius models (lines) fit to experimental data (benzyl chloride) (circles) respectively below and above T^*. (Source: (Rault 2000)).

1.3.3 Williams-Landel-Ferry model

The Williams-Landel-Ferry relationship (WLF) is one of the classic kinetic models, describing dependence of relaxation time and viscosity on the temperature (Williams et al. 1955). This model was developed on the basis that most inorganic and organic glass formers showed similar decreases in relaxation times and viscosity over the temperature range of T_g to T_g + 100K (Figure 1.6) (Roos 2013).

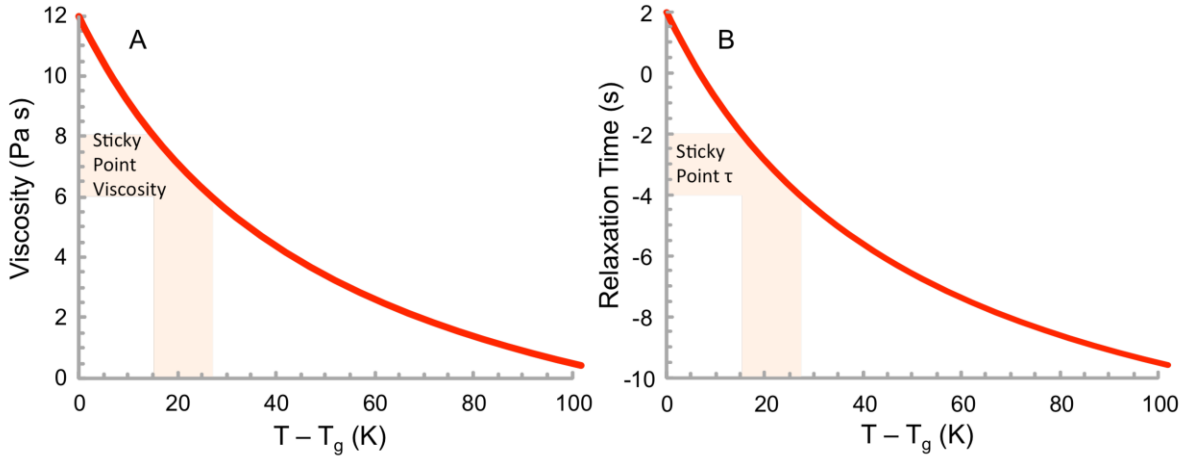

Figure 1.6. Viscosity (A) and relaxation time (B) above the glass transition temperature (T_g) predicted by the Williams-Landel-Ferry (WLF) equation with the universal constants: C_1 = -17.44 and C_2 = 51.6 (Source: Roos 2013).

In general form WLF relationship is (Equation 10):

$$log_{10}\frac{\tau}{\tau_s} = log_{10}\frac{\eta}{\eta_s} = -\frac{C_1(T-T_g)}{C_2+(T-T_g)} \quad (10)$$

where, τ is relaxation time, τ_s - reference relaxation time, η - viscosity, η_s - reference viscosity, T - temperature, T_g - glass transition temperature, C_1 and C_2 - constants.

Williams et al (Williams et al. 1955) offered "universal" values for WLF constants: $C_1 = 17.44$ and $C_2 = 51.6$ and suggested their use for a wide range of materials. However, many authors (Ferry 1980; Roos and Drusch 2015) advised against the use of these "universal" coefficients and suggest determining the real constants for each system using experimental data. To do this, the WLF equation may be used in form (Equation 11). It suggests that the plot of $1/\lg(\tau/\tau_s)$ versus $1/(T - T_g)$ gives a straight line:

$$\frac{1}{lg\frac{\tau}{\tau_s}} = \frac{1}{-C_1} - \frac{C_2}{C_1(T-T_g)} \quad (11)$$

The WLF constants C_1 and C_2 derive from the slope and intercept of the straight line (Roos and Drusch 2015).

C_1 and C_2 constants could describe the state of the material, in relation to its free volume, becouse changes in the free volume reflect the changes at the molecular level (Sanford and McCullough 1990). While C_1 gives the number of decades for decreasing of τ (limiting τ in the solids), C_2 shows the temperature below T_g where τ becomes infinitive (Landel and Nielsen 1993). Application of WLF equation is successful for temperatures well above T_g. However, when the WLF kinetics are extrapolated to the lower temperatures, a significant disagreement between the model and experimental data at the higher temperatures appears (Peleg and Chinachoti 1996). Several studies have confirmed that WLF model is suitable for amorphous materials to describe relaxation time and viscosity dependence on the temperature. Also this relation was used to relate viscosities of supercooled liquids to their stickiness (Downton et al. 1982; Boonyai et al. 2004).

The WLF relationship is often used to define mobility in terms of the non-Arrhenius temperature behavior of structural relaxation processes at temperatures above T_g. WLF relationship uses structural relaxation times at a reference temperature and the corresponding relaxation time above the glass transition (T_s) (at a certain conditions: $T_s = T_g$ (Slade et al. 1991; Peleg 1992; Roos and Drusch 2015)). Numerous studies have reported a good fit of the WLF model with unfixed constants to experimental data at temperatures above T_g (Peleg 1992; Slade and Levine 1995; Peleg and Chinachoti 1996). However, the extrapolation of the WLF equation to the range around T_g, proposes non-realistic fit for systems (Peleg and Chinachoti 1996). The use of calculated C_1 and C_2 constants gives WLF plot matching the experimental data, but does not allow predicting system behavior under changing conditions (composition, water content, etc.).

1.3.4 "Fragility" model

Angell (1991) classified glass materials using fragility parameter (Angell 1991). According to this concept, "fragile" materials have significant change in the molecular mobility at temperatures close to T_g, while "strong" materials are following the Arrhenius relationship (Figure 1.7).

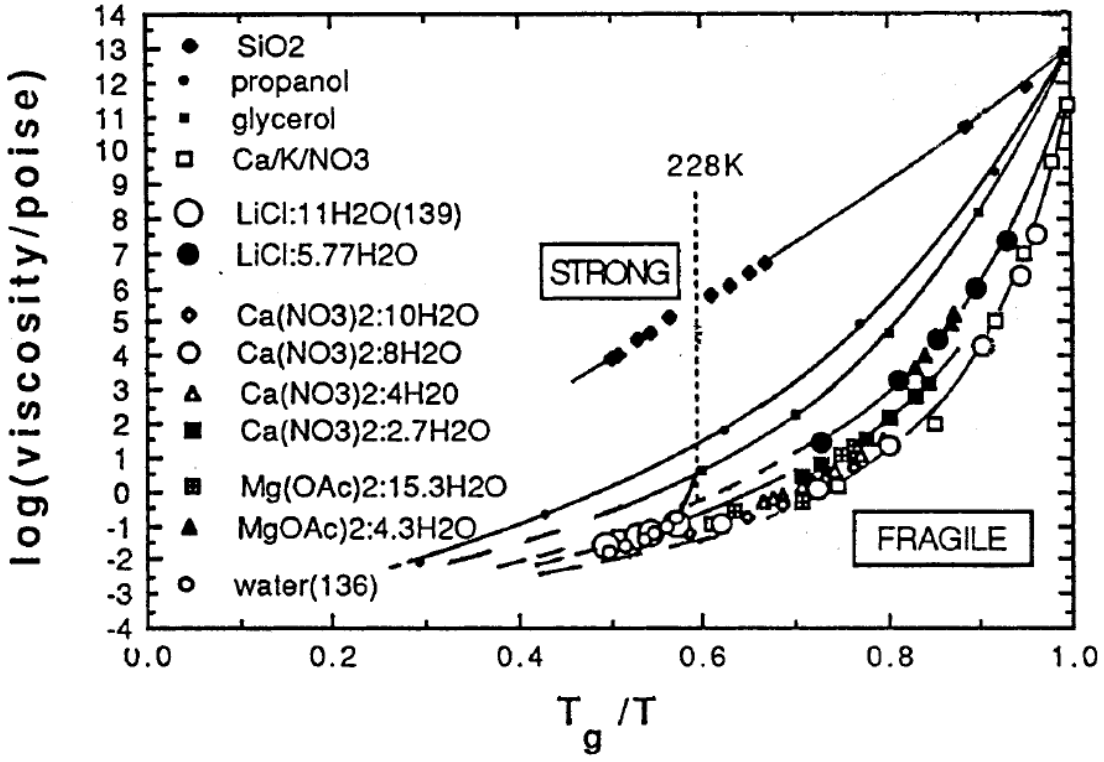

Figure 1.7. The "Angell Plot". Arrhenius plot of "Fragility" of glass formation, including "strong" material (SiO_2) and "fragile" materials (others). (Sourse: (Angell 2002)).

The typical metric to quantify kinetic "fragility" is the steepness index (m) (Equation 12) (Böhmer et al. 1993; Weng and Elliott 2015):

$$m = \frac{d\, log_{10}(\tau)}{d(T_g/T)} \Big|_{T=T_g} \quad (12)$$

where τ is structural relaxation time, T_g - calorimetric glass transition temperature, T - temperature.

"Fragility" may also relate to conventional Arrhenius activation energy (E_a) by equation (Equation 13) (Angell 2002):

$$m = \frac{E_a}{2.303RT_g} \quad (13)$$

where $R \approx 8.31$ is the universal gas constant and T_g is the glass transition temperature.

Also, "Fragility" may be expressed in terms of the VTF equation as $F_{VTF} = 1/D_{VTF}$, which varies from 0 to 1 (Roos 2013).

By combining WLF equation (Equation 10) and steepness index (Equation 12), the "Fragility" index (m) can be connected with WLF equation (Equation 14) (Alves et al. 2004; Weng and Elliott 2015):

$$m = \frac{C_1 T_g}{C_2} \quad (14)$$

where T_g is the glass transition temperature in K; C_1 and C_2 are "non-universal" WLF constants.

The "fragility" approach shows that SiO_2 is a strong glass former with Arrhenius behaviour above T_g (Figure 1.7), while water and other organic and inorganic glass formers show highly fragile behaviour. Although the fragility indexes of some materials are different, they show similar changes in viscosity and relaxation times above T_g and should be noted as equally fragile (Roos 2013). The difference in the apparent "fragility" of these materials is a serious problem and limitation of the "fragility" approach, which results in the differences in the individual T_g values and the T_g/T – scaling (Roos 2013).

Water shows the highest "fragility" and water-plasticised food components can assume to increase in "fragility" with increasing water plasticisation. However the "fragility" of water plasticised food materials decreases with increasing water content (Roos 2013). For many examples, materials may have different "fragilities", although their viscosities and relaxation times at any $T\text{-}T_g$ values are the same, therefore they should have the same "fragility", which is nonsense. However, for many different materials, the same value of $T\text{-}T_g$ corresponds to the same relaxation time and viscosity, but the T_g/T values is not the same because materials have different values of T_g (Roos et al., 2015; Fan and Roos, 2016). Thus, this model applies only for materials with the same T_g and T_g/T plot (Figure 1.7) and cannot explain variations in structural relaxation time and viscosities above T_g (Roos, 2013). This reason makes the "fragility" model unusable for complex food systems.

Despite the fact that traditional kinetic models are widely usable, the complicity of real multicomponent systems reduces their validity. More detailed investigation and

development of a convenient and appropriate mathematical model to describe material characteristics at different contents of components and water is often required.

1.4 Structural relaxations in various food systems

Knowing the physical parameters of individual food components and their mixtures allows predicting changes in their behaviour, applied to improve their stability and shelf life.

Generally, at the onset T_g, the relaxation times are typically 100s and assumed to approach 10^{-14} s at high temperatures (Figure 1.6 B) (Williams et al. 1955; Angell 2002). Relaxation times of food systems usually decrease to 10^{-3} s at 20-30°C above T_g, which corresponds to a decrease in viscosity from 10^{12} Pa*s to 10^{5} Pa*s (Roos 2013). This is in agreement with critical viscosities for collapse in freeze-drying and stickiness in spray drying (Bellows and King 1973; Downton et al. 1982; Roos 2013).

Amorphous food components have been studied in detail for water sorption, glass transition, dielectrical and mechanical relaxation, spectroscopic properties and other characteristics, showing changes in molecular mobility at and around the glass transition (Roos 2013). However, the properties of complex food solids with different carbohydrate and protein composition are still not well investigated. Some possibilities for structure formation in dairy and food formulations are described schematically in Figure 1.8 (Roos 2013).

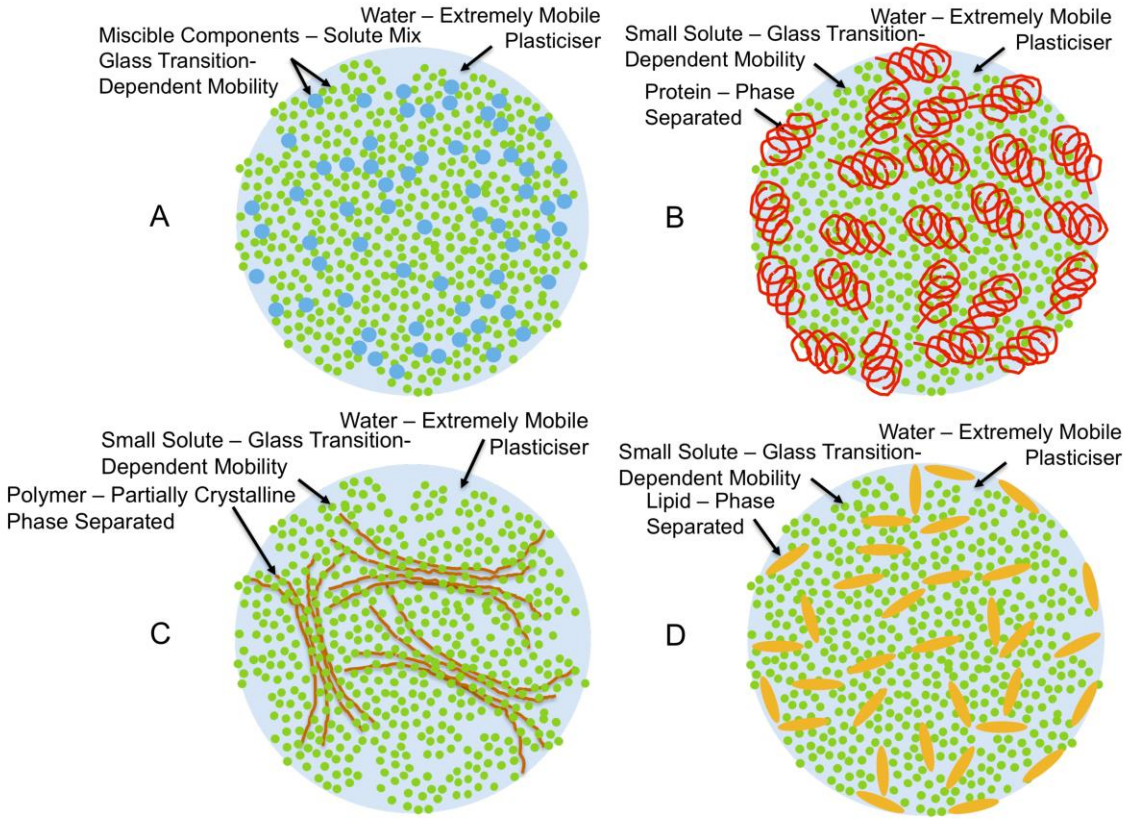

Figure 1.8. Food components at high solids contents. Typical compositions of solids and water in food ingredients. A. Miscible components, e.g., sugars and polysaccharides of various molecular sizes; B. Carbohydrates and partially or fully phase separated high molecular weight components, e.g., lactose and proteins in dairy powders; C. Mixtures of noncrystalline and crystalline components, e.g., partially crystallized lactose in dairy powders; D. Phase separated systems, e.g., lipids dispersed in noncrystalline solids in dairy powders, such as infant formula. (Sourse: (Roos 2013)).

1.4.1 Relaxations in food components at high content of solids (food powders)

Miscible systems (Figure 1.8 A) are formulations containing carbohydrate mixtures. One example of such system is lactose-trehalose mixture that has components with similar glass transition properties, but can provide improved stability to nutrient delivery systems because of the higher solubility of trehalose and decreased tendency of component for crystallization (Zhou and Roos, 2011). Miscible materials have been studied for their sticky points, glass transition and structural relaxations at various water activities. Significant differences in the glass transition and structural relaxation behaviour were detected for systems containing low molecular weight carbohydrates and high molecular weight

maltodextrins. Systems with maltodextrin of low DE usually form mixtures with sugars, that have higher T_g than pure sugars (Silalai and Roos, 2011).

Carbohydrate-protein systems (Figure 1.8 B) represent partially miscible systems and are probably the most important food powders as they are typical in infant formula powders and all dairy-based food ingredients. These materials tend to exist as amorphous, noncrystalline structures at low water content (White and Cakebread, 1966; Slade et al., 1991; Roos and Drusch, 2015). Carbohydrates and proteins can also form phase-separated regions in food systems (Roos, 2013). In the DSC measurements of carbohydrate-protein system, the carbohydrate phase showed protein content-independent glass transition temperature. However, proteins, as high molecular weight components, can exhibit challenging glass transition and structural relaxation behaviour over a wide temperature range and slowly develop plasticization above the T_g (Roudaut et al., 2004; Roos, 2008). On the other hand, systems with the high content of protein as macromolecular component show higher structural α-relaxation temperature than pure carbohydrate systems due to the physical barrier of proteins to the molecular mobility of amorphous carbohydrates (Fan and Roos, 2016).

Precrystallization of carbohydrates (Figure 1.8 C) is often important in the improvement of the stability of various foods and dairy powders. Crystalline and amorphous materials show significantly different physicochemical properties (Bhandari et al., 2013), due to differences in microstructure. Crystalline structures have long range molecular order, while amorphous structures are more disordered (short range molecular alignment) (Nurhadi and Roos, 2016). Crystalline phase ussually has no effect on the glass transition temperature of partially crystalline systems but slightly decrease structural α-relaxation temperature. Study of partially crystalline systems could be higly relevant to dairy and food manufactures as it may indicate possible problems in precrystallization processes during dehydration and encapsulation, what can affect stability and shelf life of the product.

Carbohydrate solids and proteins have important functions as hydrophilic encapsulant matrices (Vega and Roos, 2006). The *encapsulant systems* (Figure 1.8 D) have liquid (sunflower oil) or solid (hydrogenated fat) lipid phase on the continuous carbohydrate-protein (trehalose-WPI) phase. Proteins may separate onto dispersed lipid particles and significantly affect glass transition and structural relaxation behaviour of the systems (Cornacchia and Roos, 2011). The assembly of the protein components, the particle size (micro- vs. nanosize)

and physical structure of the dispersed lipid phase may affect the relaxation chracteristics of the encapsulant phase and the core stability (Roos, 2013).

1.5 Conclusions

Fundamental knowledge of the physical state of materials provides practically important information for food and pharmaceutical industry. Understanding glass trasition, structural relaxations and their application to engineering properties of amorphous food materials are important tasks for the futher desing of complex food and nutrient delivery carriers. Calorimetric glass transition temperature of material does not provide sufficient information about kinetics of the transition process. Therefore, investigations of the time-depending characteristics of thermal, electric and mechanical changes (DMA, DEA, rheology) gives important practical data. By now numerous theoretical kinetic models, which describe structural relaxation, were developed and elaborated. However, the complicity of real multicomponent systems limits the validation of such models. Existing kinetic models fail to explain glass forming properties of food and biological systems, hence a simple approach, which is based on structural relaxations around and above the glass transition, to describe relaxation characteriscs of various systems is often required.

CHAPTER II

Journal of Food Engineering 188 (2016) 21–31

Contents lists available at ScienceDirect

Journal of Food Engineering

journal homepage: www.elsevier.com/locate/jfoodeng

Modification of the WLF model for characterization of the relaxation time-temperature relationship in trehalose-whey protein isolate systems

V.A. Maidannyk, Y.H. Roos*

School of Food and Nutritional Sciences, University College Cork, Ireland

Source: (Maidannyk and Roos, 2016).

2 Modification of the WLF model for characterization of the relaxation time-temperature relationship in trehalose-whey protein isolate systems

2.1 Abstract

Understanding of structural relaxations is an important task for materials engineering in biological, food, polymer and pharmaceutical areas. By now a number of theoretical models for describing structural relaxation were developed. Nevertheless, the complicity of real systems requires more detailed investigation and development of appropriate mathematical models. In the present study trehalose-WPI system was used as a carbohydrate-protein model. The ratio of components was varied over the range 0-100% with 20% intervals. The experimental part consisted of tree main sections: (1) sample preparation and preliminary analysis (water content, water sorption, freeze drying), (2) thermal (DSC) and mechanical (DMA) analyses, (3) rheology of high water content systems. Water sorption isotherms were plotted, glass transition and α-relaxation temperature were obtained for each system. Based on the WLF relationship, the "strength" parameter: $S = \frac{dC_2}{C_1 - d}$, was defined, where d is the critical decrease of τ on the logarithmic scale, C_1 and C_2 – the "non-universal" constants in WLF equation. For all systems dependence of the "strength" parameter on the composition and water content was established.

Keywords: "strength" parameter, WLF, trehalose, whey protein isolate, relaxation.

2.2 Introduction

Thermodynamic properties and surrounding conditions define the physical state of materials. Pressure and temperature control the equilibrium of crystalline, liquid and gaseous states. As a result of comprehensive studies of physical properties (heat capacity, thermal conductivity, viscosity etc.), Parks (Parks and Huffman, 1927) defined the glassy state as the fourth state of matter, distinct from the liquid and crystalline states. Based on this definition, any material under certain conditions can be present as a nonequilibrium solid in the glassy state. However, the glassy state is metastable state of matter with time-dependent characteristics, which affect material behavior during processing and storage (Troy and Sharp, 1930; Levine and Slade, 1986).

The amorphous solid (e.g., glass) and supercooled liquid (e.g., rubber) are characterized by a lack of molecular order in structure and they exhibit a larger volume than the same material in the equilibrium crystalline state (Slade and Levine, 1995; Roos, 2008). The glassy state has extremely high viscosity (10^{12} Pa s) (Levine and Slade, 1986) and can be transformed to the more liquid-like "rubbery" state over the temperature region of the glass transition (T_g). The definition of glass transition is not clear and its properties are continuously discussed (Angell, 2002). Glass transition results in dramatic changes in molecular mobility and consequently in dielectric and mechanical properties (Williams et al., 1955; Slade et al., 1991; Roos, 1993). Below T_g amorphous materials demonstrate higher thermodynamic parameters (enthalpy, entropy, free volume) than their equilibrium state at the same conditions. The transition from the amorphous solid state to the rubbery state results in a rapid change in structural relaxation times (Angell et al., 2000; Priestley et al., 2005). Traditionally – Arrhenius (Peleg et al., 2002), Vogel-Tammar-Fultcher (VTF) (Rault, 2000) and Williams-Landel-Ferry (WLF) (Williams et al., 1955) relationships have been used to model temperature dependence of structural relaxation times. Structural relaxation time may be a characteristic of mechanical properties which control the stability and quality of food during storage (the particle structure, viscosity, collapse, flow characteristics). The complicity of real multicomponent systems reduces the validity of such models, although a simple approach to describe material characteristics is often required.

Carbohydrates and proteins are important components of numerous food solids and particularly dairy powders and infant formulae. Such hydrophilic materials tend to exist as amorphous, noncrystalline structures at low water content (White and Cakebread, 1966; Slade et al., 1991; Roos and Roos, 1995). In the present study systems of trehalose-whey protein isolate (WPI) were used to investigate structural relaxation times in complex food solids. Trehalose is a naturally occurring disaccharide of glucose monomers with high T_g (Green and Angell, 1989) and significant ability to support cell viability in stress conditions (Clegg, 1965; Miller et al., 1999) and dormancy of multicellular organisms (Elbein et al., 2003). High molecular weight components, such as proteins WPI, may exhibit challenging glass transition behavior over a wide temperature range and slowly developing plasticization above the T_g (Roudaut et al., 2004; Roos, 2008). WPI due to its molecular composition (β-lactoglobulin ~ 50% , α-lactalbumin ~ 20%, bovine serum albumin ~ 10% of whey protein) and the complex tertiary structure does not have clear representative glass transition temperature (Roos and Potes, 2015).

The T_g of binary systems depends on the component properties and miscibility (Roos, 2008). Proteins with carbohydrates are reported to cause a slight increase of the T_g of the sugar, however, the hydrolysis of proteins can also dramatically decrease an overall T_g value (Aguilera et al., 1993; Netto et al., 1998). The T_g of carbohydrates and proteins significantly depends on the water content and often become significantly plasticized by water (Slade and Levine, 1995; Roos, 2008). The T_g of dehydrated solids decreases as a result of water sorption and their properties may change from glassy solids to viscous liquids (e.g. sugar systems) or leathery materials (e.g. protein systems) in an isothermal process (Roos, 2008). The T_g of water is very low (-135°C) (Angell, 2002), and its experimental determination for system with high water content is often inhibited because of crystallization. For such systems T_g can be derived from the Gordon-Taylor relationship (Arvanitoyannis et al., 1993).

The calorimetric T_g is often measured by differential scanning calorimeter (DSC) Glass transition of amorphous solids, including most mono- and disaccharides (Roos, 1993; Roos, 2008) occurs at about 100-150°C below their equilibrium melting temperature. Despite the fact, that the value of T_g is an important material property it does not provide information on the kinetics of the transition. In general, amorphous structures are fairly stable in the glassy state (Sperling, 1991; Slade and Levine, 1995; Roos, 2008). However, at temperatures close to T_g, more rapid time-dependent flow appears (White and Cakebread, 1966; Roos and Roos, 1995; Roudaut et al., 2004). Changes in mechanical properties around the glass transition result in α-relaxation which can be investigated by dynamic mechanical analysis (DMA) and detected from changes in loss modulus (E'', mechanical energy dissipation), storage modulus (E', mechanical energy storage) and tan δ (tan $\delta = E''/E'$). DMA has been applied for the analysis of carbohydrates (Roos and Karel, 1991; Kalichevsky and Blanshard, 1993; Silalai and Roos, 2011; Potes et al., 2012) and proteins (Kokini et al., 1994; Gearing et al., 2010). DMA studies in multi-frequency mode demonstrated a significant decrease in relaxation times around the T_g (Roos, 2013). On the other hand, rheometry allows determination of time-temperature dependence of relaxations for systems of high water contents (Ollett and Parker, 1990; Miller et al., 1999). Measurements of viscosity in the T_g region are extremely difficult (Ferry, 1980; Peleg et al., 2002). Knowledge of the relaxation times during temperature changes is fundamental for understanding of properties of food materials.

The WLF equation is one of the popular models, describing dependence of relaxation time and viscosity on the temperature. Originally this relation showed that inorganic and organic glass materials possessed similar decreases in relaxation times and viscosity over the temperature range of T_g to T_g+100K. Williams et al. (Williams et al., 1955) offered "universal" values for WLF constants: C_1 = 17.44 and C_2 = 51.6 and suggested their use for a wide range of materials. However, many authors (Ferry, 1980; Peleg, 1992; Roos and Roos, 1995) advised against the use of these "universal" coefficients and suggested to determine the real constants for each system using experimental data (Eq. 11). The WLF relationship is often used to define mobility in terms of the non-Arrhenius temperature behavior of structural relaxation processes at temperatures above the T_g. WLF relationship uses structural relaxation times at a reference temperature and the corresponding relaxation time above the glass transition (T_s) (at a certain conditions: $T_s = T_g$ (Williams et al., 1955; Peleg, 1992; Roos and Roos, 1995). Numerous studies have reported a good fit of the WLF model with unfixed constants to experimental data at temperatures above the T_g (Peleg, 1992; Slade and Levine, 1995; Peleg and Chinachoti, 1996). However, the extrapolation of the WLF equation to the range around T_g, proposes non-realistic fit for systems (Peleg and Chinachoti, 1996). The use of calculated C_1 and C_2 constants gives WLF plot matching the experimental data, but does not allow predicting system behavior under changing conditions (composition, water content and i.e.).

The objective of the present study was to determine structural relaxation times of sugar-protein systems and assess the use of the WLF equation in a simple and convenient form, that allows describing of the relaxation time-temperature dependence over a wide temperature range, including region around T_g. A new parameter for system characterization was introduced and the influence of protein and water contents on structural relaxation times in tertiary systems was investigated.

2.3 Materials and Methods

2.3.1 Materials

D-(+)-Trehalose crystalline dihydrate (Hayashibara Co., Ltd., Okayama, Japan) and whey protein isolate (Isolac®, Carbery Food Ingredients, Ballineen, Cork, Ireland) were used without purification. De-ionized water (KB Scientific, Cork, Ireland) was used for all experimental work.

2.3.2 Determination of the initial water content

The initial water content of trehalose-WPI mixtures was determined using WTB Binder vacuum oven (Mason Technology®, Tuttingen, Germany). Six samples with different contents of trehalose and WPI were prepared in glass vials (10 ml) by mixing of pure powders. The amounts of components were varied over the range 0-100% with 20% intervals. Samples with the final weight 0.5-1 g were dried at 70°C and absolute pressure P_{abs}<10 mbar during 20 hours. The water content in samples was calculated as the weight loss and expressed in percentage.

2.3.2 Preparation of amorphous freeze-dried materials

Freeze-dried amorphous solids of trehalose-WPI mixtures were obtained from the solution with 20% (w/w) of total solids. The ratios of components trehalose:WPI in solids were 100:0, 80:20, 60:40, 40:60, 20:80, 0:100. Aliquots of these trehalose-WPI solutions (5 ml, approximately 1g of freeze-dried material) were frozen in pre-weighted and semi-closed with septum 10 ml glass vials at -20°C for 24 h, then at -80°C for 3 h, followed by freeze-drying for 60 h at pressure p < 0.1 mbar (Lyovac GT2, Steris®, Hürth, Germany) to obtain amorphous materials. All vials were hermetically sealed under vacuum inside the freeze dryer at p < 0.1 mbar and stored over P_2O_5 in vacuum desiccators (Roos and Karel, 1990) at room temperature (23 ± 2°C) to protect samples from water uptake.

2.3.3 Water sorption analysis

Samples with different ratios of trehalose-WPI (described above) were freeze-dried and stored in vacuum desiccators over P_2O_5. Each sample was monitored during storage in vacuum desiccators at 23 ± 2 °C for 120 h over the saturated solutions of CH_3COOK, $MgCl_2$, K_2CO_3, $Mg(NO_3)_2$, $NaNO_2$, NaCl and KCl (Sigma Chemical Co., St. Louise, MO, U.S.A.), which provided 0.23, 0.33, 0.44, 0.545, 0.66, 0.76 and 0.85 a_w respectively. Samples were weighted at the time points 0, 2, 4, 6, 8, 10, 24, 48, 72, 96 and 120 hours upon storage. Possible crystallization of trehalose was detected from loss of sorbed water. To check the water activity for each samples AQUALAB 4 (TE) (Decagon Devices Inc., NE) water activity meter was used. The water content in the mixtures was plotted as a function of time, and the Guggenheim-Anderson-de Boer (GAB) equation was fit to the data (Eq. 2).

2.3.4 Differential Scanning Calorimetry (DSC)

The T_g was determined by DSC (Mettler Toledo Schwerzenbach, Switzerland) for anhydrous solids and solids at 0.23, 0.33, 0.44 and 0.545 a_w. Freeze-dried anhydrous materials were transferred to the pre-weighted DSC aluminium pans (40 μL, Mettler Toledo Schwerzenbach, Switzerland) and hermetically sealed. The lids of DSC aluminium pans, for anhydrous systems only, were punctured to allow evaporation of residual water upon the measurement. The freeze-dried materials at different a_w were transferred to the pre-weighted DSC aluminium pans and stored in evacuated desiccators over saturated salt solutions at room temperature (23±2°C) until constant weight. After equilibration the pans were hermitically sealed and reweighed. An empty pan with punctured lid was used as reference. The DSC was calibrated for temperature and heat flow. Samples were scanned from ~ 30°C below to over the T_g region at 5°C/min heating and then cooled at 10°C/min to the starting temperature. The second heating scan was performed to well above the T_g. STARe software version 8.10 (Mettler Toledo Schwerzenbach, Switzerland) was used to calculate the onset, midpoint and endset T_g values. For high water content systems (10, 20, 30, and 40% of total solids) the onset T_g values were calculated by Gordon-Taylor equation (Eq. 4).

2.3.5 Dynamical Mechanical Analyses (DMA)

Dynamic mechanical analyzer DMA (Tritec 2000 DMA, Triton Technology Ltd., UK) was used to measure dynamic-mechanical properties of the freeze-dried materials. Samples as described for the DSC experiments were analyzed and recorded using DMA control software version 1.43.00. A metal pocket-forming sheet (Triton Technology Ltd., UK) with approximately 60 mg of the powdered sample was fixed directly between the stationary and the driveshaft clamps (balanced to zero) inside the measuring head of the DMA. All three dimensions of the sample - length, width and thickness - were determined. Then sample was scanned over the temperature range -50°C - +180°C with cooling rate 5°C/min and heating rate 1°C/min at frequencies 0.1, 0.2, 0.5, 1, 2, 5, 10 Hz by using the single cantilever bending mode. To provide efficient cooling, the DMA device was connected to a liquid nitrogen tank (1 l; Cryogun, Brymill Cryogenic Systems, Labquip Ltd., Dublin, Ireland). The α-relaxation temperature (T_α) of freeze-dried anhydrous and humidified (0.23, 0.33, 0.44 a_w) trehalose-WPI systems above the onset T_g was measured by DSC and calculated from peak temperature of tangents δ, measured by DMA in multi-frequency mode

(Fig. 4). This calculation provided higher accuracy, than data from decreasing of loss modulus (Hardy et al., 2001).

The relaxation times (τ) of peak T_α, measured by DMA at various frequencies (f), were calculated using the Equation 5 (Noel et al., 2000; Potes et al., 2012).

2.3.6 Rheology

Trehalose and WPI were dissolved separately in water (considering the initial water contents in the powders) and mixed together at ratios 100:0, 80:20, 60:40, 40:60, 20:80 after 2 hours. The total solids contents were 10, 20, 30 and 40%. Apparent viscosities of solutions were measured using a rheometer ARES-G2 (TA Instruments®, USA) with aluminum "plane-plane" (40 mm) geometry. The shear rate $100s^{-1}$ was constant for all systems. The temperature range was 0 - 50°C. To convert the raw viscosity (η) data into shear relaxation times (τ_s), the Maxwell relation (Eq. 15) was used (Angell, 2002):

$$\eta = G_\infty \tau_S \qquad (15)$$

where, G_∞ is the infinite frequency shear modulus.

We determined the apparent viscosity for high water content (10, 20, 30, 40 % of total solids) trehalose-WPI systems with components ratios 100:0, 80:20, 60:40, 40:60 and 20:80.

The WLF relation in a form (Eq. 10) was used to fit DMA and rheometry data (Roos, 2013; Williams et al., 1955). The WLF equation in the form Eq. 11 suggests that the plot of $1/lg(\tau/\tau_s)$ versus $1/(T-T_g)$ gives a straight line. The WLF constants C_1 and C_2 derive from the slope and intercept of the straight line (Roos, 1995).

2.3.7 Data analysis

Mean values of the water content, glass transition and α-relaxation temperatures were calculated from 3 replicates with standard deviations expressed in error bars. To ensure consistency, all the experiments were performed in triplicates.

2.4 Results and discussion

2.4.1 Water sorption analysis

Water contents in the freeze-dried trehalose-WPI systems, equilibrated in desiccators with different water activities (a_w), are given in Table 2.1.

Table 2.1. Water content of freeze-dried Trehalose-WPI systems stored at different water activities for 120 hours at 23±2°C.

	Water content (g/100 g of solids)					
a_w	**100:0**	**80:20**	**60:40**	**40:60**	**20:80**	**0:100**
0.23	4.13±0.44	4.98±0.03	5.12±0.19	5.97±0.23	6.50±0.09	7.33±0.09
0.33	5.92±0.39	6.61±0.02	7.02±0.21	7.73±0.16	8.27±0.13	9.24±0.12
0.44	9.00±0.21	8.75±0.06	8.66±0.13	9.24±0.34	9.98±0.05	11.24±0.21
0.55	9.49±0.11	12.25±0.17	11.14±0.22	11.05±0.08	11.04±0.22	13.04±0.24
0.65	9.45±0.27	12.00±0.16	15.95±0.15	14.62±0.14	13.38±0.17	16.20±0.19
0.76	9.28±0.40	12.52±0.07	14.46±0.25	21.23±0.24	18.88±0.18	19.82±0.15
0.85	9.46±0.41	13.65±0.21	17.66±0.29	22.21±0.22	26.19±0.19	24.96±0.24

The sorption kinetic profiles of trehalose-WPI mixtures 100:0 (Figure 2.1 a), 80:20 (Figure 2.1 b), 60:40 (Figure 2.1 c), 40:60 (Figure 2.1 d), 20:80 (Figure 2.1 e) and 0:100 (Figure 2.1 f) at different relative humidities demonstrate the time required for the system equilibration.

Figure 2.1 show that samples reached the equilibrium water content in about 96 hours, except for the "40:60" system, which required about 120 hours. All systems demonstrated an overall increase of the water content for the higher water activity and with an increase in the WPI concentration for the certain water activity. We observed a spike in the water content for "100:0" trehalose-WPI system at the water activity 0.55-0.85 a_w, for "80:20" system at 0.65-0.85 a_w, for "60:40" system at 0.76-0.85 a_w and for "40:60" system at 0.85 a_w. The further decrease of the water content for these systems during several hours of monitoring may indicate trehalose *crystallization* above 0.55 a_w; above 0.65 a_w for "80:20" system; above

0.76 a_w for "60:40" system and above 0.85 a_w for "40:60" system. For all further experiments in this work, only the amorphous noncrystallizing systems were used. To study the influence of water content on the system, all samples were equilibrated in desiccators with 0, 0.23, 0.33 and 0.44 a_w.

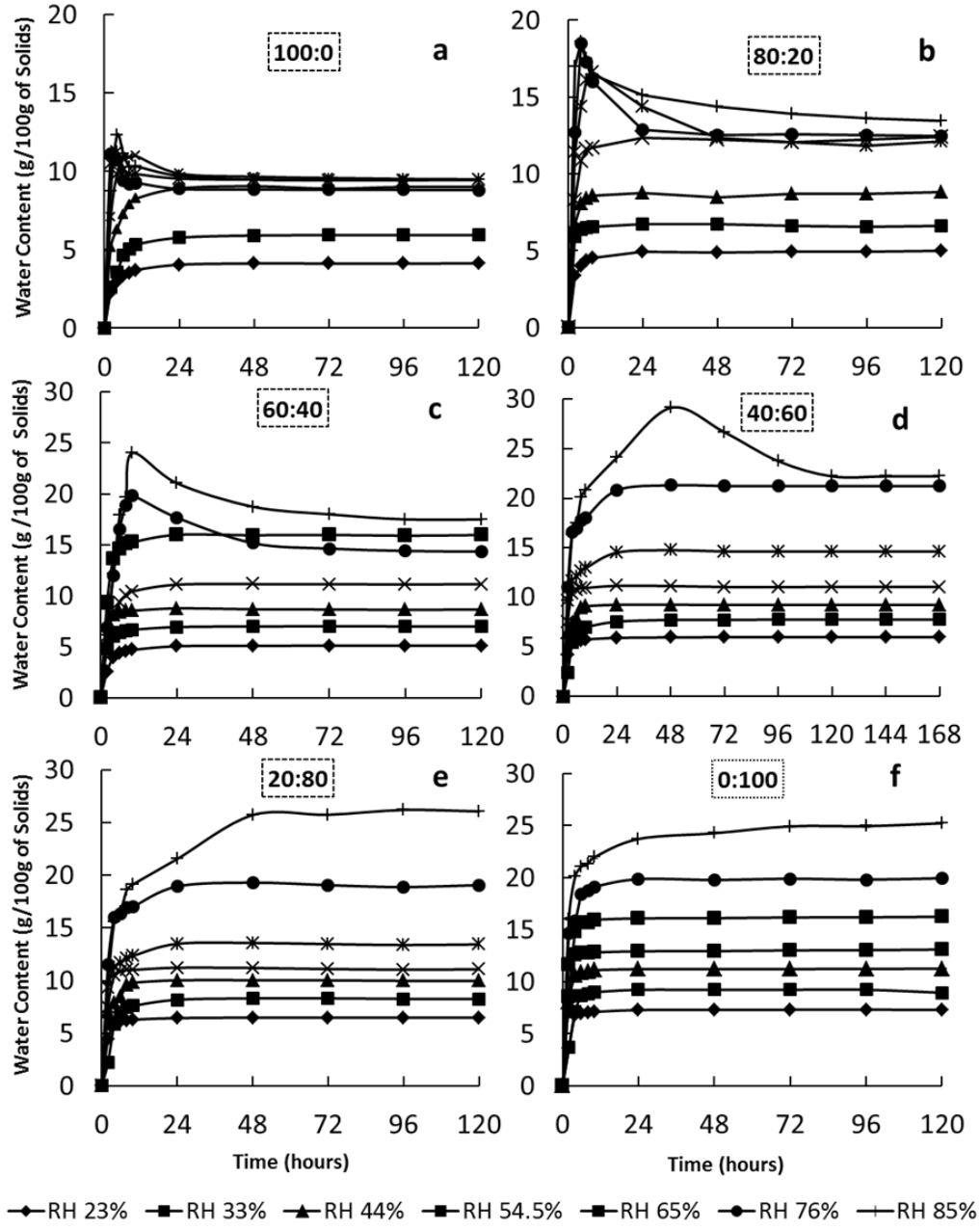

Figure 2. 1. Sorption kinetics for freeze-dried trehalose-WPI mixtures 100:0 (a), 80:20 (b), 60:40 (c), 40:60 (d), 20:80 (e) and 0:100 (f), at different relative humidities 23, 33, 44, 55, 65, 76, 85%, monitored during 120 hours at 23±2°C.

The GAB sorption isotherms (lines), experimental data (solid symbols) and predicted water contents (clear symbols) for non-crystalline trehalose-WPI system are shown at Figure 2.2. Previous studies suggested that the GAB equation could be used to fit to the experimental data of amorphous trehalose below $0.55a_w$ at 20°C (Bell and Labuza, 2000). However, the extrapolated sorption data above 0.44 a_w provided false results of sorbed water contents.

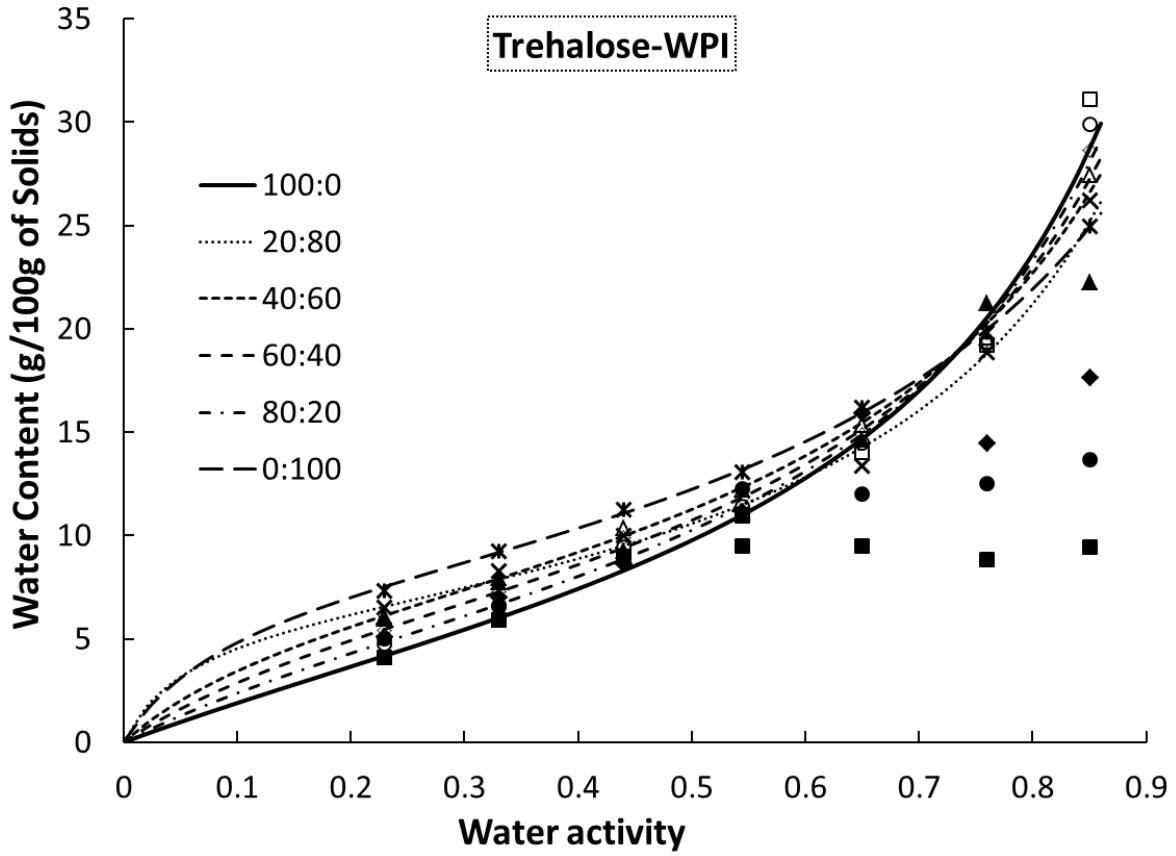

Figure 2.2. The GAB sorption isotherms at 23±2°C (lines), experimental data (solid symbols) and calculated water contents (clear symbols) for amorphous trehalose-WPI systems with components ratios 100:0 (▪,▫), 80:20 (●,○), 60:40 (♦,◇), 40:60 (◢,◿), compared to experimental data for trehalose-WPI 20:80(x) and 0:100(✖) systems.

In the present study the water sorption data for non-crystalline trehalose-WPI systems were obtained from the sum of water contents of amorphous component at different a_w (0.11-$0.85a_w$), i.e. the sorbed water contents of trehalose-WPI systems were matched and compared with the sum of water contents of individual amorphous components at each a_w (Potes et al., 2012) according to Equation 3 (Potes, 2014).

Calculated water contents were derived from experimental water sorption data of trehalose-WPI "20:80" and WPI systems (steady-state sorbed water contents of non-crystalline components). The experimental data of water contents are in agreement with calculated water contents at 0.11-0.44 a_w for pure trehalose; at 0.11-0.55a_w for "80:20" trehalose-WPI system; at 0.11-0.65 a_w for "60:40" system and at 0.11-0.76 a_w for "40:60" system. This result allows obtaining the GAB sorption isotherms for non-crystalline trehalose-WPI systems with different ratios of components.

2.4.2 Glass transition temperature

The onset of calorimetric glass transition T_g for anhydrous and humidified (0-0.44 a_w) freeze-dried trehalose-WPI systems are shown in the Table 2.2. As expected, the T_g decreased with increasing the water content (Figure 2.3). For anhydrous trehalose we obtained the same T_g value, that has been reported by numerous authors such as Green and others (Green and Angell, 1989), Miller and others (Miller et al., 1999). The T_g of trehalose-WPI systems were slightly higher than those of pure trehalose in the anhydrous state. The increase of T_g in the presence of WPI may be explained by the effect of the high molecular weight molecules, which can interact with trehalose to some extent. On the other hand, trehalose was unable to form strong hydrogen bonds between molecules in the anhydrous amorphous state, which explained strong interactions with protein compare to the other saccharides (López-Dıez and Bone, 2004). These changes in T_g are in agreement with previous study (Haque and Roos, 2004), where an increase of lactose T_g after addition of WPI was reported.

For the pure WPI glass transition temperature was not observed. It is known, that T_g of globular proteins is difficult to detect due to their complex secondary and tertiary structures, which results in gradual increase of the heat capacity during glass transition (Zhou and Labuza, 2007). For humidified samples (0.23-0.44 a_w) the differences in T_g for pure trehalose and trehalose-WPI systems are not significant. Haque and others (Haque and Roos, 2004) explained similar changes in T_g for lactose-WPI systems with various water sorption properties. Indeed, during storage at $a_w \leq 0.33$, trehalose sorbed less water than trehalose-WPI systems. However, the amounts of sorbed water at 0.44 aw for pure trehalose and trehalose-WPI systems are almost equal (table 2.1), what is in agreement with detected changes of T_g.

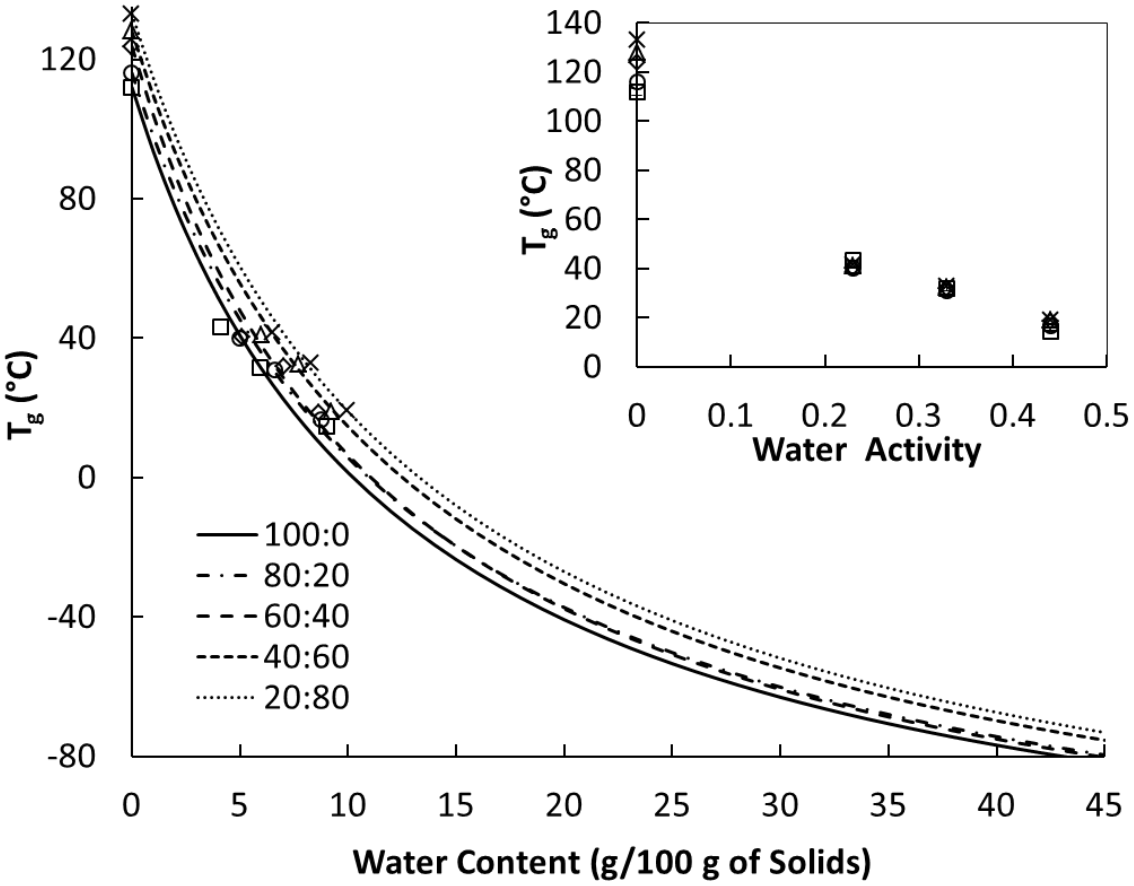

*Figure 2.3. Dependence of the glass transition temperatures (T_g) on the water content and water activity (a_w) of freeze-dried trehalose-WPI system with ratios 100:0 (▫), 80:20 (○), 60:40 (◇), 40:60 (△), 20:80 (**x**). Anhydrous samples were stored for 48 hours at 23±2°C and various water activities (0, 0.23, 0.33, 0.44 a_w). Lines correspond to the T_g predicted by the Gordon-Taylor equation.*

Table 2.2. Measured by DSC the onset of calorimetric glass transition temperatures (T_g) of freeze-dried trehalose-WPI systems stored for 48 hours at 23±2°C and various water activities.

	Glass transition temperatures (T_g) of trehalose-WPI (w/w) systems, °C				
a_w	**100:0**	**80:20**	**60:40**	**40:60**	**20:80**
0	112.0±1.4	116.1±1.2	123.7±1.8	128.0±0.2	133.0±0.1
0.23	43.2±2.1	40.0±1.4	40.2±0.2	41.0±1.2	41.5±1.1
0.33	31.6±0.9	30.9±1.1	31.8±1.0	38.4±1.0	32.8±1.1
0.44	14.5±0.4	16.5±0.7	18.4±1.1	18.8±0.9	19.1±1.3

Table 2.3 gives predicted by Gordon-Taylor equation (Eq. 4) values of T_g for high water content trehalose-WPI systems (10, 20, 30 and 40% of total solids). We used experimental T_{g1} (Table 2.2) for anhydrous trehalose-WPI systems, and T_{g2} = *-135°C* (Angell, 2002) for water. This equation was successfully used to fit the experimental data of amorphous trehalose-WPI systems (Figure 2.3). We obtained the following constants k for trehalose-WPI systems: 8.1±1.0 at ratio 100:0; 7.9±0.4 at 80:20; 8.3±0.7 at 60:40; 7.6±0.2 at 40:60 and 7.4±0.6 at 20:80.

Table 2.3. Glass transition temperatures (T_g) predicted by Gordon-Taylor equation for trehalose-WPI systems with high water contents.

Water content, %	Glass transition temperatures (T_g) of trehalose-WPI (w/w) systems, °C				
	100:0	**80:20**	**60:40**	**40:60**	**20:80**
90	-132.0	-131.9	-131.9	-131.6	-131.4
80	-129.0	-128.8	-128.9	-128.3	-127.9
70	-126.2	-125.8	-125.9	-125.0	-124.6
60	-123.4	-122.9	-123.1	-121.9	-121.3

2.4.3 Dynamic-mechanical properties

The α-relaxation temperature (T_α) calculated from peak temperature of tangent δ, measured by DMA in multi-frequency mode is presented on Figure 2.4.

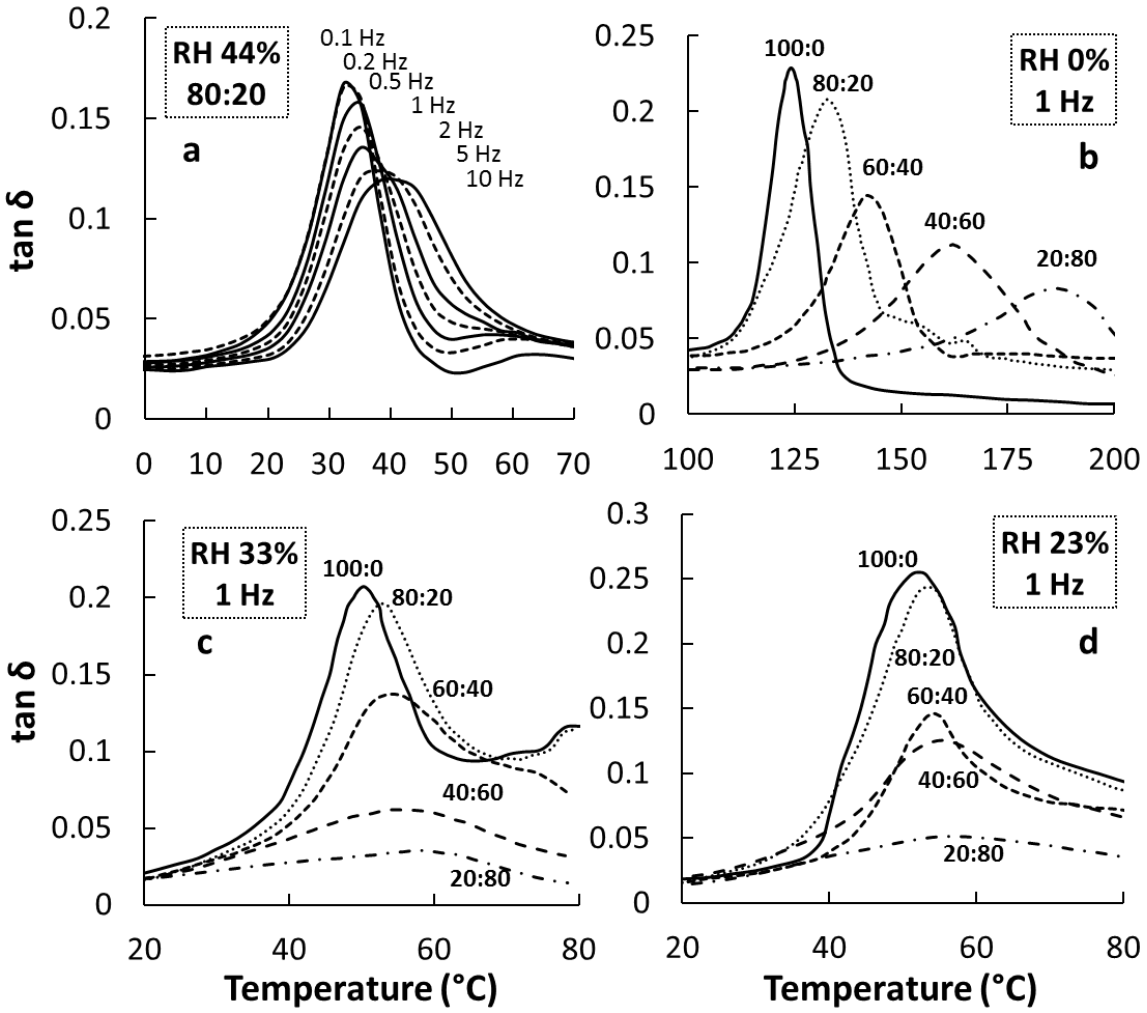

Figure 2.4. (a) Temperature dependence of dynamic tangents δ for humidified (0.44 a_w) trehalose-WPI "80:20" system in multi-frequency mode (0.1, 0.2, 0.5, 1, 2, 5, 10 Hz). (b,c,d) Temperature dependence of dynamic tangents δ for anhydrous and humidified (0.23, 0.33 a_w) trehalose-WPI mixtures (100:0, 80:20, 60:40, 40:60, 20:80) at 1 Hz.

The value of T_α for amorphous trehalose and trehalose-WPI systems was highly dependent on the water content (Table 2.4), which is in agreement with previous works (Silalai and Roos, 2011; Potes et al., 2012). For example, the value of T_α at 10 Hz for pure trehalose varies from 128.5°C for anhydrous system to 33.6°C for humidified system at 0.44 a_w. These changes in systems and increase of diffusivity could be explained by the free

volume theory (Royall et al., 2005; Meinders and van Vliet, 2009). Probably, water increases the free volume in the system and molecular mobility of amorphous material consequently.

For anhydrous and humidified (0.23, 0.33, 0.44 a_w) systems the T_α of amorphous trehalose and trehalose-WPI systems occurred at ~20-30°C above the onset T_g. Table 2.4 gives T_α from peak temperature of tangents δ measured by DMA. It is well known, that T_α from the mechanical analysis are highly dependent on the frequencies of the measurements (Talja and Roos, 2001) (Figure 2.4 a).

The presence of WPI in the system significantly increased the T_α values (Table 2.4). The amorphous trehalose showed lowest T_α, while 20:80 trehalose-WPI system - the highest T_α for all humidities. This dependence demonstrated that the WPI could affect the molecular mobility of amorphous trehalose. The WPI is macromolecular component and could reduce diffusion process in the system. The intensity of tan δ showed independence on the water content (Figure 2.4 b,c,d), however, it inversely correlates with T_α values. During this study, we show that presence of water or proteins is important due to the changes of molecular mobility, which could be detected by DMA.

Table 2.4. α-relaxation temperature (T_α) detected by DMA for trehalose-WPI mixtures equilibrated at different relative humidities (RH), measured at different frequencies (f) and relaxation times ($log_{10}\tau$, s).

RH 0%		**Trehalose-WPI systems**				
		100:0	**80:20**	**60:40**	**40:60**	**20:80**
f, Hz	**lgτ, s**	**T_α, °C**	**T_α, °C**	**T_α, °C**	**T_α, °C**	**T_α, °C**
0.1	**0.20**	123.0	130.1	143.3	161.2	179.8
0.2	**-0.09**	124.2	131.4	144.1	163.1	182.3
0.5	**-0.49**	125.2	131.9	147.1	166.2	184.5
1.0	**-0.80**	127.3	133.9	147.6	166.5	184.4
2.0	**-1.09**	127.4	134.8	149.0	166.7	187.5
5.0	**-1.50**	128.4	135.8	150.8	168.8	189.5
10.0	**-1.80**	128.5	136.5	151.1	169.6	189.6
RH 23%		**Trehalose-WPI systems**				
		100:0	**80:20**	**60:40**	**40:60**	**20:80**
f, Hz	**lgτ, s**	**T_α, °C**	**T_α, °C**	**T_α, °C**	**T_α, °C**	**T_α, °C**
0.1	**0.20**	54.8	54.5	57.3	64.8	69.1
0.2	**-0.09**	56.0	55.5	59.1	66.5	71.2
0.5	**-0.49**	57.9	57.0	61.4	67.9	71.6
1.0	**-0.80**	58.3	58.0	61.5	68.7	72.8

2.0	**-1.09**	58.5	58.8	62.1	69.4	73.2
5.0	**-1.50**	60.2	60.3	63.6	70.2	73.8
10.0	**-1.80**	60.9	61.0	64.2	70.9	74.2
RH 33%			**Trehalose-WPI systems**			
		100:0	**80:20**	**60:40**	**40:60**	**20:80**
f, Hz	**lgτ, s**	**T_{α}, °C**	**T_{α}, °C**	**T_{α}, °C**	**T_{α}, °C**	**T_{α}, °C**
0.1	**0.20**	43.9	45.4	49.7	58.2	62.0
0.2	**-0.09**	45.1	46.5	49.8	59.6	62.4
0.5	**-0.49**	46.5	47.5	52.5	60.9	63.4
1.0	**-0.80**	46.7	48.9	53.4	61.6	63.7
2.0	**-1.09**	48.3	50.3	53.8	62.2	64.7
5.0	**-1.50**	48.9	50.8	55.5	62.8	65.1
10.0	**-1.80**	50.0	51.4	55.6	63.3	66.2
RH 44%			**Trehalose-WPI systems**			
		100:0	**80:20**	**60:40**	**40:60**	**20:80**
f, Hz	**lgτ, s**	**T_{α}, °C**	**T_{α}, °C**	**T_{α}, °C**	**T_{α}, °C**	**T_{α}, °C**
0.1	**0.20**	28.1	30.9	37.7	45.0	48.2
0.2	**-0.09**	28.4	32.3	38.8	46.1	49.8
0.5	**-0.49**	30.1	33.8	41.0	47.1	50.1
1.0	**-0.80**	31.4	34.7	41.2	47.8	50.6
2.0	**-1.09**	31.8	35.6	41.3	48.2	50.9
5.0	**-1.50**	32.7	36.5	42.8	49.2	51.6
10.0	**-1.80**	33.6	36.8	43.5	49.4	51.9

2.4.4 Rheology

Figure 2.5 is a graphical presentation of apparent viscosity of aqueous trehalose and trehalose-WPI systems.

The apparent viscosity values for trehalose solution increased with increasing content of solids in a system that correlates with the previous study (Miller et al., 1999). The addition of WPI significantly increased apparent viscosity, especially for systems with 30 and 40% of total solids. Such behavior of systems is typical for addition of WPI macromolecules to carbohydrate aqueous solution (Adhikari et al., 2007). As expected, the values of apparent viscosity are decreasing upon heating (Parks and Gilkey, 1929; Miller et al., 1999).

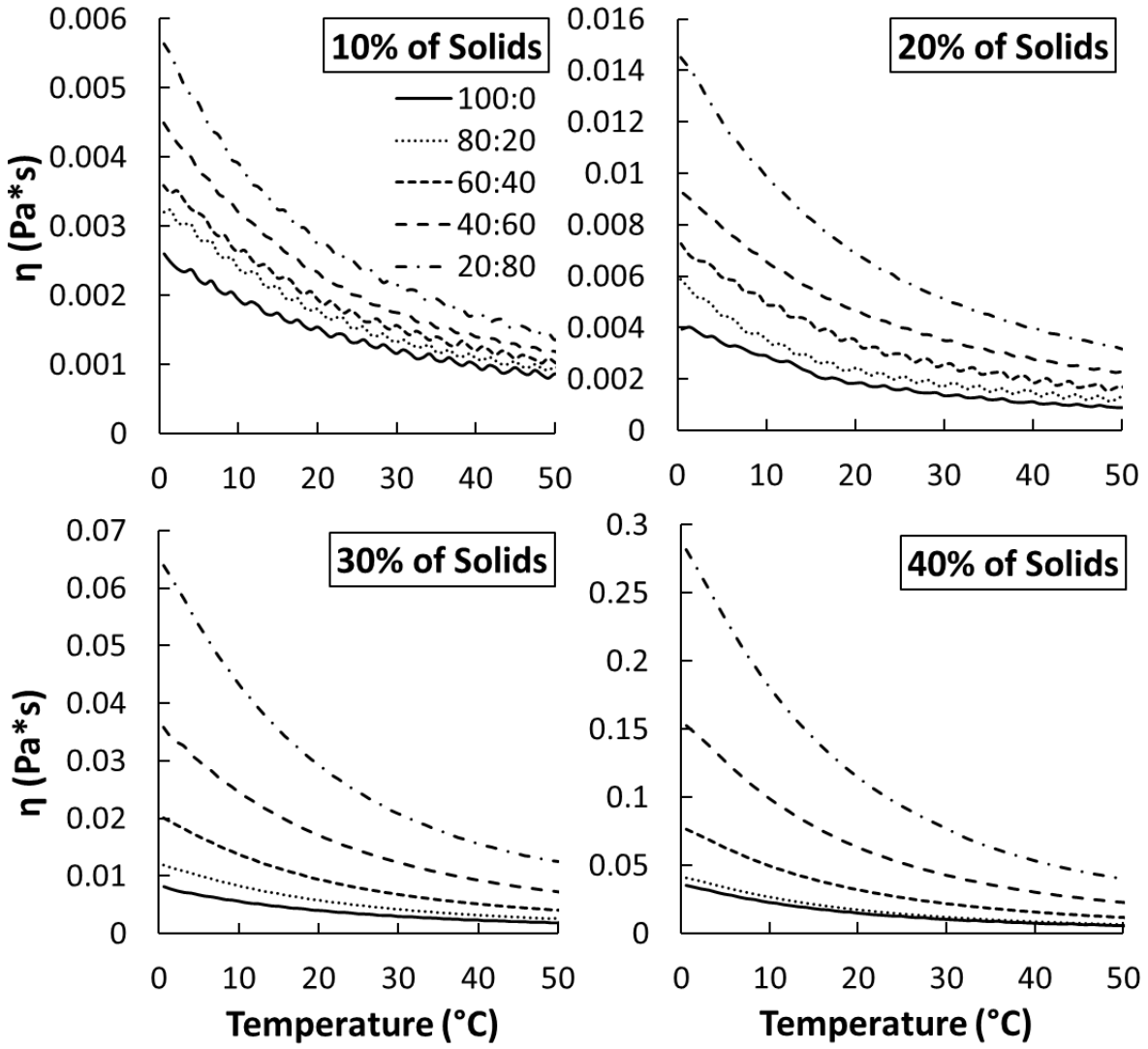

Figure 2.5. Temperature dependence of the apparent viscosity of aqueous trehalose-WPI (100:0; 80:20; 60:40; 40:60; 20:80) systems at 10, 20, 30 and 40% of total solids.

2.4.5 Application and modification of the WLF equation

In the present study we determined the constants C_1 and C_2 for both low and high water content systems. In our calculations we considered that relaxation time was typically 100s and assumed to approach 10^{-14}s at high temperatures, which corresponds to decrease in viscosity from 10^{12}Pa s to 10^{5}Pa s (Angell, 1991; Angell, 2002; Roos, 2013).

Depending on the positive or negative values of C_1 and C_2 we obtained different types (I-IV) of hyperbole for WLF curves (Figure 2.6).

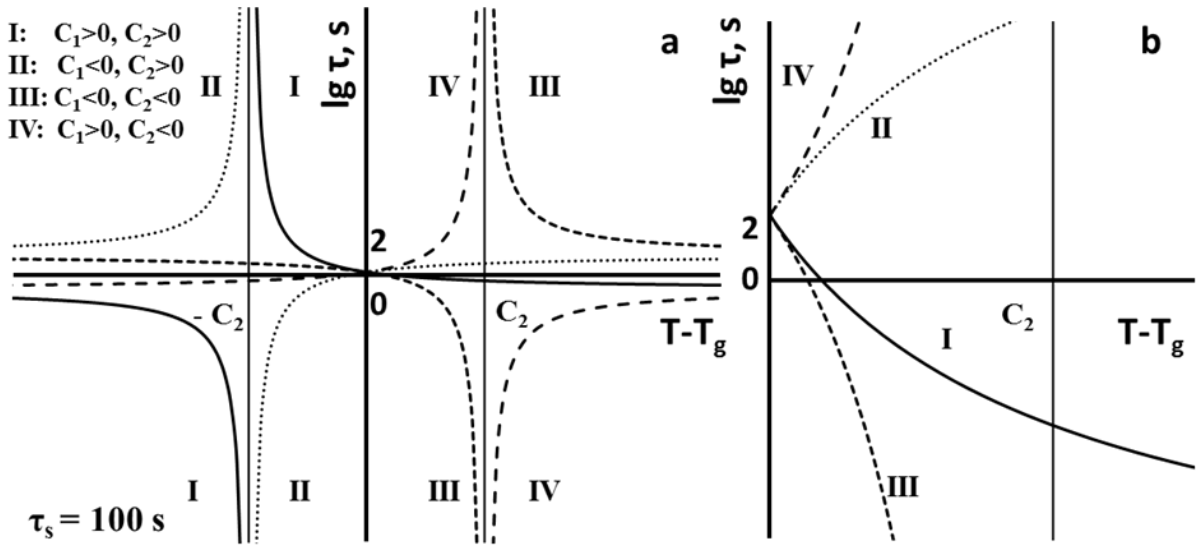

Figure 2.6. Calculated WLF curves with positive and negative values of C_1 and C_2 constants.

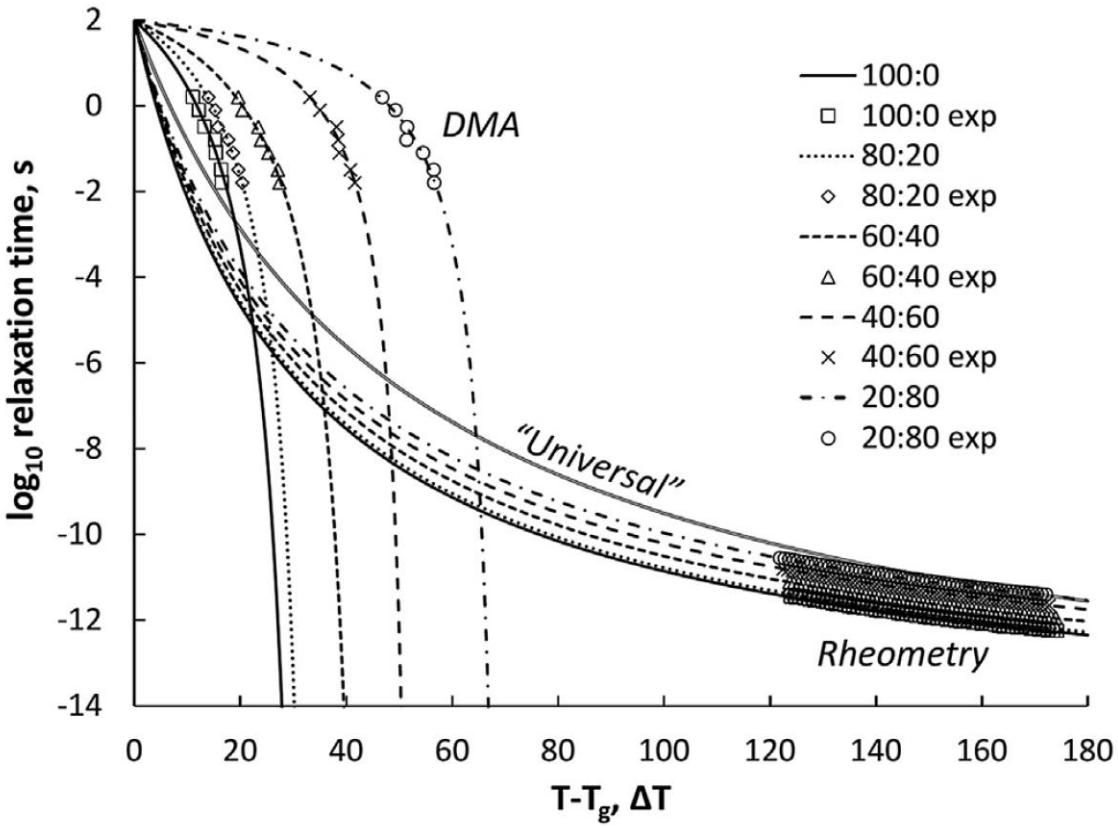

Figure 2.7. "Universal" and calculated WLF curves (lines) and experimental data (symbols) for anhydrous (DMA data) and dissolved (rheometry data) 40% of total solids trehalose-WPI mixtures (100:0, 80:20, 60:40, 40:60, 20:80).

In the real situation $T-T_g > 0$, which is shown with magnification on the Figure 2.6b. At the low temperatures: $T-T_g < C_2$, the behavior of WLF curves is different from those of

"universal" WLF curves. The type I of hyperbole corresponds to the liquid phase state, while type III is typical for the amorphous state (Figure 2.7).

For both amorphous and "liquid" systems, the WLF equation was used to fit the experimental data. The calculated C_1 and C_2 constants are given in tables 2.5 and 2.6.

Table 2.5. Calculated WLF constants C_1, C_2 for trehalose-WPI systems humidified at different relative humidities (RH).

Trehalose-WPI	**RH 0%**		**RH 23%**		**RH 33%**		**RH 44%**	
	$-C_1$	$-C_2$	$-C_1$	$-C_2$	$-C_1$	$-C_2$	$-C_1$	$-C_2$
100:0	3.85	34.5	3.30	32.9	2.88	31.9	2.47	31.3
80:20	2.83	35.5	2.60	35.0	2.48	34.0	2.34	33.3
60:40	2.47	45.6	2.14	37.8	2.09	37.4	1.40	34.2
40:60	1.12	53.9	1.09	35.5	0.81	37.6	0.68	36.1
20:80	0.94	70.7	0.74	39.3	0.57	37.8	0.46	36.8

Table 2.6. Calculated WLF constants C_1 and C_2 for aqueous trehalose systems with high water contents.

Trehalose-WPI	**10% of total solids**		**20% of total solids**		**30% of total solids**		**40% of total solids**	
	C_1	C_2	C_1	C_2	C_1	C_2	C_1	C_2
100:0	16.58	18.0	17.18	25.0	16.64	22.9	16.75	30.3
80:20	16.81	21.1	17.01	24.6	16.67	25.0	16.72	30.9
60:40	16.72	20.8	16.86	24.5	16.58	26.6	16.56	32.5
40:60	16.81	22.46	16.47	21.6	16.29	26.6	16.31	33.6
20:80	16.72	22.8	16.56	25.1	16.18	28.4	16.18	35.3

Angell (1991) classified glass materials using fragility parameter. According to this concept, "fragile" materials have significant change in the molecular mobility at temperatures close to T_g, while "strong" materials are following the Arrhenius relationship. However, this approach is not suitable for biological and food systems (Roos, 2013). Characterization of the glass-forming properties of those systems is an important question. Several studies have confirmed that WLF model is suitable for amorphous food and biological materials for

describing relaxation time and viscosity dependence on temperature. Also, this equation was used for relating supercooled liquids viscosities to their stickiness (Downton et al., 1982; Boonyai et al., 2004).

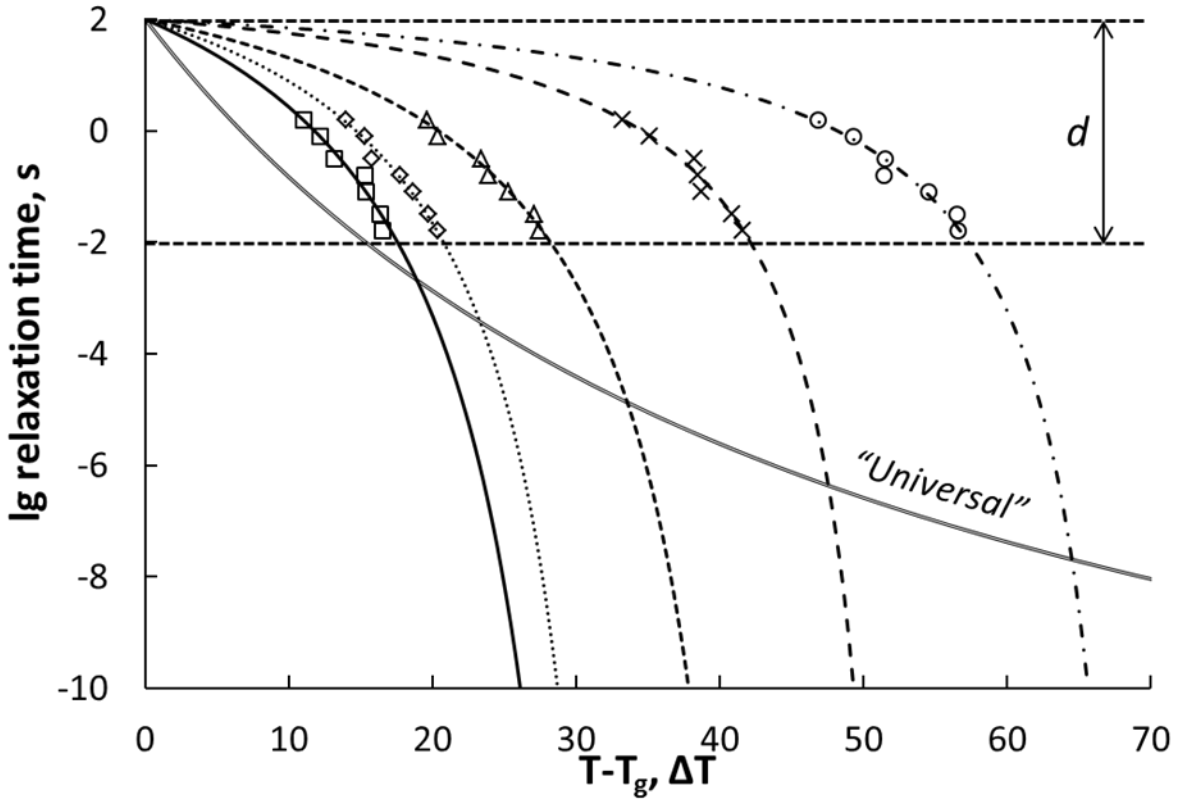

Figure 2.8. "Universal" and calculated WLF curves (lines) and experimental data (symbols) for anhydrous trehalose-WPI mixtures (100:0, 80:20, 60:40, 40:60, 20:80).

During heating above the onset of calorimetric T_g, amorphous materials rapidly lose their solid characteristics, expressed in decreasing of viscosity and increasing of the systems flowability (Levine and Slade, 1988; Lillie and Gosline, 1990). Equation 11 allows calculating C_1 and C_2 constants from the WLF relation for each system. Figure 2.8 shows that upon heating, the structural relaxation time dropped rapidly from 100s to 0.01s (from 2 to -2 in logarithmic scale). This decrease of structural relaxation is critical for material and can be defined as parameter *d*. We defined the temperature difference $T-T_g$ at which this critical change happens as "strength" (S) parameter (Eq. 16):

$$S = \frac{dC_2}{C_1 - d} \tag{16}$$

where d is a parameter showing the critical decrease of τ (from 100 to 0.01s) in the

logarithmic scale (can be chosen for each system as an integer depending on the required accuracy), C_1 and C_2 – the "non-universal" constants in the WLF equation that define *S.*

However, at the temperatures well above the glass transition *(rheometry data* on Figure 2.7) the structural relaxation time is almost unchanged. This *shows the physical limit of change of the structural relaxation time.*

The "strength" parameter combines the characterization of material state of the system and practically important time factor. This parameter is simple in calculation and allows describing the strength of glass forming material. To summarize, S parameter shows the critical temperature difference, at which a sharp change in properties of the system occurs.

To prove the concept the "strength" parameter was calculated for each system at d = 4 (Figure 2.9) and summarized in the Table 2.7. Importantly, the new parameter S correlates with the system resistance to changes: higher value of S refers to the stronger system.

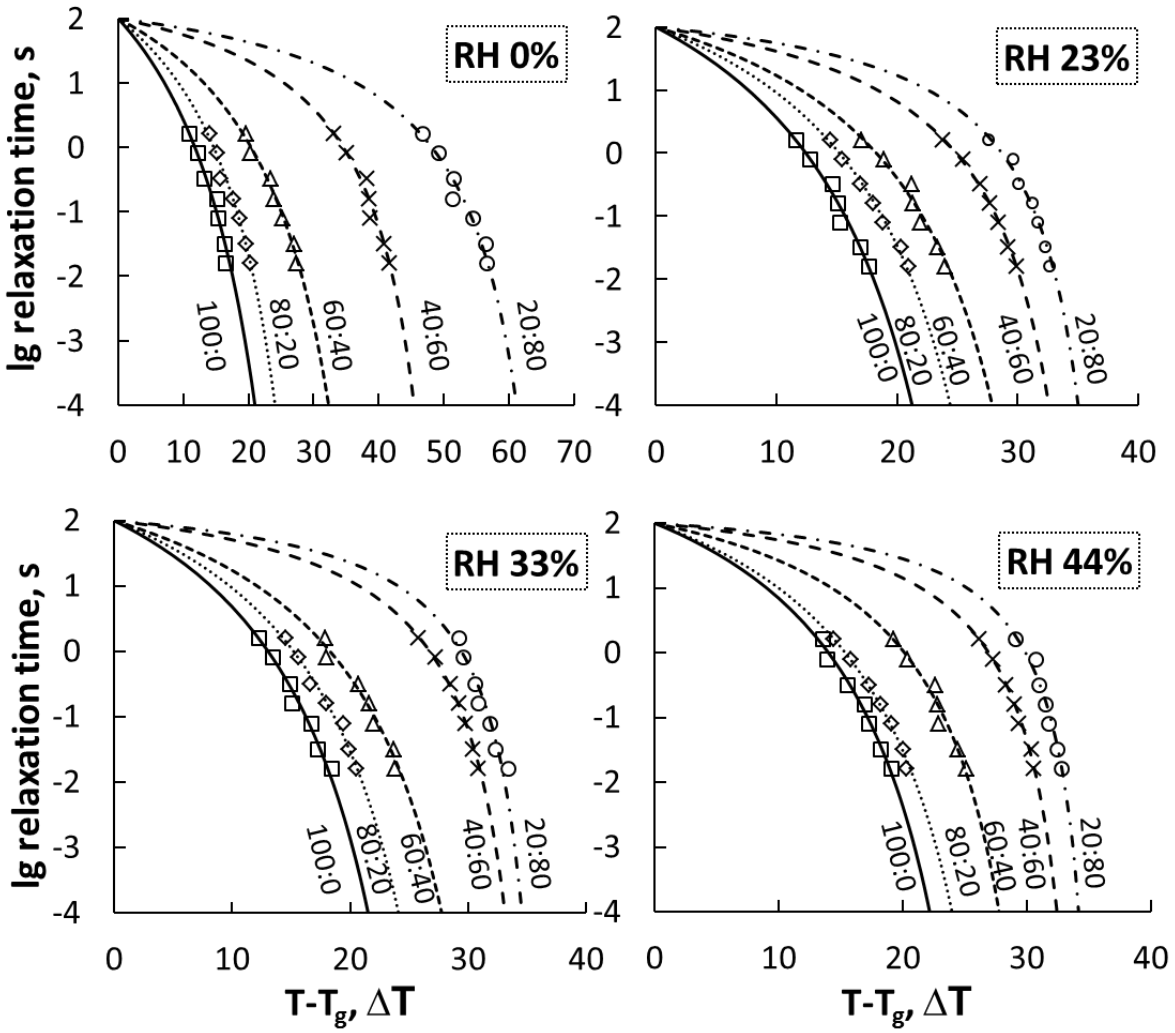

Figure 2.9. Calculated WLF curves (lines) and experimental data (symbols) for trehalose-WPI mixtures (100:0, 80:20, 60:40, 40:60, 20:80) stored for 48 hours at various water activity (0, 0.23, 0.33, 0.44 a_w) at 23±2°C.

Table 2.7. The "strength" parameter S (at d = 4) for trehalose-WPI systems humidified at different relative humidities (RH).

Trehalose-WPI	RH 0%	RH 23%	RH 33%	RH 44%
100:0	17.6	18.0	18.5	19.3
80:20	20.8	21.2	21.0	21.0
60:40	28.2	24.6	24.6	25.4
40:60	42.1	30.2	31.2	30.8
20:80	57.3	33.2	33.1	33.0

Knowing the C_1 and C_2 parameter values for the pure substances allows predicting S values for any mixtures of these substances. The "strength" parameter is linearly depends on the protein content of the systems (Figure 2.10).

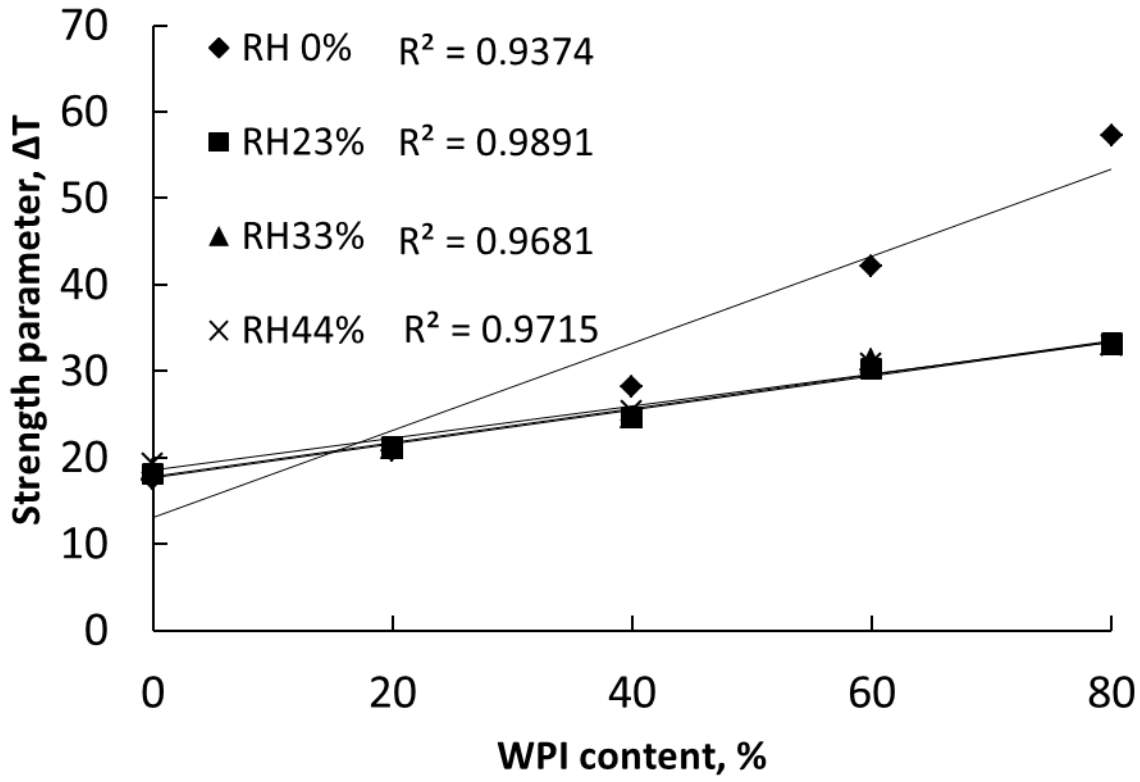

Figure 2.10. "Strength" parameter versus WPI concentration (%) for anhydrous and humidified (0.23, 0.33, 0.44 a_w) trehalose-WPI systems.

Anhydrous trehalose, with S = 17.6, have a minimal value of S, while anhydrous 20:80 trehalose-WPI system have a highest value with S = 57.3. Consequently, the "Strength" parameter is increasing upon addition of the protein to the system. The presence of water in the system has less impact than the protein amount. However, for the systems with high protein levels (60:40, 40:60, 20:80) the addition of water (RH 23%) significantly decreases the "strength" parameter. Further water addition (RH 33%, 44%) to the system does not have a strong influence on parameter.

2.5 Conclusions

In the present study we have presented the new approach describing structural relaxation time-temperature dependence, using trehalose-WPI system as a carbohydrate-protein model. Preliminary, calorimetric and mechanical analyses were carried out. Water sorption isotherms show crystallization during water sorption above 0.65, 0.76, 0.85 a_w in samples with 20%, 40% and 60% of protein respectively. The glass transition temperature, measured by DSC, was strongly decreased by the addition of water and in a lesser extent by the addition of the carbohydrate. The α-relaxation temperature, measured by DMA had a similar behavior with glass transition temperature. We introduced the "strength" parameter, which shows the linear dependence on the concentration of components. This parameter may be used for stability and quality control during food processing and storage. Knowing values of parameter for pure substances allows predicting the S values for any mixtures of these components. The "strength" parameter combines the material state of the system and a practically important time factor. The parameter is increasing upon addition of protein to the system. The anhydrous systems with high level of protein (40%-80%) had significant decreasing S parameter with addition of water. Further water addition for humidified systems did not have a strong influence on parameter.

CHAPTER III

Food Hydrocolloids 70 (2017) 76–87

Contents lists available at ScienceDirect

Food Hydrocolloids

journal homepage: www.elsevier.com/locate/foodhyd

Water sorption, glass transition and "strength" of lactose – Whey protein systems

V.A. Maidannyk, Y.H. Roos*

School of Food and Nutritional Sciences, University College Cork, Ireland

Source: (Maidannyk and Roos, 2017).

3 Water sorption, glass transition and "strength" of lactose – whey protein systems

3.1 Abstract

Freeze-dried lactose-whey protein isolate (WPI) systems with various ratios of components were used as a carbohydrate-protein food model. The Guggenheim-Anderson-de Boer (GAB) water sorption relationship was used as a tool to model fractional water sorption, including higher water activities. Structural relaxation times were measured by DMA and rheology and combined to cover a broad range for strength assessment. The C_1 and C_2 constants for WLF equation and a structural "strength" parameter were calculated for each system. Strength showed linear dependence on composition of the mixtures. Strength was predicted for pure water and calculated for pure WPI at different water contents.

Keywords: "Strength", WLF, lactose, whey protein isolate, structural relaxation.

3.2 Introduction

Lactose and whey protein isolate (WPI) are widely used food ingredients, obtained from milk. Their physicochemical properties are important for storage stability and quality of milk powders. At sufficiently low temperatures (below the glass transition temperature, T_g) lactose is an amorphous glass (Troy and Sharp, 1930; Herrington, 1934; Jouppila and Roos, 1994). In this temperature region amorphous materials have higher thermodynamic characteristics (entropy, enthalpy, free volume etc.) than their equilibrium state at the same conditions. When they are heated to above T_g, the materials soften in transition region from amorphous solid (e.g., glass) to supercooled liquid (e.g., rubber) (Roos, 2008). During this transition amorphous materials display dramatic physical changes: a decrease of viscosity, increase of molecular mobility, rapid decrease in structural relaxation times (Williams et al., 1955; Levine and Slade, 1986; Angell et al., 2000). Structural relaxation time correlates with the time during which long-range molecular motion (displacement, deformation, diffusion, migration) occurs (Chung and Lim, 2003; Surana et al., 2005). It relates to the time-dependent changes of mechanical, electrical and thermodynamic properties of materials (Haque et al., 2006; Liu et al., 2006). An analysis of structural relaxation times above the T_g of noncrystalline solids allowed introduction of a "strength" parameter by Roos and co-workers (Roos et al., 2015; Roos and Drusch, 2015; Fan and Roos, 2016a,b; Maidannyk and Roos, 2016). The Strength, S, measures a critical temperature difference above the T_g where structural relaxation time becomes equal to that critical in processing of solids of biological

materials, e.g., foods and pharmaceutical solids. The control of water sorption behavior may also be used to manipulate structural relaxation times of noncrystalline solids, where water is crucial for the control of production, processing and storage of dairy powders.

Lactose is a disaccharide sugar showing a high T_g (>105 °C for anhydrous lactose) (Roos and Karel, 1990; Haque and Roos, 2004b; Shrestha et al., 2007). Water plasticization significantly lowers T_g of lactose (Roos and Karel, 1992; Shrestha et al., 2007). In dairy powders lactose occurs typically in noncrystalline mixtures with proteins. Whey proteins do not have clear representative T_g due to the complex protein structures and composition of bovine whey (β-lactoglobulin ~ 50%, α-lactalbumin ~ 20%, bovine serum albumin ~ 10%) (Roos and Potes, 2015; Maidannyk and Roos, 2016). Measured T_g values of solids of biological materials depend on the miscibility of components (Roos, 2008), which is poorly understood for carbohydrate-protein systems. Molecular size and supramolecular structures of carbohydrate – protein systems are different and vary with water content (Roos and Potes, 2015). Proteins are macromolecular particles and interact differently with water molecules to compare with small carbohydrates (Swenson and Cerveny, 2015). Proteins often have hydrophobic structures, which cause poor miscibility and molecular segregation of aqueous carbohydrates and proteins (Halle, 2004; Roos and Potes, 2015).

T_g is often measured by the differential scanning calorimetry (DSC). However, T_g alone does not provide kinetic information at molecular level. In the glassy state amorphous structures are fairly stable (Roos, 1995; Slade and Levine, 1995). But at temperatures close to T_g slow structural relaxations relate to "aging" and as the transformation from solid state to supercooled liquid state occurs more rapid time-dependent flow appears (White and Cakebread, 1966; Roos, 1995; Roudaut et al., 2004). Dynamic mechanic analysis (DMA) can measure structural relaxation times from mechanical properties undergoing α-relaxation around the glass transition. DMA has been applied for the analysis of carbohydrates (Roos and Karel, 1991; Silalai and Roos, 2011; Potes et al., 2012) and proteins (Kokini et al., 1994; Gearing et al., 2010). The multi-frequency mode of DMA allows monitoring of relaxation times at temperatures close to T_g. For systems with high water contents volume rheometry can be used for investigation of relaxation time-temperature dependence.

The present study focused on further developing of our strength concept. That is, mechanical α-relaxation, glass transition, water sorption behavior of freeze-dried and

humidified noncrystalline lactose-WPI mixtures and volume rheology of high water content lactose –WPI systems were studied.

3.3 Materials and Methods

3.3.1 Materials

α-lactose monohydrate (Sigma-Aldrich, St. Louis, Mo., U.S.) and whey protein isolate (WPI; Isolac®, Carbery Food Ingredients, Co., Ballineen, Ireland; minor components including carbohydrates or lipids < 3%) were used without purification. De-ionized water (KB Scientific, Cork, Ireland) was used for all experimental work.

3.3.2 Determination of initial water content

Six powder mixtures with different contents of lactose and WPI (the amount of components were varied over the range 0-100% with 20% intervals) and with final weight 0.5-1.0 g were dried at 70°C and absolute pressure P_{abs}<10 mbar during 20 hours, using WTB Binder vacuum oven (Tuttingen, Germany) for determination of the initial water content. The water content in samples was calculated as the weight loss and expressed in percentage.

3.3.2 Preparation of amorphous freeze-dried materials

Lactose and WPI were dissolved separately to obtain 20% (w/w) solutions in water. Lactose solution was heated up to~ 80°C and cooled to room temperature to ensure full dissolution. Thereafter WPI solution, which was stirred 3 hours to dissolve, was added to lactose solutions in required proportion. The ratios of solid components lactose:WPI were 100:0, 80:20, 60:40, 40:60, 20:80, 0:100. Aliquots of these lactose-WPI solution (5 ml) were frozen in pre-weighted and semi-closed with septum 10 ml glass vials at -20°C for 24 h, then at -80°C for 3 h, followed by freeze-drying for 60 h at pressure p < 0.1 mbar (Lyovac GT2, Steris®, Hürth, Germany) to obtain amorphous materials. All vials were hermetically sealed under the vacuum conditions inside the freeze-dryer at p < 0.1 mbar and stored over P_2O_5 in vacuum desiccators (Roos and Karel, 1990) at room temperature (23 ± 2°C) to protect samples from water uptake.

3.3.3 Water sorption analysis

Samples with different ratios of lactose-WPI (described above) were freeze-dried and stored in vacuum desiccators over P_2O_5. Samples were stored in vacuum desiccators at 23 ± 2°C for 120 h over the saturated solutions of CH_3COOK, $MgCl_2$, K_2CO_3, $Mg(NO_3)_2$, $NaNO_2$, NaCl and KCl (Sigma Chemical Co., St. Louise, MO, U.S.A.) which at equilibrium provided 0.23, 0.33, 0.44, 0.545, 0.66, 0.76 and 0.85 a_w respectively. AQUALAB 4 (TE) (Decagon Devices Inc., NE) water activity meter was used to measure water activity for each system. Samples were weighted at the time points 0, 2, 4, 6, 8, 10, 24, 48, 72, 96 and 120 hours upon storage. The crystallization of lactose was assessed by the loss of sorbed water. The water content in each mixture was plotted as a function of time, and the Guggenheim-Anderson-de Boer (GAB) equation was used to fit the data (Eq. 2):

3.3.4 Differential Scanning Calorimetry (DSC)

Differential scanning calorimeter (DSC) (Mettler Toledo Schwerzenbach, Switzerland) was used to determine T_g of anhydrous powders and powders at 0.23, 0.33 and 0.44 a_w. Freeze-dried anhydrous materials were transferred to the pre-weighted DSC aluminium pans (40 μL, Mettler Toledo Schwerzenbach, Switzerland) and hermetically sealed. For anhydrous systems only, the lids of DSC aluminium pans were punctured to allow evaporation of residual water upon the measurement. The freeze-dried samples were transferred to the pre-weighted DSC aluminium pans and stored in evacuated desiccators over saturated salt solutions (with different humidity, described above) at room temperature (23±2°C) until constant weight. After equilibration the pans were hermitically sealed and reweighed. An empty pan with punctured lid was used as a reference. The DSC was calibrated for temperature and heat flow. Samples were scanned from ~ 30°C below to over the T_g region at 5°C/min heating and then cooled at 10°C/min to the starting temperature. The second heating scan was performed to well above the T_g. STARe software version 8.10 (Mettler Toledo Schwerzenbach, Switzerland) was used to calculate the onset, midpoint and endset T_g values. For high water content systems (60, 70, 80, and 90% of water) the onset T_g values were calculated by Gordon-Taylor equation (Eq. 4).

3.3.5 Dynamical Mechanical Analyses (DMA)

To measure dynamic-mechanical properties of the freeze-dried solids dynamic mechanical analyzer (DMA) (Tritec 2000 DMA, Triton Technology Ltd., UK) was used.

Samples (described above for the DSC experiments) were analyzed and recorded using DMA software version 1.43.00. A metal pocket-forming sheet (Triton Technology Ltd., UK) with approximately 60 mg of the powdered sample was fixed directly between the stationary and the driveshaft clamps (balanced to zero) inside the measuring head of the DMA. All three geometric dimensions of the sample - length, width and thickness - were measured. Then sample was scanned over the temperature range from T_α-50°C to T_α+50°C (with cooling rate 5°C/min and heating rate 1°C/min at frequencies 0.1, 0.5, 1, 5, 10 Hz) by using the single cantilever bending mode. For efficient cooling, the DMA device was connected to the liquid nitrogen tank (1 l; Cryogun, Brymill Cryogenic Systems, Labquip Ltd., Dublin, Ireland). The α-relaxation temperature (T_α) was calculated from peak temperature of tangents δ, measured by DMA in multi-frequency mode (Hardy et al., 2001).

To calculate the relaxation times (τ) of peak T_α, measured by DMA at various frequencies (f), we use the Equation 5 (Noel et al., 2000; Potes et al., 2012).

3.3.6 Rheology

Lactose and WPI were dissolved separately in water (considering the initial water contents in the powders) and mixed together at ratios 100:0, 80:20, 60:40, 40:60, 20:80 after 3 hours. The total contents of solids were 10, 20, 30 and 40%. Rheometer ARES-G2 (TA Instruments®, USA) with aluminum "plane-plane" (40 mm) geometry was used to determine apparent viscosities of solutions. The shear rate 100 s was constant for all systems. The temperature range was 0 - 50°C. To convert the apparent viscosity (η) data into shear relaxation times (τ_s), the Maxwell relation (Eq. 15) was used (Angell, 2002).

3.3.7 Calculation of WLF model constants

To calculate the Structural strength, the constants C_1 and C_2 from WLF equation were obtaining as described by Roos (Roos, 1995).

The WLF equation in the form of (Eq. 10) was fitted to DMA, DSC and rheometry data (Williams et al., 1955). The WLF equation in the form of (Eq. 11) suggests that the plot of $1/lg(\tau/\tau_s)$ versus $1/(T-T_g)$ gives a linear correlation. The WLF constants C_1 and C_2 were derived from the slope and intercept of the straight line (Roos, 1995).

3.3.8 Data analysis

All experiments were performed in triplicate. Mean data of the water sorption analyses, DSC, DMA and rheometry were calculated from 3 replicates with standard deviations expressed in error bars. Statistical analysis was performed by Paired-samples t-test using Microsoft Office Excel 2011 (Microsoft, Inc., U.S.A.). Means without a common letter differ significantly from each other ($p<0.05$-significantly, $p<0.01$- very significantly, $p>0.05$ statistically the same).

3.4 Results and discussion

3.4.1 Water sorption analysis

The experimental content of water, sorbed by freeze-dried lactose-WPI systems at different water activities at equilibrium after 120 hours of storage is given in Table 3.1.

Table 3.1. Water content of freeze-dried lactose-WPI systems (ratios of components 100:0, 80:20, 60:40, 40:60, 20:80) stored at different water activities (0.23, 0.33, 0.44, 0.55, 0.65, 0.76, 0.85) for 120 hours at 23±2°C. The 0:100 system data from Maidannyk and Roos, 2016.

	Experimental water content for lactose:WPI systems (g/100 g of solids)					
a_w	**100:0**	**80:20**	**60:40**	**40:60**	**20:80**	**0:100**
0.23	4.33±0.43	4.93±0.09	5.48±0.21	6.12±0.09	6.72±0.12	7.33±0.09
0.33	5.58±0.24	6.05±0.11	7.09±0.03	7.77±0.15	8.51±0.08	9.24±0.12
0.44	8.75±0.33	9.24±0.13	9.75±0.12	10.24±0.06	10.75±0.05	11.24±0.21
0.55	2.08±0.17	6.42±0.82	12.37±0.23	12.03±0.12	12.70±0.21	13.04±0.24
0.65	2.33±0.06	5.46±0.11	14.88±0.30	15.32±0.17	15.76±0.04	16.20±0.19
0.76	2.58±0.38	6.13±0.07	9.80±0.32	19.58±0.41	19.59±0.14	19.82±0.15
0.85	2.62±0.44	7.37±0.09	13.60±0.27	22.28±0.13	25.19±0.37	24.96±0.24

120 hours was enough for all systems to reach the equilibrium water content (Figure 3.1). As expected, water contents correlated with water activities. Systems with high WPI content had significantly higher water content in comparison with lactose, stored at the same humidity (Haque and Roos, 2004a). During the first hours of monitoring a sharp increase of the water content was observed in 100:0 and 80:20 lactose-WPI systems at 54.5 – 85% relative humidities (RH); in 60:40 system at 76 – 85% RH and in 40:60 system at 85% RH.

The further rapid decrease in water content refers to crystallization above 0.55 a_w for 100:0 and 80:20 lactose – WPI systems; above 0.76 a_w for 60:40 and above 0.85 a_w for 40:60 system. Hence, the presence of WPI may prevent lactose crystallization. For non-crystalline systems, water content increased linearly (with R^2 0.9998; 0.9943 and 1 for RH 23, 33 and 44% respectively) with increasing WPI content in system.

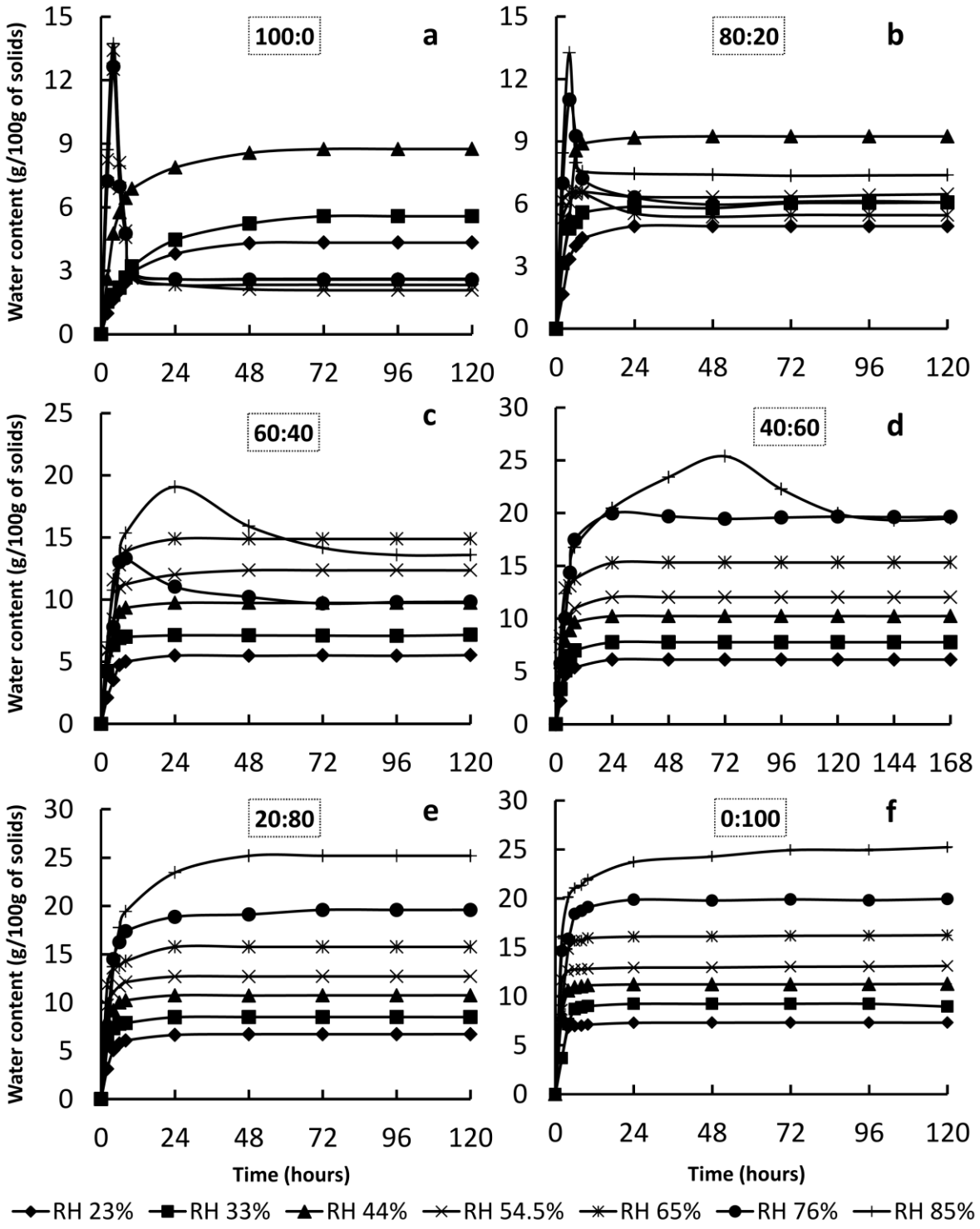

Figure 3.1. Sorption kinetics profiles for freeze-dried lactose-WPI mixtures 100:0 (a), 80:20 (b), 60:40 (c), 40:60 (d), 20:80 (e) and 0:100 (f),stored at 0.23, 0.33, 0.44, 0.55, 0.65, 0.76 and 0.85 a_w, monitored during 120 hours at 23±2°C. Data for 0:100 system from Maidannyk and Roos, 2016.

Many authors reported that the GAB equation could be a useful tool to model water sorption data for lactose (Roos and Karel, 1990; Jouppila and Roos, 1994; Bronlund and Paterson, 2004; Shrestha et. al., 2007; Silalai and Roos, 2010; Zhou and Roos, 2011). However, the extrapolated sorption data of amorphous (non-crystalline) components using the GAB model obtained from water sorption data over a narrow water activity range (≤0.44 a_w) overestimated sorbed water contents and resulted in significant errors (Potes et. al., 2012). Potes et. al. (Potes, 2014) showed that the method, which allowed counting *fractional water contents* of lactose stored at high water activities (Eq. 3) was more accurate.

In the present study, fractional water contents were derived from experimental water sorption data of lactose-WPI 20:80 and 0:100 systems, which showed *no crystallization* even at 0.85 a_w. The *experimental data* of water contents are in agreement with *fractional water contents* at 0.11-0.44 a_w for pure lactose and 80:20 lactose-WPI system; at 0.11-0.65 a_w for 60:40 system and at 0.11-0.76 a_w for 40:60 system. Using fractional and experimental data of water content, we obtained valid GAB sorption isotherms for non-crystalline lactose systems with different ratios of components at high water activities (Figure 3.2).

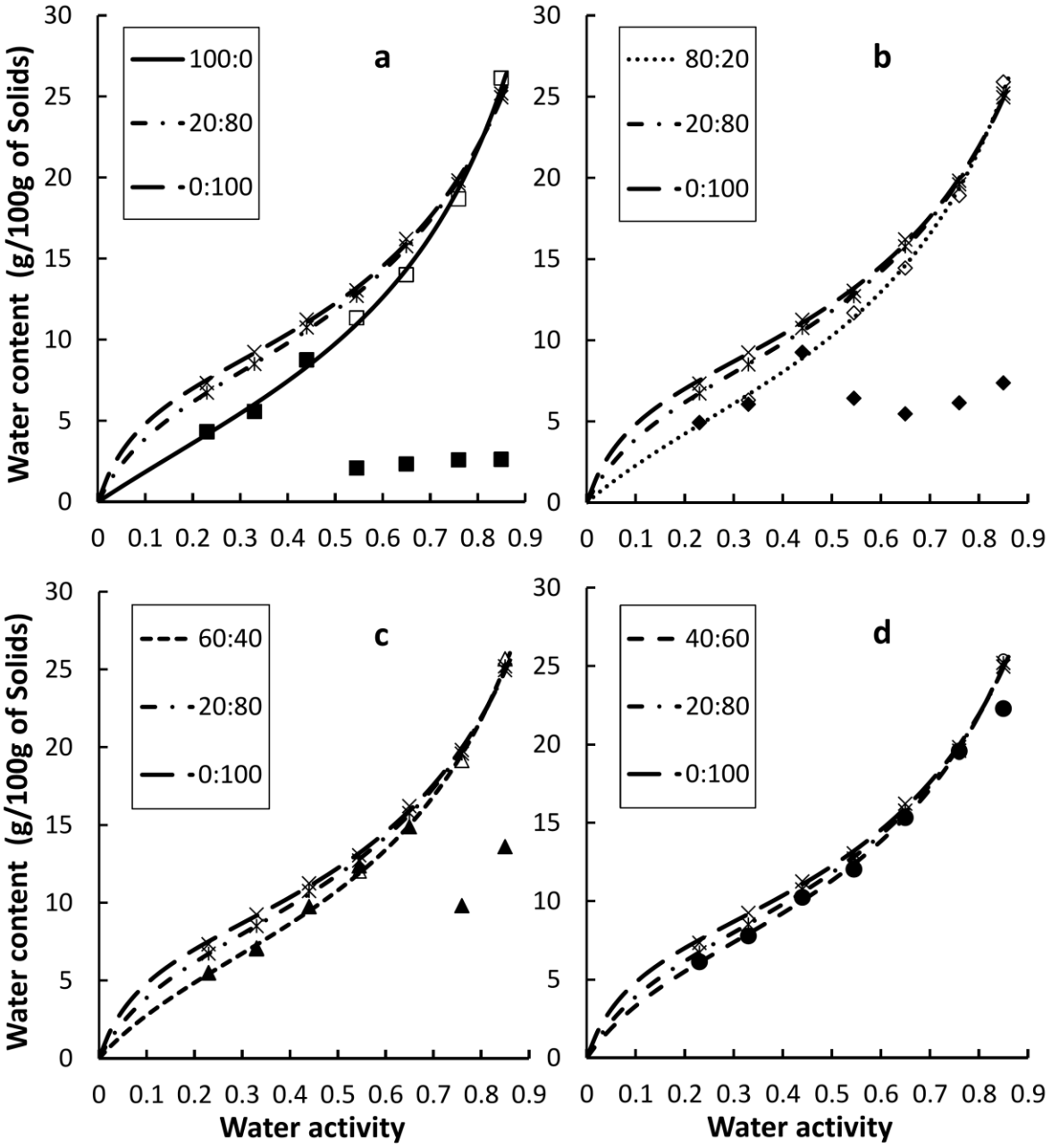

Figure 3.2. The GAB sorption isotherms at 23±2°C (lines), experimental data (solid symbols) and calculated water contents (clear symbols) for amorphous lactose-WPI system with components ratios 100:0 (a); 80:20 (b); 60:40 (c) and 40:60 (d) compared to experimental data for lactose-WPI 20:80 and 100:20 systems.

3.4.2 Glass transition temperature

Table 3.2 shows the onset of calorimetric glass transition temperature from the second heating scan of amorphous (0 – 0.44 a_w) lactose-WPI systems. The T_g of anhydrous lactose

was in agreement with many published results (Roos and Karel, 1990; Haque and Roos, 2004a; Potes et al., 2012). While glass transition temperature of pure WPI was not observed.

Table 3.2. Measured by DSC the onset of calorimetric glass transition temperatures (T_g) of freeze-dried lactose-WPI systems stored for 120 hours at 23±2°C and various water activities.

	Glass transition temperatures (T_g) of lactose-WPI (w/w) systems, °C				
a_w	**100:0**	**80:20**	**60:40**	**40:60**	**20:80**
0	108.6±2.4	112.7±0.9	118.9±2.7	123.4±1.1	128.7±0.6
0.23	45.3±2.3	44.2±1.9	43.2±1.5	42.9±2.2	42.6±1.6
0.33	34.5±1.8	33.9±0.8	32.1±1.4	31.9±1.0	31.5±3.1
0.44	19.5±2.8	18.8±3.3	18.6±2.7	17.7±3.2	17.5 ±2.7

For anhydrous conditions, T_g values of higher WPI content systems were higher ($p<0.05$) than those of low protein content systems due to plasticization. WPI is a macromolecular component with high molecular weight, so increasing of its concentration leads to increasing of systems average molecular weight. Systems with higher molecular weight have a higher glass transition temperature (Slade and Levine, 1991). These results were in agreement with Roos and Karel, 1992; Shamblin and others, 1996; Biliaderis and others, 2002; Haque and Roos, 2004b and Maidannyk and Roos, 2016, who demonstrated that the addition of protein slightly increased the T_g of different anhydrous carbohydrate systems (lactose, trehalose, sucrose).

The T_g was decreasing ($p<0.01$) upon increasing of water content in a system (Figure 3.3). T_g values of humidified lactose-WPI systems were almost composition-independent ($p>0.05$) due to the phase separation of components (MacNaughtan and Mitchell, 2000; Silalai and Roos, 2010; Fan and Roos, 2016a). T_g of humidified systems was mostly dependent on the lactose component. The slight differences in T_g values of humidified systems related to the changes of water content in systems (Table 3.1, 3.2).

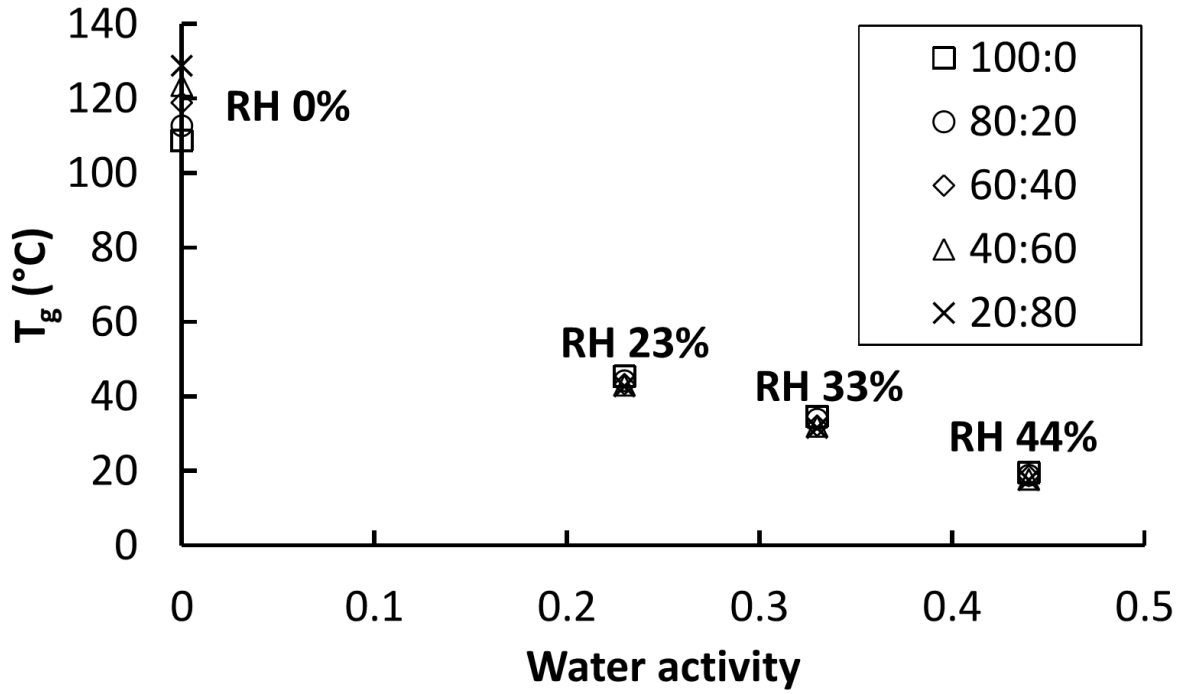

Figure 3.3. Dependence of the glass transition temperatures (T_g) on the water activity (a_w) of freeze-dried lactose-WPI systems.

3.4.3 Rheology

The apparent viscosity for the temperature range 0 to 50°C is shown on Figure 3.4. As expected, the apparent viscosity of lactose and lactose-WPI solutions was decreasing ($p<0.01$) with an increase in temperature (Parks and Gilkey, 1929). The presence of WPI with lactose gave a significantly higher apparent viscosity, especially with 60 and 70% of water. For both, carbohydrate and carbohydrate-protein solutions, the apparent viscosity increased ($p<0.01$) with concentration of the components (Morison and Mackay, 2001; Adhikari and others, 2007).

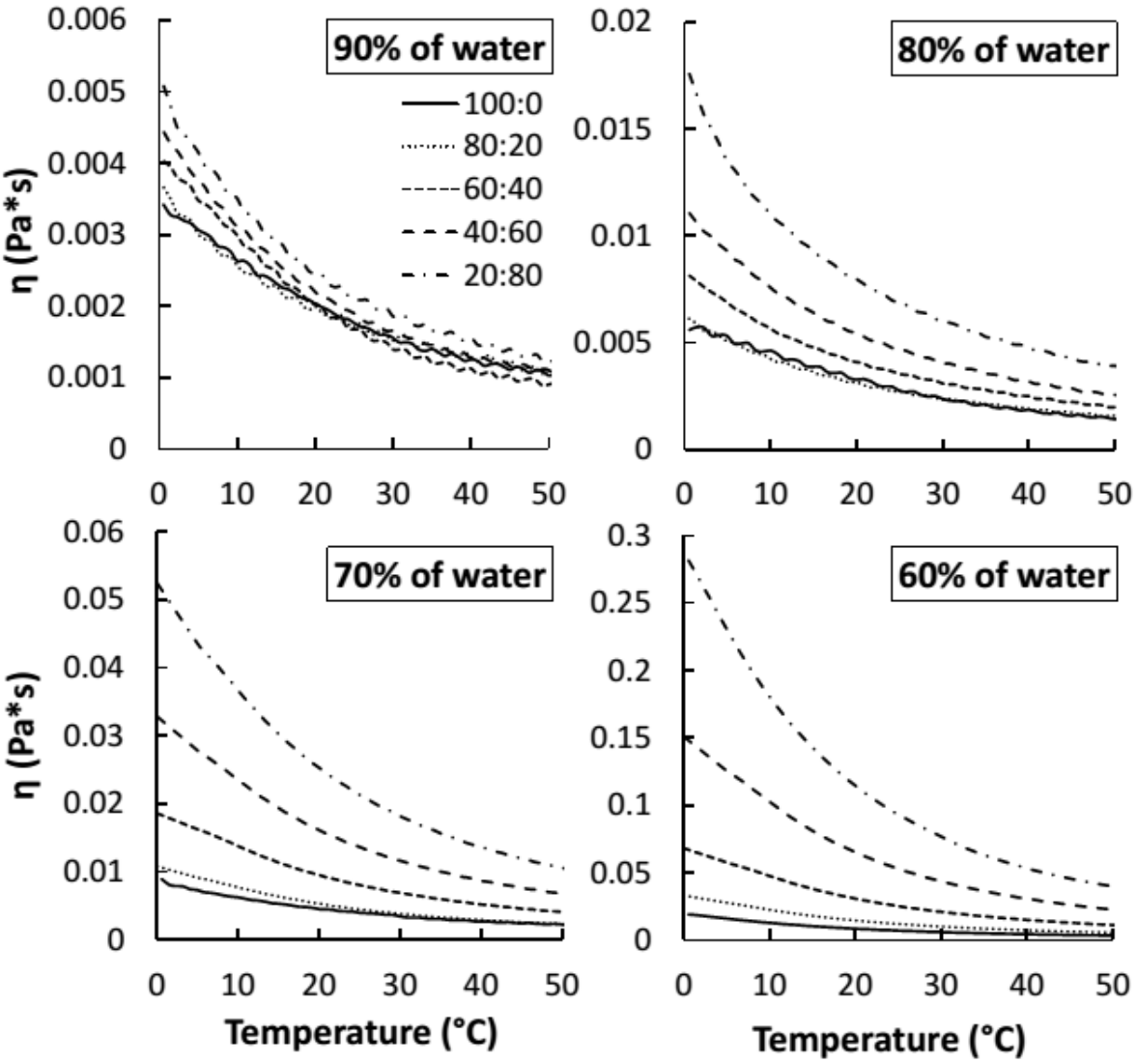

Figure 3.4. Temperature dependence of the viscosity of aqueous (90, 80, 70 and 60% of water) lactose-WPI (100:0; 80:20; 60:40; 40:60; 20:80) systems.

For high water content system (60, 70, 80 and 90% of water) the T_g values were obtained from the Gordon-Taylor relationship (Eq. 4). We used -135°C for glass transition temperature of water (Angell, 2002), and experimental T_g (Table 3.2) for anhydrous and humidified lactose-WPI systems (Table 3.3). The constant *k* was 6.96±0.49 for 100:0 system, 6.9±0.3 for 80:20, 6.7±0.3 for 60:40, 6.5±0.2 for 40:60 and 6.4±0.3 for 20:80 system.

Table 3.3. Glass transition temperatures (T_g) predicted by Gordon-Taylor equation for 100:0, 80:20, 60:40, 40:60 and 20:80 lactose-WPI systems with high water contents (60, 70, 80, 90% of water).

Water content, %	Calculated glass transition temperature, (T_g) of lactose-WPI (w/w) systems, °C				
	100:0	**80:20**	**60:40**	**40:60**	**20:80**
60	-113.7±0.7	-112.9±0.6	-112.1±0.7	-111.0±0.5	-110.3±1.2
70	-120.9±1.1	-120.3±1.3	-119.8±0.4	-119.0±0.5	-118.5±0.8
80	-126.6±0.9	-126.1±0.4	-125.9±0.9	-125.4±0.6	-125.1±0.4
90	-131.2±1.1	-130.9±1.1	-130.9±1.3	-130.7±0.3	-130.5±0.4

3.4.4 Dynamical Mechanical Analyses (DMA)

DMA in multi-frequency mode was used for scanning amorphous (0 – 0.44 a_w) lactose-WPI systems. Figure 3.5a shows an example of typical spectra for pure lactose system, humidified in a desiccator at 0.33 a_w. DMA measurements allowed detecting changes in different material properties such as molecular interaction and water plasticization (Lopes-Diez and Bone, 2004; Silalai and Roos, 2011).

The T_α data were obtained from the temperature peak of tanδ, which showed exactly the same values as temperature peak of loss modulus. Using Equation 5, we obtained the relaxation time – temperature dependence for amorphous lactose-WPI systems. For anhydrous and humidified lactose-WPI systems the T_α occurred at ~20-30°C above the onset T_g.

Peak of tan δ was significantly dependent on the protein content of the system (Figure 3.5b). For pure lactose the sharp peak was observed, while systems with high amount of WPI showed broadened peaks with less intensity. T_α value was increasing ($p<0.05$) upon increasing of the protein content in carbohydrate-protein system (Table 3.4, Figure 3.5b). The reason for that was a physical barrier of WPI as macromolecular component to the molecular mobility of amorphous lactose (Fan and Roos, 2016b).

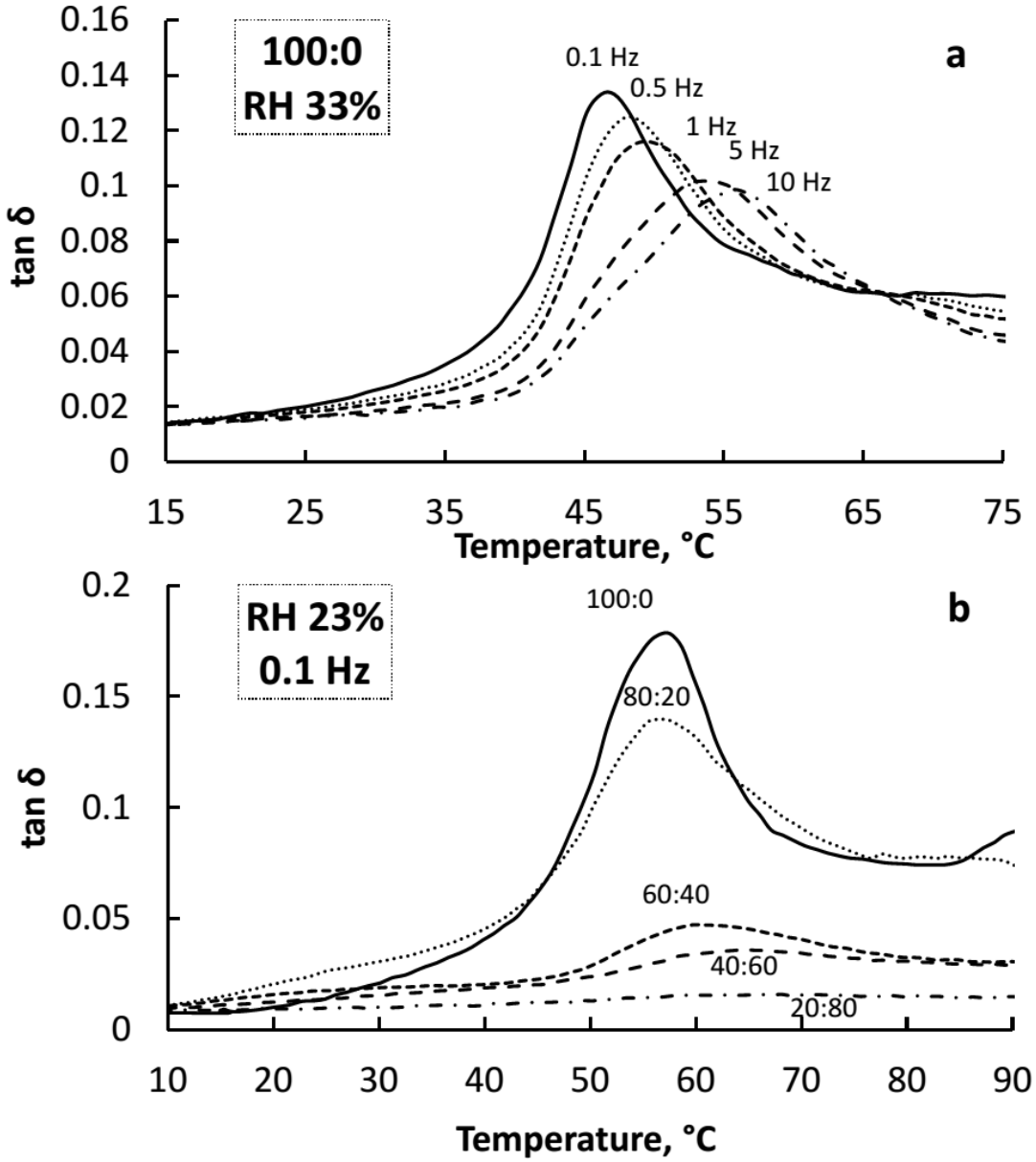

Figure. 3.5. (a) Temperature dependence of dynamic tangents δ for humidified (0.33 a_w) lactose system in multi-frequency mode (0.1, 0.5, 1, 5, 10 Hz). (b) Temperature dependence of dynamic tangents δ for humidified (0.23 a_w) lactose-WPI mixtures (100:0, 80:20, 60:40, 40:60, 20:80) at 0.1 Hz.

Water is important factor that affects the value of T_α (Table 3.4). The tan δ peaks were decreasing ($p<0.01$) for every system with increasing of the water content. For example, the T_α for 80:20 (f = 0.1 Hz) lactose-WPI system decreased from 163.5°C at RH 0% to 42.8°C at RH 44%, what was in agreement with many authors (Silalai and Roos, 2011; Potes

et al., 2012; Fan and Roos, 2016). These changes could be explained by the free-volume theory, which shows that the presence of water (good plasticizer) increases free volume in the system as well as molecular mobility of amorphous sugar (Slade and Levine, 1991; Royall et al., 2005; Meinders and van Viet, 2009).

Table 3.4. α-relaxation temperature (T_α) detected by DMA for lactose-WPI mixtures equilibrated at different relative humidities (RH) and measured at different frequencies (f) and relaxation times (logτ, s).

RH 0%		**Lactose-WPI systems**				
		100:0	**80:20**	**60:40**	**40:60**	**20:80**
f, Hz	**logτ, s**	**T_α, °C**	**T_α, °C**	**T_α, °C**	**T_α, °C**	**T_α, °C**
0.1	**0.20**	124.4±0.9	130.5±3.1	140.3±0.6	151.8±1.0	163.5±4.3
0.5	**-0.49**	126.3±1.2	133.7±1.2	142.4±1.2	155.7±0.7	167.1±2.2
1.0	**-0.80**	127.8±2.1	135.8±2.3	146.7±1.2	157.1±1.2	169.5±2.2
5.0	**-1.50**	130.3±0.8	139.0±1.5	147.8±2.4	161.0±1.9	172.1±2.5
10.0	**-1.80**	131.7±1.1	140.1±1.3	148.9±2.5	163.0±1.8	173.6±3.4
RH 23%		**Lactose-WPI systems**				
		100:0	**80:20**	**60:40**	**40:60**	**20:80**
f, Hz	**logτ, s**	**T_α, °C**	**T_α, °C**	**T_α, °C**	**T_α, °C**	**T_α, °C**
0.1	**0.20**	56.5±0.9	58.3±1.4	60.0±2.6	61.3±0.9	69.6±2.1
0.5	**-0.49**	59.7±1.0	61.0±2.7	62.3±2.1	62.7±1.2	70.1±3.2
1.0	**-0.80**	61.1±1.8	62.0±2.2	64.5±0.4	64.0±3.3	72.6±2.8
5.0	**-1.50**	64.0±1.6	65.2±3.2	66.3±1.8	68.3±1.2	74.3±2.2
10.0	**-1.80**	67.1±1.7	66.7±4.0	67.9±3.5	70.1±2.5	76.7±1.8
RH 33%		**Lactose-WPI systems**				
		100:0	**80:20**	**60:40**	**40:60**	**20:80**
f, Hz	**logτ, s**	**T_α, °C**	**T_α, °C**	**T_α, °C**	**T_α, °C**	**T_α, °C**
0.1	**0.20**	46.7±0.6	48.6±2.1	49.2±3.3	51.9±2.4	57.8±2.7
0.5	**-0.49**	48.2±1.1	50.0±1.4	50.3±1.1	53.0±1.5	59.2±2.0
1.0	**-0.80**	49.2±1.3	51.4±2.3	52.5±2.7	54.2±2.3	60.3±3.1
5.0	**-1.50**	53.5±2.9	53.5±2.5	53.6±1.2	55.2±1.9	61.3±1.2
10.0	**-1.80**	55.6±1.2	56.3±1.0	55.8±3.1	56.2±2.3	62.5±1.9
RH 44%		**Lactose-WPI systems**				
		100:0	**80:20**	**60:40**	**40:60**	**20:80**
f, Hz	**logτ, s**	**T_α, °C**	**T_α, °C**	**T_α, °C**	**T_α, °C**	**T_α, °C**
0.1	**0.20**	24.6±2.3	32.6±3.1	34.7±2.2	38.2±0.8	42.8±1.4
0.5	**-0.49**	24.8±1.6	35.9±2.5	36.9±1.1	39.5±1.3	44.8±1.9
1.0	**-0.80**	30.0±3.4	36.9±1.9	37.9±3.1	40.4±2.4	45.9±2.6
5.0	**-1.50**	32.2±1.1	39.1±1.2	40.7±1.6	41.5±3.3	46.9±0.6
10.0	**-1.80**	34.3±1.1	40.1±1.8	41.3±2.7	43.2±2.3	47.9±2.8

3.4.5 WLF modeling and Strength

Understanding and characterization of glass-forming process is an important task in food materials science. Angell and co-workers (1991) introduced classification of glass formers to "fragile" and "strong" materials. According to their model, structural relaxation times of "strong" glass formers above T_g followed the Arrhenius relationship while "fragile" materials showed non-Arrhenius characteristics near the glass transition temperature. This concept allowed classifying materials according to the plot of viscosity (or structural relaxation time) versus T_g/T.(Angell, 2002). However, a plot of T_g/T varies according to differences in T_g values, while the same $T-T_g$ value often shows similar viscosity (or relaxation time). Thus, this concept applies only for materials with the same T_g and T_g/T plot cannot explain variations in structural relaxation times (or viscosities) above the T_g (Roos, 2013).

The WLF model is often used for glass-formers to model relaxation time - temperature relationships close to the onset T_g (Peleg, 1992; Harnkarnsujarit et al., 2012; Roos, 2013; Roos and Drusch, 2015). This relationship uses structural relaxation times at a reference temperature and the corresponding relaxation time above the glass transition (T_s) at a certain conditions: $T_s = T_g$ (Williams et al., 1955; Peleg 1992; Roos and Drusch, 2015). In calculations we assumed that the viscosity and relaxation time of supercooled liquid approached 10^{12} Pa s and 100 s respectively. Upon heating, values of viscosity and relaxation time are decreasing down to 10^5 Pa s and 10^{-14} s. (Angell, 1991; Angell et al., 2000; Angell, 2002; Roos, 2013; Roos et al., 2015).

The WLF constants C_1 and C_2 were obtained for amorphous (0 - 0.44 a_w) and high water content systems (60, 70, 80, 90% of water) using Equation 11. These data are provided in tables 3.5 and 3.6.

Table 3.5. Calculated WLF (τ_s = 100s; $\eta_s = 10^{12}$Pa s) constants C_1 and C_2 for amorphous lactose-WPI systems storage at different relative humidities (RH).

Trehalose-WPI	**RH 0%**		**RH 23%**		**RH 33%**		**RH 44%**	
	-C_1, s	***-C_2, °C***	***-C_1, s***	***-C_2, °C***	***-C_1, s***	***-C_2, °C***	***-C_1, s***	***-C_2, °C***
100:0	2.71±0.31	38.4±0.4	13.57±0.41	94.2±0.5	8.09±0.53	62.1±0.7	-8.27±0.32	-18.1±0.5
80:20	3.68±0.43	53.5±0.6	4.15±0.27	45.7±0.4	3.25±0.22	39.1±0.3	3.83±0.14	41.8±0.3
60:40	2.66±0.23	51.3±0.4	2.77±0.31	41.9±0.5	2.11±0.17	35.6±0.3	2.36±0.15	36.1±0.2
40:60	2.06±0.37	59.9±0.5	3.37±0.22	49.5±0.3	0.93±0.15	29.7±0.2	1.09±0.27	30.7±0.4
20:80	1.33±0.09	60.0±0.1	1.41±0.13	45.5±0.3	0.71±0.08	36.3±0.2	0.85±0.09	35.8±0.1

Table 3.6. Calculated WLF constants C_1 and C_2 for high water content (60, 70, 80 and 90% of water) lactose-WPI systems.

Trehalose-WPI	90% of water		80% of water		70% of water		60% of water	
	C_1, s	C_2, °C	C_1, s	C_2, °C	C_1, s	C_2, °C	C_1, s	C_2, °C
100:0	16.67±0.81	19.7±0.9	16.67±0.44	21.9±0.5	16.42±0.35	20.4±0.5	16.58±0.29	23.9±0.4
80:20	16.89±0.73	22.3±0.8	16.72±0.67	23.2±0.8	16.64±0.61	23.2±0.7	16.50±0.69	25.6±0.8
60:40	16.98±0.75	23.8±0.8	16.75±0.56	23.8±0.7	16.39±0.45	23.5±0.5	16.23±0.73	26.7±0.8
40:60	17.09±0.83	25.1±0.9	16.67±0.83	24.4±0.9	16.21±0.78	24.4±0.9	16.05±0.52	28.5±0.6
20:80	17.06±0.56	25.2±0.7	16.47±0.78	24.5±0.9	16.03±0.97	24.6±1.0	15.87±0.33	29.5±0.4

Roos et al. (2015) introduced a *"strength" parameter* as a measure of variations in structural relaxation times. This parameter or *flow characteristics* of the glass formers and their interactions with other solids contribute to noncrystalline solids characteristic (Roos et al., 2015). Figure 3.6 shows that for systems with differences in water contents, upon heating, critical and large variation in the structural relaxation time occurred between 100 s and 0.01 s (between 2 and -2 in logarithmic scale).

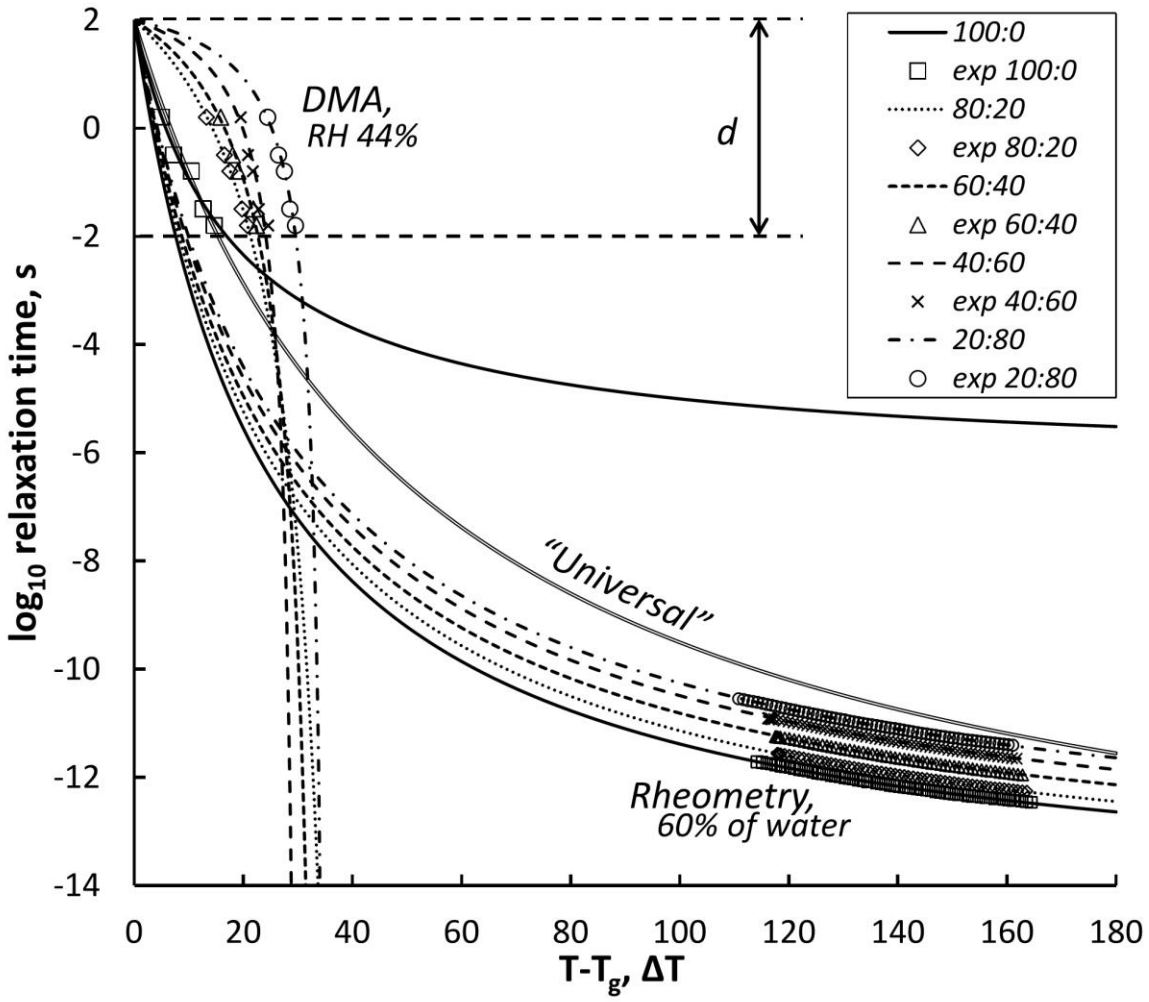

Figure 3.6. Modified WLF curves with calculated and "universal" constants (lines) and experimental data (symbols) for humidified (RH 44%) and high water content (60% of water) lactose-WPI systems.

The temperature difference, $T\text{-}T_g$, at which structural relaxation times exceed time factors critical to processing characteristics of the materials (for example particle stickiness in spray drying) was defined as "strength" parameter S (Eq.16).

Our rheometry data on the Figures 3.6 and 3.7 showed that at temperatures well above the onset of the T_g, the structural relaxation time decreased very slowly. For example for 20:80 lactose-WPI system, structural relaxation decreased from -10.5 to -11.4 s in logarithmic scale at temperature differences of 124.1 to 169.3°C. Hence, these data give a *physical limitation of relaxation time change*.

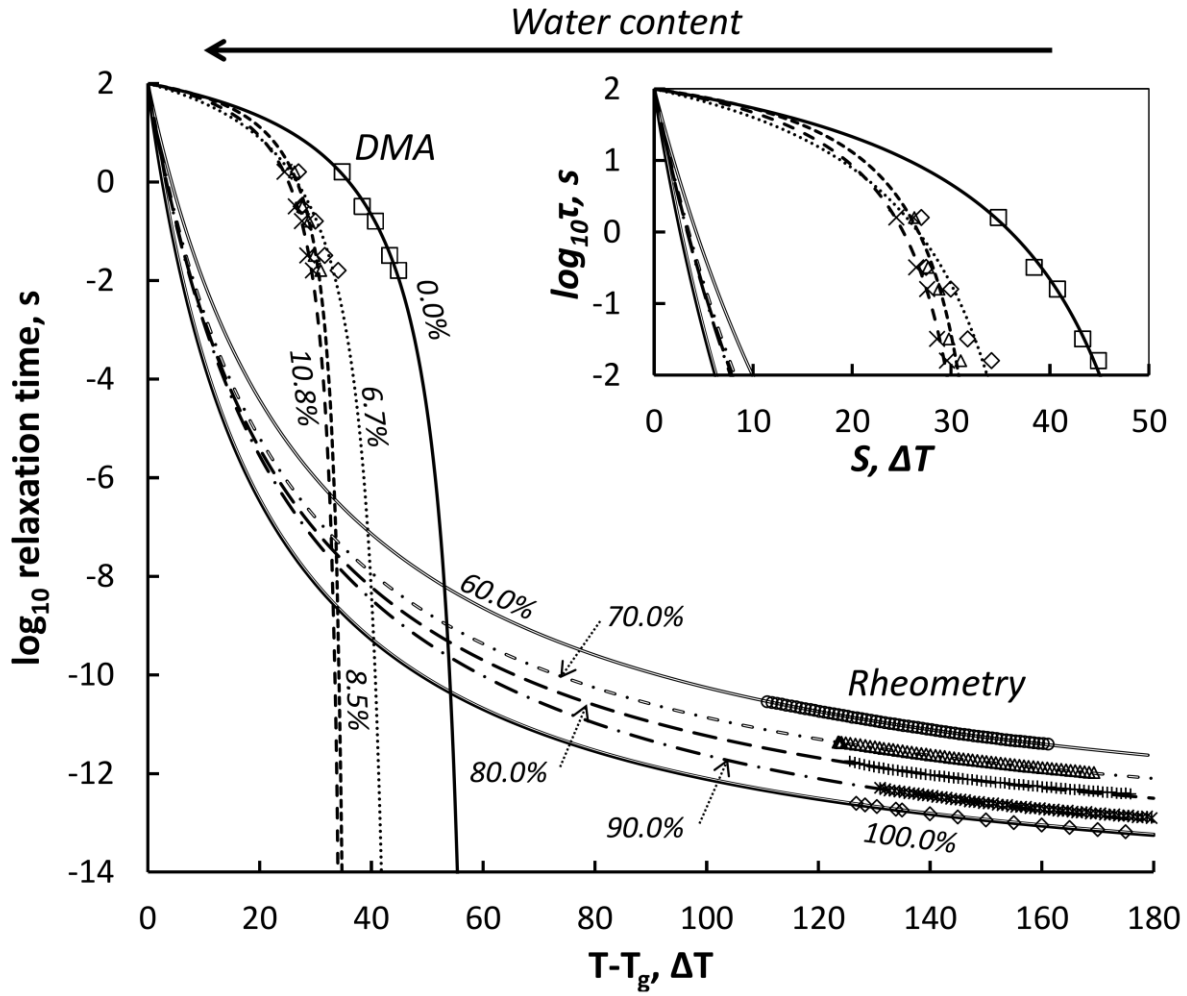

Figure 3.7. Modified WLF curves (lines) and experimental data (symbols) for 20:80 lactose-WPI system with different water contents (g/100 g of dry solids, %). Data for pure water are from Kestin et al. (1978).

The Strength, S, was found for every lactose-WPI system at different relative humidities and water contents at $d = 4$. These data are summaries in the Table 3.7.

Table 3.7. Strength S (at d = 4) for lactose-WPI systems at different relative humidities (RH) and water contents.

Trehalose-WPI	**90% of water**		**80% of water**		**70% of water**		**60% of water**	
	C_1, *s*	C_2, *°C*	C_1, *s*	C_2, *°C*	C_1, *s*	C_2, *°C*	C_1, *s*	C_2, *°C*
100:0	16.67±0.81	19.7±0.9	16.67±0.44	21.9±0.5	16.42±0.35	20.4±0.5	16.58±0.29	23.9±0.4
80:20	16.89±0.73	22.3±0.8	16.72±0.67	23.2±0.8	16.64±0.61	23.2±0.7	16.50±0.69	25.6±0.8
60:40	16.98±0.75	23.8±0.8	16.75±0.56	23.8±0.7	16.39±0.45	23.5±0.5	16.23±0.73	26.7±0.8
40:60	17.09±0.83	25.1±0.9	16.67±0.83	24.4±0.9	16.21±0.78	24.4±0.9	16.05±0.52	28.5±0.6
20:80	17.06±0.56	25.2±0.7	16.47±0.78	24.5±0.9	16.03±0.97	24.6±1.0	15.87±0.33	29.5±0.4

Table 3.7 shows that when water content in the system increased, its flow characteristics decreased significantly (P<0.01), especially between anhydrous and humidified lactose-WPI systems (Fig. 7). Probably, due to water plasticization and molecular mobility of amorphous lactose. Fan and Roos (2016b) showed relationships similar to Gordon-Taylor (Equation 17) which allowed to calculate S at different water contents. Authors used S_2 = 1°C, as a strength of pure water. Using literature data, at this work we predict strength of pure water around 6°C.

$$S = \frac{w_1 S_1 + k w_2 S_2}{w_1 + k w_2}, \quad (17)$$

where w_1 – weight fraction of dry solid; w_2 – weight fraction of water; k – coefficient; S_1 – structural strength for anhydrous system; S_2 – structural strength of water (S_2 = 6.0, was calculated from viscosity data of Kestin et al., (1978)).

Figure 3.8 shows modeled and experimental data for lactose-WPI systems. The value of k was 5.7, 5.7, 5.2, 7.2 and 5.7 for 100:0, 80:20, 60:40, 40:60 and 20:80 lactose-WPI systems respectively.

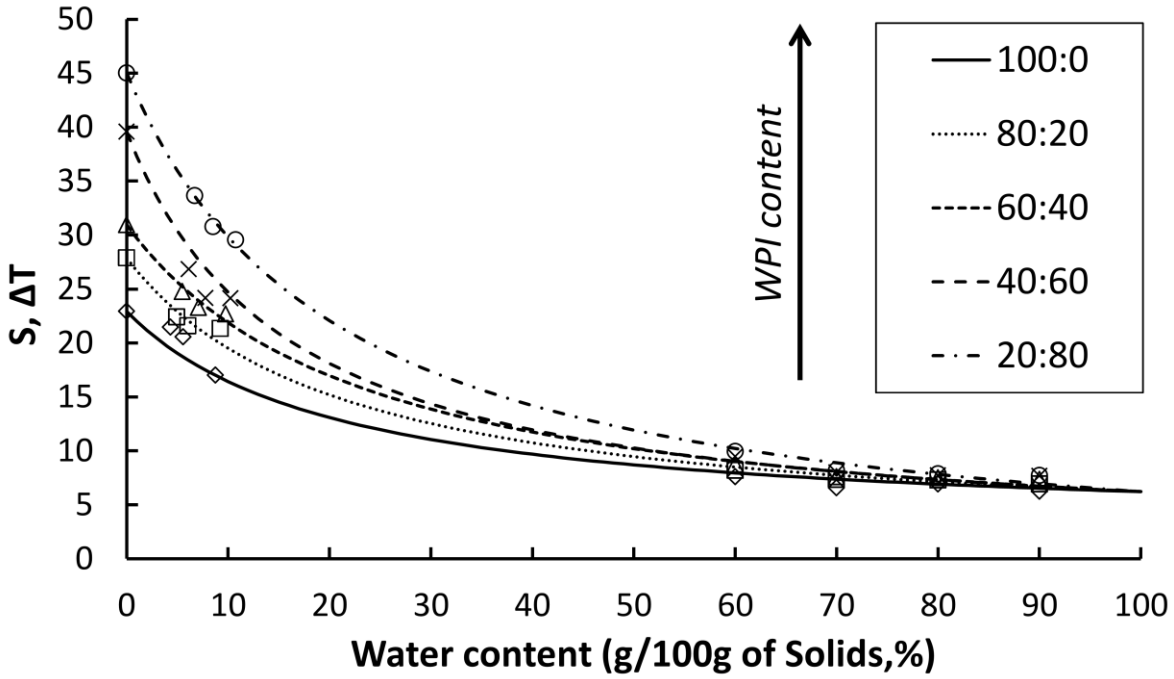

Figure 3.8. Modelled by equation 17 (lines) and experimental (symbols) S of lactose-WPI (100:0; 80:20; 60:40; 40:60; 20:80) systems at different water contents.

The structural strength of materials was strongly dependent on the protein content in the system (Figure 3.9).

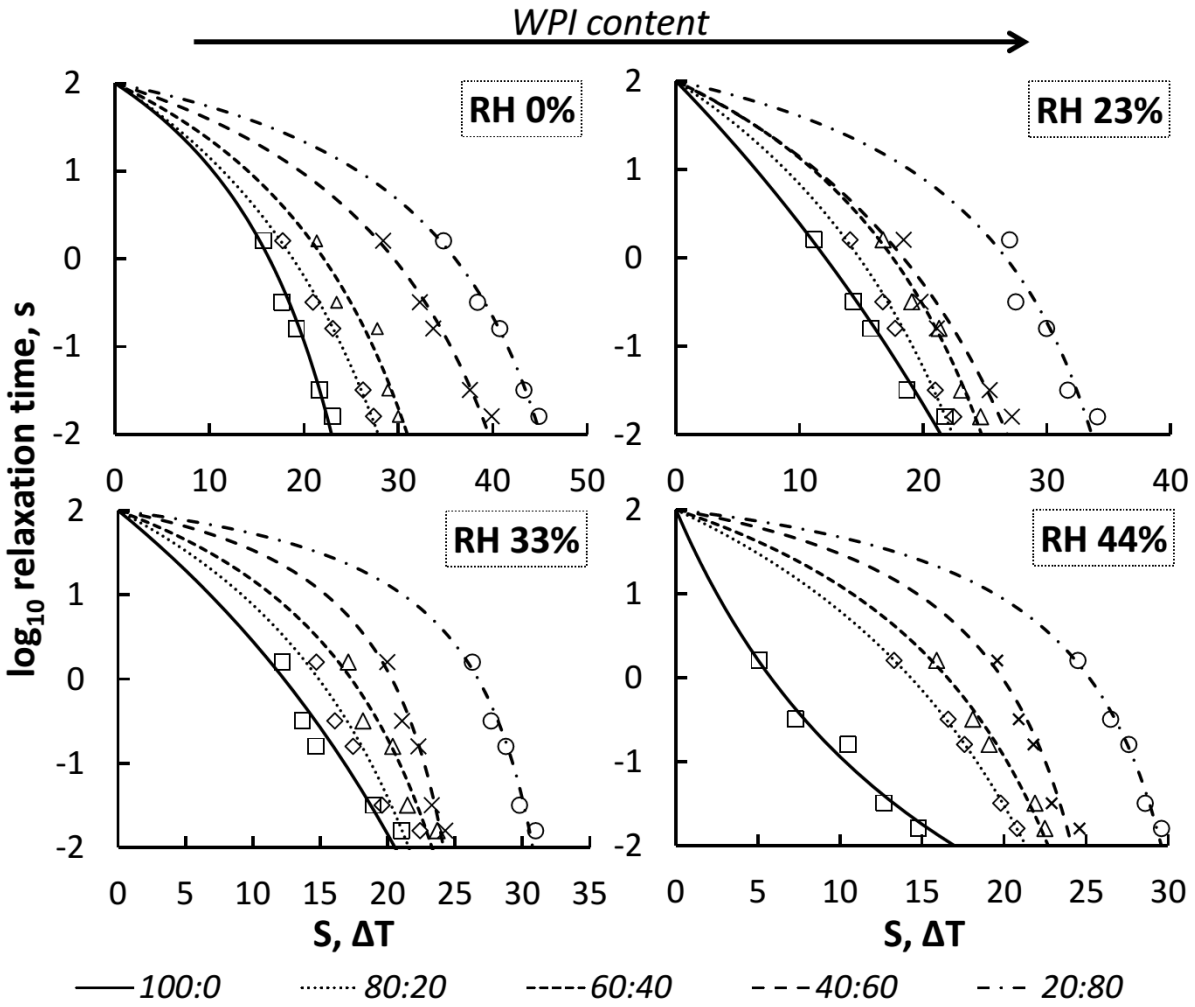

Figure 3.9. Modified WLF curves (lines) and experimental data (symbols) for lactose-WPI mixtures (100:0, 80:20, 60:40, 40:60, 20:80) stored for 120 hours at various water activity (0, 0.23, 0.33, 0.44 a_w) at 23±2°C.

Figure 3.9 shows that systems with a high amount of protein were "stronger" than pure carbohydrate systems. Hence, lactose-WPI systems showed that structural relaxation times achieved a critical level at higher temperatures than pure carbohydrate systems. These results were in agreement with our previous studies (Maidannyk and Roos, 2016; Fan and Roos, 2016a,b).

The experimental (solid symbols) and modeled by equation 17 (empty symbols) data of S for lactose-WPI systems at different water and WPI contents are shown on Figure 3.10.

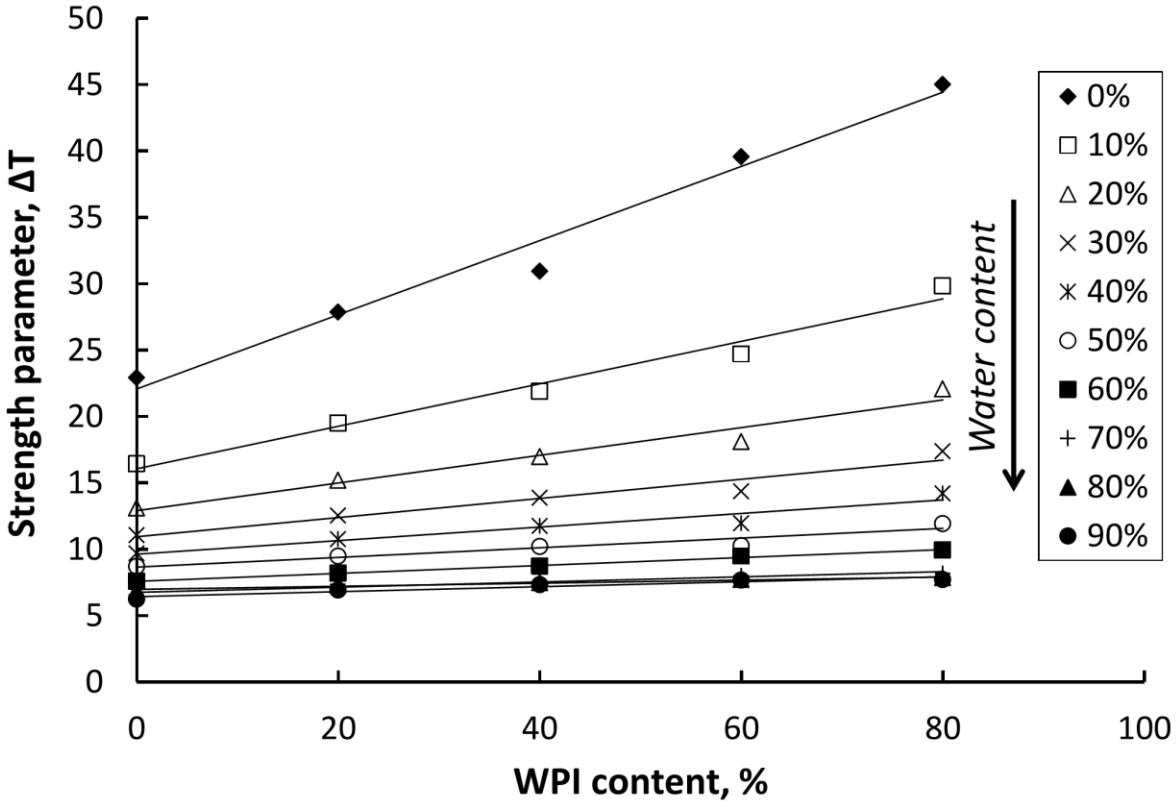

Figure 3.10. The dependence of S from WPI content (%) for lactose-WPI system at different water contents (0%, 60%, 70%, 80%, 90% - experimental data; 10%, 20%, 30%, 40%, 50% - the data predicted by Eq. 9).

S is increasing *linearly* (with 0.9783, 0.9774, 0.9583, 0.9413, 0.9279, 0.9174, 0.9965, 0.9342, 0.9710 and 0.9109 R^2 for 0%, 10%, 20%, 30%, 40%, 50%, 60%, 70%, 80% and 90% of water respectively) with increasing of protein concentration in the system (Fig. 10). Thus, *strength shows linear dependence on composition in a system.* Calculated S for WPI was 50.0, 32.1, 23.4, 18.2, 14.7, 12.3, 10.6, 8.7, 8.2 and 8.3 for 0%, 10%, 20%, 30%, 40%, 50%, 60%, 70%, 80% and 90% of water respectively. Knowing structural strength of pure components (for example lactose and WPI) we can calculate S for their mixture. Therefore, the present work showed that structural strength approach allows controlling quality and stability of different amorphous mixtures.

3.5 Conclusions

This work focused on further development of the strength approach. The effects of the composition and water content on the structural strength were under investigation. Systems with different amounts of lactose and WPI were used as carbohydrate-protein model. Fractional water sorption analysis allowed controlling water content in amorphous mixtures. The presence of WPI may prevent lactose crystallization. Structural strength showed linear dependence on composition in a mixture. The S significantly depended on the water content in the system. The S value for pure water was found to be 6.0 by estimation from viscosity data. Knowing S of lactose-WPI mixtures, the "strength" parameter of pure WPI at different water content was predicted. Knowing S of pure components allows to estimate S for their mixtures. This data may be suitable for stability and quality control during food production and storage as well as for other amorphous materials.

CHAPTER IV

Food Research International 96 (2017) 121–131

Contents lists available at ScienceDirect

Food Research International

journal homepage: www.elsevier.com/locate/foodres

Structural strength analysis of amorphous trehalose-maltodextrin systems

V.A. Maidannyk [a], B. Nurhadi [b], Y.H. Roos [a,*]

[a] School of Food and Nutritional Sciences, University College Cork, Ireland
[b] Faculty of Agro-Industrial Technology, University Padjadjaran, Indonesia

Source: (Maidannyk et al., 2017).

4 Structural strength analysis of amorphous trehalose-maltodextrin systems

4.1 Abstract

Fundamental knowledge of physical state of materials gives practically important information for food, biological and pharmaceutical industry. Based on Williams-Landel-Ferry (WLF) equation, the strength concept was introduced. This concept provides a simple parameter, S, to express resistance of solids to flow above the glass transition temperature. To develop this approach, miscible trehalose-maltodextrin (0:100; 20:80; 40:60; 60:40; 80:20 and 100:0) systems with different ratios of components were used in the present study. Such systems represent various food products including infant formula and many nutritional formulations. Amorphous solids were prepared from 20% solids in water solutions by freeze-drying. Fractional water sorption analysis of trehalose-maltodextrin miscible systems allows controlling water content at high water activities. Glass transition temperature was measured by DSC. DMA and DEA in a multi-frequency mode allowed determination of the α-relaxation temperatures at various structural relaxation times. Volume rheology gives structural relaxation time – temperature dependence for high water content systems. The strength shows linear dependence on maltodextrin concentration and significantly decreases with increasing water content in miscible systems.

Keywords: Structural relaxation, WLF, "Strength" parameter, trehalose, maltodextrin.

4.2 Introduction

Knowledge of thermodynamic and kinetic characteristics is fundamental for understanding of processing and storage of materials. The glass transition temperature (T_g) is an important physical parameter which is often measured by differential scanning calorimeter (DSC). At temperatures below T_g low molecular weight sugars (mono- and disaccharides) exist in an amorphous solid form. However, during heating to above the T_g, physical properties such as molecular mobility, viscosity, etc. are significantly changing and amorphous solids (e. g. glass) are converted to supercooled liquids (e. g. rubber), showing time-dependent flow (rapid change in structural relaxation time) (Angell et al., 2000; Roos, 2008). Unfortunately, T_g of a material alone does not provide sufficient information about kinetics of the transition process. Therefore, measurements of the time-dependent characteristics of electric, thermal and mechanical changes give very important practical data. Structural strength determination, proposed by Roos and co-workers is a simple approach,

which combines temperature change and practically important time factors (Roos et al., 2015; Fan and Roos, 2016a, b; Maidannyk and Roos, 2016). The strength (S) shows a temperature difference ($T-T_g$), at which a critical change in structural relaxation time happens (Roos et al., 2015; Fan and Roos, 2016a, b; Maidannyk and Roos, 2016).

T_g of complex multicomponent systems depends on components miscibility (Roos, 2008). In the present study systems of trehalose-maltodextrin with various component contents were used as a miscible carbohydrate model. Trehalose is a natural disaccharide of glucose monomers with a high T_g (Green and Angell, 1989) and it a suitable material for uses in food and biotechnological areas due to its physicochemical properties (stabilization of protein structure and membrane structure in a dry state, inhibition of biological damage) (Xie and Timasheff, 1997; Crowe et al., 1985). Maltodextrins are starch hydrolysis products which the molecular size/weight can be characterized by Dextrose Equivalent (DE). Even with the same DE, maltodextrin is a mixture of different carbohydrates, therefore usually maltodextrins have a very complex composition (Linden and Lorient, 1999; Nurhadi et al., 2016). Systems with maltodextrin of low DE usually form mixtures with sugars which have higher T_g than pure sugars (Silalai and Roos, 2011).

The presence of water dramatically decreased T_g of anhydrous carbohydrates as a result of water sorption. Water sorption isotherm for each system allows knowing water content during storage at various relative humidities (Blahovec and Yanniotis, 2009; Potes et al., 2012). Measurement of T_g, at a very high water content in the system, is practically complicated, thereby T_g may be obtained from the Gordon-Taylor relationship (Arvanitoyannis et al., 1993).

Dynamic mechanical (DMA) and dielectric (DEA) analyses in a multi-frequency mode are suitable methods to measure α-, β- and γ- relaxation which happens due to molecular mobility below T_g. These methods were applied for analyses of different amorphous carbohydrates at low water contents (Moates et al., 2001; Kilmartin et al., 2004; Ermolina et al., 2007; Silalai and Roos, 2011; Potes et al., 2012). The structural relaxation time of α-relaxation process can be obtained from the frequency of primary α-relaxation (Noel et al., 2000). For systems with high water contents, data of the structural relaxation times may be obtained from volume rheology (Angell, 2002).

Structural strength analysis was successfully applied for various carbohydrate-protein and carbohydrate-carbohydrate models such as trehalose-whey protein isolate (WPI) (Maidannyk and Roos, 2016a; Fan and Roos, 2016a, b), lactose-WPI (Fan and Roos, 2016a, b; Maidannyk and Roos, 2016 b) and lactose-trehalose (Fan and Roos, 2016a), these studies have confirmed that structural strength linearly depends on composition and significantly decreases upon increasing of the water content of the material. However, structural strength analysis including water sorption, glass transition, rheological, mechanical and dielectric properties of miscible carbohydrates systems has not been addressed. The main purpose of the present study was to develop the strength concept, using trehalose-maltodextrin miscible systems. For this, the effect of maltodextrin on structural strength of amorphous trehalose was under investigation. In addition, effects of water content on structural strength of miscible systems were also in focus.

4.3 Materials and Methods

4.3.1 Materials

D-(+)-Trehalose crystalline dihydrate (Hayashibara Co., Ltd., Okayama, Japan) and Maltodextrin (M 100) with DE 9-12 or in average DE 10 (Grain Processing Corporation, IA, USA) were used without purification. De-ionized water was obtained from KB scientific, Cork, Ireland.

4.3.2 Determination of the initial water content

Samples of powders with various ratios of trehalose and maltodextrin (0:100; 20:80; 40:60; 60:40; 80:20 and 100:0 trehalose-maltodextrin systems) with final mass 0.5-1.0 g were dried at 70°C with absolute pressure P_{abs}<10 mbar for 24 hours in a WTB Binder vacuum oven (Mason Technology®, Tuttingen, Germany) to measure the initial water content of the materials. The difference in mass of samples before and after drying was defined as initial water content.

4.3.2 Preparation of amorphous freeze-dried materials

Trehalose and maltodextrin solutions (total solid of 20%) in water were prepared separately. After that, solutions were mixed in required proportions. The ratio of solid components trehalose : maltodextrin were 0:100; 20:80; 40:60; 60:40; 80:20 and 100:0. 5 ml

aliquots of these solutions were frozen in pre-weighted and semi-closed with septum 10 ml glass vials at -20°C for 24 h, then at -80°C for 3 h, followed by freeze-drying for 60 h at pressure p < 0.1 mbar (Lyovac GT2, Steris®, Hürth, Germany) to obtain amorphous materials. All vials were hermetically sealed under the vacuum conditions inside the freeze dryer at p < 0.1 mbar and stored over P_2O_5 in vacuum desiccators (Roos and Karel, 1990) at room temperature (25 ± 1°C) to protect samples from water uptake.

4.3.3 Water sorption analysis

Freeze-dried and closed under vacuum conditions samples with various ratios of trehalose and maltodextrin (described above) were stored in desiccators over P_2O_5. Each system was stored at an evacuated desiccator (25±1°C) for 10 days over the saturated solutions of LiCl, CH_3COOK, $MgCl_2$, K_2CO_3, $Mg(NO_3)_2$, $NaNO_2$, NaCl and KCl (Sigma Chemical Co., St. Louise, MO. U.S.A.), which at equilibrium provided 0.11, 0.23, 0.33, 0.44, 0.545, 0.66, 0.76 and 0.85 a_w, respectively. AQUALAB 4 (TE) (Decagon Devices Inc., NE) water activity meter was used to measure water activity for each material after storage. Samples were weighted at intervals of 0, 2, 4, 6, 8, 10, 24, 48, 72, 96, 120 and 144 hours (up to 192 hours for 0:100 trehalose:maltodextrin system) upon storage. Possible crystallization of trehalose was assessed from the loss of sorbed water. The water content in each mixture was plotted as a function of time, and the Guggenheim-Anderson-deBoer (GAB) relationship was fitted to data to know water activity-water content dependence of amorphous trehalose-maltodextrin systems (Eq. 2). The fractional water sorption method, shown by Potes et al. (Potes, 2014) allows calculation of fractional water content of material, stored at high water activities (Eq. 3).

4.3.4 Differential Scanning Calorimetry (DSC)

Differential scanning calorimeter (DSC) (Mettler Toledo Schwerzenbach, Switzerland) was used to measure the glass transition temperature of amorphous trehalose-maltodextrin mixtures with 0, 0.11, 0.23, 0.33 and 0.44 a_w. Samples of all mixtures were transferred to pre-weighted standard DSC aluminium pans (40 μL, Mettler Toledo Schwerzenbach, Switzerland) and hermetically sealed. An empty punctured pan was used as a reference. For anhydrous systems only, the lids of DSC aluminium pans were punctured to allow evaporation of residual water upon the measurement. All samples were scanned from ~ 30°C below to over T_g region with 5°C/min heating rate and cooled at 10°C/min to initial

temperature. Then, second heating scan was run to well above (>50°C) the T_g at 5°C/min heating rate. The onset of T_g was determined by the STAR^e software version 8.10 (Mettler Toledo Schwerzenbach, Switzerland). The Gordon-Taylor equation (Eq. 4) was used to estimate T_g for high water content systems (60, 70, 80 and 80% of water).

4.3.5 Dynamical Mechanical Analyses (DMA)

Dynamic mechanical analyzer (DMA) (Tritec 2000 DMA, Triton Technology Ltd., UK) was used to measure mechanical properties (E'' – loss modulus, E' – storage modulus and tanδ = E''/E') of anhydrous and humidified trehalose-maltodextrin systems (described above for the DSC experiments). The DMA instrument was balanced or set at zero to determine the zero displacement position before starting. Approximately 60 g of grinded samples were spread on a metal pocket-forming a sheet (Triton Technology Ltd., UK). This sandwich sheet was fixed between the stationary and drive shaft clamps inside the measuring head of the DMA. Length, width and thickness were measured for each sample. All results were obtained using 1.43.00 DMA software version. To control temperature the DMA was connected to a liquid nitrogen tank (1l; Cryogun, Brymill Cryogenic Systems, Labquip Ltd., Dublin, Ireland). Samples were scanned from ~ 50°C below to over the α-relaxation region with cooling rate of 5°C/min and heating rate of 2°C/min using the single cantilever bending mode (Potes et al., 2012; Fan and Roos, 2016a, b; Maidannyk and Roos, 2016). The α-relaxation temperatures (T_α) were determined from peak of tangent δ above the glass transition.

4.3.6 Dielectric analysis (DEA)

Samples (described above for DSC and DMA experiments) of each material were analyzed by dielectric spectrometer, DEA (DS6000, Triton Technology Ltd., UK) with titanium sample holders as the electrodes. The LCR meter (LCR-819) and the DEA instrument were calibrated at frequency 0.103 kHz with open-short circuit of the electrodes and zeroed in bridge RQ on a regular basis at 1 kHz with open-short circuit of the electrodes to ensure that the electrodes were ready to use (resistance value < 2 Ω). Approximately 100 mg of grinded samples were transferred onto the lower cup electrode (40 mm diameter) and then pressed with the upper electrode (33 mm diameter). Two electrodes were placed into a dielectric cell. The thickness (< 2 mm) was measured for each sample. The DEA was connected to a liquid nitrogen tank (1l; Cryogun, Brymill Cryogenic Systems, Labquip Ltd.,

Dublin, Ireland). Samples were scanned from ~ 50°C below to over the α-relaxation region with cooling rate of 5°C/min and heating rate of 2°C/min at frequencies of 0.012 – 20 kHz (Silalai and Roos, 2011; Potes et al., 2012). The T_α was determined from the peak temperature above T_g of dielectric loss (ε''). All results were obtained by Triton Laboratory DEA software, version 1.0.330.

Equation 5 was used to calculate the relaxation times (τ) of peak T_α, measured by DMA and DEA at various frequencies (f) (Noel et al., 2000; Potes et al., 2012).

4.3.7 Rheology

Trehalose and maltodextrin were separately dissolved in water (considering the initial water contents in the powders) and mixed together at ratios 100:0, 80:20, 60:40, 40:60, 20:80 and 0:100 after 1 hour. The total contents of water were 60, 70, 80 and 90%. Rheometer ARES-G2 (TA Instruments®, USA) with aluminum "plane-plane" (40 mm) geometry was used to determine apparent viscosities of solutions. The shear rate 100 s was constant for all measurements. The temperature range was 0 - 80°C. The Maxwell relation (Eq. 15) was used (Angell, 2002) to convert the apparent viscosity (η) data into shear relaxation times (τ_s).

4.3.8 Calculation of WLF model constants and Structural strength parameter

To calculate the structural strength parameter, the constants C_1 and C_2 from Williams Landel Ferry (WLF) equation were obtaining as described by Roos and Drusch (Roos and Drusch, 2015).

The WLF equation in the form of (Eq. 10) was used to fit DMA, DEA and rheometry data (Williams et al., 1955). The WLF equation in the form of (Eq. 11) suggested that the plot of $1/lg(\tau/\tau_s)$ versus $1/(T-T_g)$ gives a linear correlation. The WLF constants C_1 and C_2 were derived from the slope and intercept of the straight line (Roos and Drusch, 2015). Mathematically, strength is based on WLF relationship and can be calculated by Equation (16). Equation 17 was used to predict the strength (S) at different water contents.

4.3.9 Data analysis

All experiments were performed in triplicate. Mean data of the water sorption analyses, DSC, DMA, DEA and rheometry were calculated from 3 replicates with standard deviations expressed in error bars.

4.4 Results and discussion

4.4.1 Fractional water sorption analysis

Experimental water contents of freeze-dried trehalose-maltodextrin systems, over the whole range of water activities at 25±1°C are shown in Table 4.1 and Figure 4.1.

Table 4.1. Water content of freeze-dried trehalose-maltodextrin systems (ratios of components 100:0, 80:20, 60:40, 40:60, 20:80, 0:100) stored at different water activities (0.11, 0.23, 0.33, 0.44, 0.55, 0.65, 0.76, 0.85) for 144 hours (192 hours for 0:100 system) at 25±1°C.

a_w	Experimental water content for trehalose:maltodextrin systems (g/100 g of solids)					
	100:0	**80:20**	**60:40**	**40:60**	**20:80**	**0:100**
0.11	2.2±0.1	2.7±0.2	2.9±0.2	3.3±0.2	3.7±0.1	4.1±0.1
0.23	4.1±0.4	4.6±0.2	5.1±0.3	5.6±0.2	6.1±0.3	6.6±0.1
0.33	5.9±0.4	6.2±0.1	6.7±0.1	7.1±0.3	7.5±0.4	7.8±0.1
0.44	9.0±0.2	8.3±0.3	8.7±0.3	8.9±0.5	9.1±0.2	9.3±0.2
0.55	9.5±0.1	11.2±0.1	11.1±0.2	11.1±0.7	11.1±0.6	11.2±0.2
0.65	9.4±0.3	14.4±0.1	14.0±0.3	13.6±0.2	13.1±0.2	12.6±0.2
0.76	8.8±0.4	19.6±0.2	16.7±0.5	17.6±0.5	16.5±0.6	15.5±0.2
0.85	9.5±0.4	26.9±0.2	19.9±0.9	18.8±0.3	23.4±1.0	22.1±0.2

Steady-state water contents of each mixture at 144 hours (except for the pure maltodextrin system, which was measured over 192 hours) were used in GAB model. The GAB model was fitted to experimental data of 100:0 trehalose-maltodextrin system below $0.55a_w$ (Labuza, 1984; Maidannyk and Roos, 2016). However, at higher water activities ($\geq 0.55\ a_w$), the crystallization of trehalose, shown by release of sorbed water (Fig. 4.1, a), occurred and extrapolated sorption data from GAB relationship give misleading results for sorbed water contents (Potes et al., 2012). Fractional water sorption analysis (Eq. 3) allows calculating water content at high water activities.

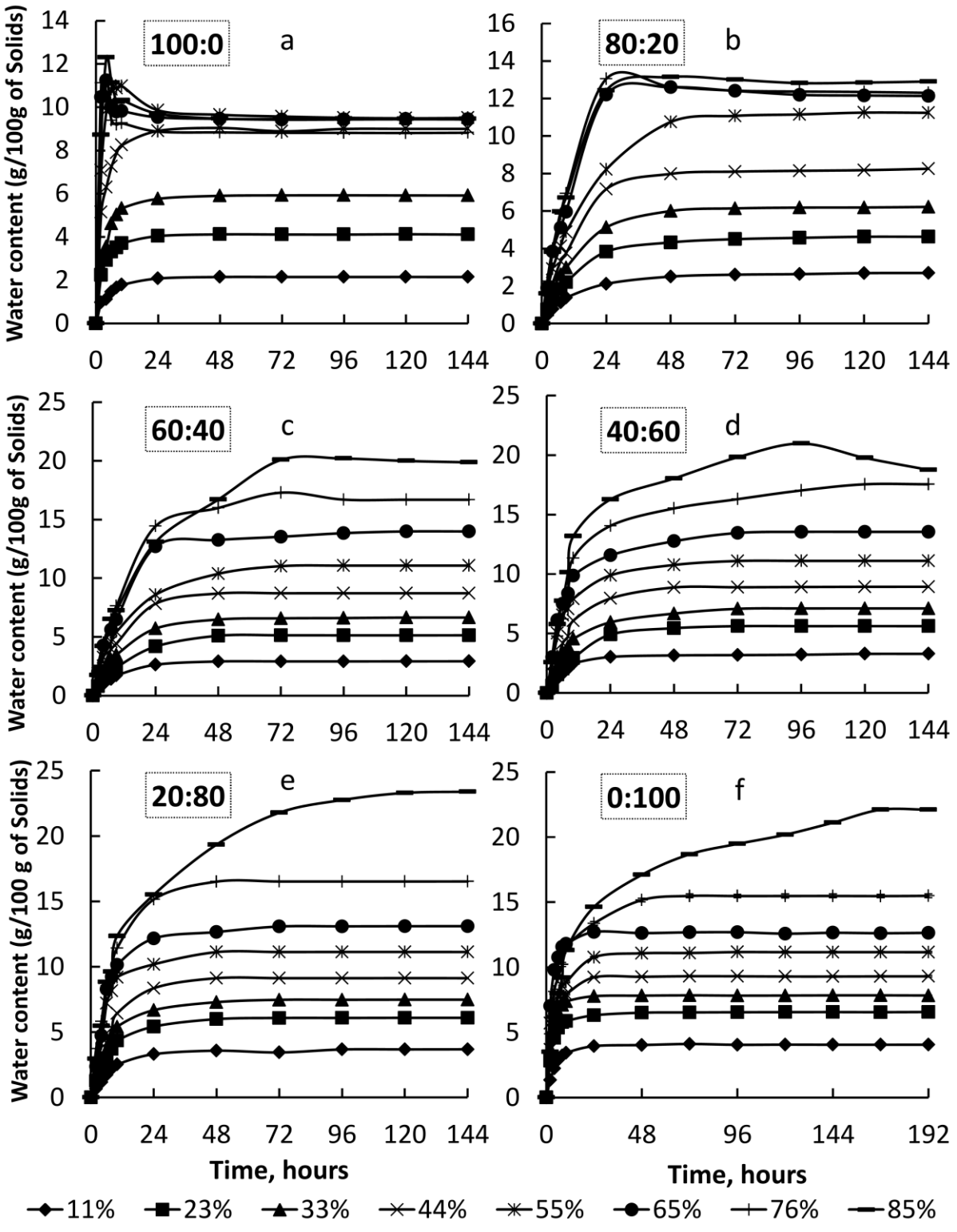

Figure 4.1. Sorption kinetics profiles for freeze-dried trehalose-maltodextrin mixtures 100:0 (a), 80:20 (b), 60:40 (c), 40:60 (d), 20:80 (e) and 0:100 (f),stored at 0.11, 0.23, 0.33, 0.44, 0.55, 0.65, 0.76 and 0.85 a_w, monitored during 144 (192 hours for 0:100 system) hours at 25±1°C.

In the present study, fractional water contents were derived from experimental water sorption data of trehalose-maltodextrin 20:80 and 0:100 systems, which showed *no crystallization* even at 0.85 a_w (Fig. 4.1, e, f). This calculated fractional water contents are in agreement with experimental data at 0.11-0.44 a_w for 100:0; at 0.11-0.545 a_w for 80:20; at 0.11-0.65 a_w for 60:40; at 0.11-0.76 a_w for 40:60 trehalose-maltodextrin systems. Using fractional and experimental data of water content, the GAB model was fitted to obtain sorption isotherms at high water activities (Figure 4.2).

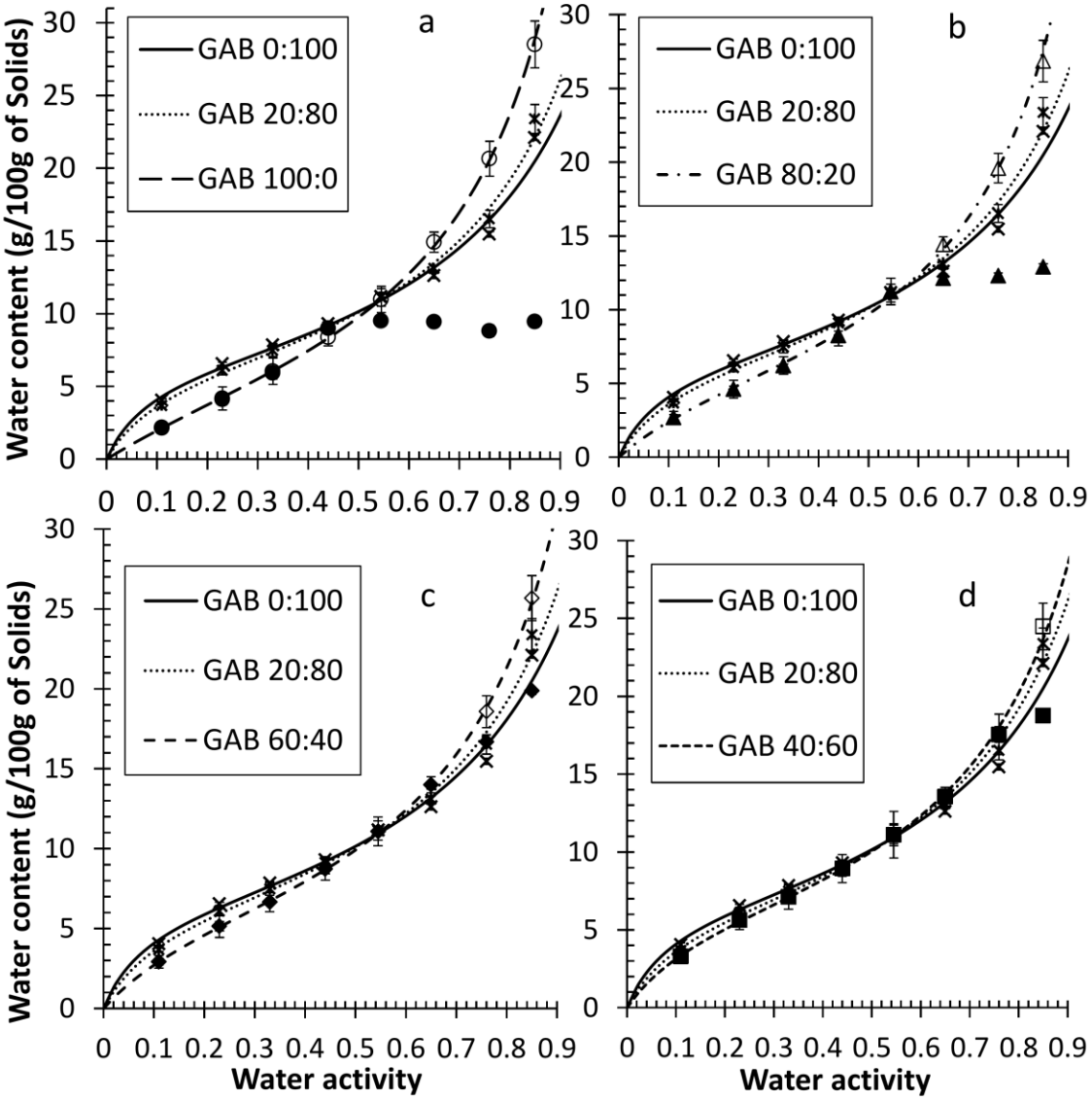

Figure 4.2. The GAB sorption isotherms at 25±1°C (lines), experimental data (solid symbols) and calculated water contents (clear symbols) for amorphous trehalose-maltodextrin system with component ratios 100:0 (a); 80:20 (b); 60:40 (c) and 40:60 (d) compared to experimental data for trehalose-maltodextrin 20:80 and 100:0 systems.

4.4.2 Glass transition temperature

The onset of calorimetric glass transition temperature (T_g) obtained from second heating scan of amorphous (0 – 0.44 a_w) trehalose-maltodextrin systems is presented in Table 4.2.

Table 4.2. The onset of calorimetric glass transition temperatures (T_g) of anhydrous (0 a_w) and humidified (0.11-0.44 a_w) trehalose-maltodextrin systems stored for 144 hours at 25±1°C.

a_w	Glass transition temperatures (T_g) of trehalose-maltodextrin (w/w) systems, °C					
	100:0	**80:20**	**60:40**	**40:60**	**20:80**	**0:100**
0	112±1	120±1	126±1	131±1	139±6	149±3
0.11	62±2	64±1	64±2	70±2	85±1	95±1
0.23	43±2	44±3	44±1	46±2	57±1	75±2
0.33	32±1	33±1	33±2	37±1	42±2	64±3
0.44	15±1	19±3	21±4	31±4	38±1	51±2

At all experimental a_w, T_g increases with increasing concentration of maltodextrin in a system. The measurement of the T_g is a common method which often is used to determine the *miscibility* of components. Miscible mixtures have T_g between the two T_g values of components and broadening of the transition is observed as the components become more immiscible (Krause, 1986; Kalichevsky and Blanshard, 1992; Silalai and Roos, 2011). Increasing the T_g of trehalose-maltodextrin systems with increasing maltodextrin content can be explained by its higher molecular weight (Roos and Karel, 1991a; Buera et al., 1992; Bhandari et al., 1997; Bhandari and Howes, 1999; Avaltroni et al., 2004; Silalai and Roos, 2011).

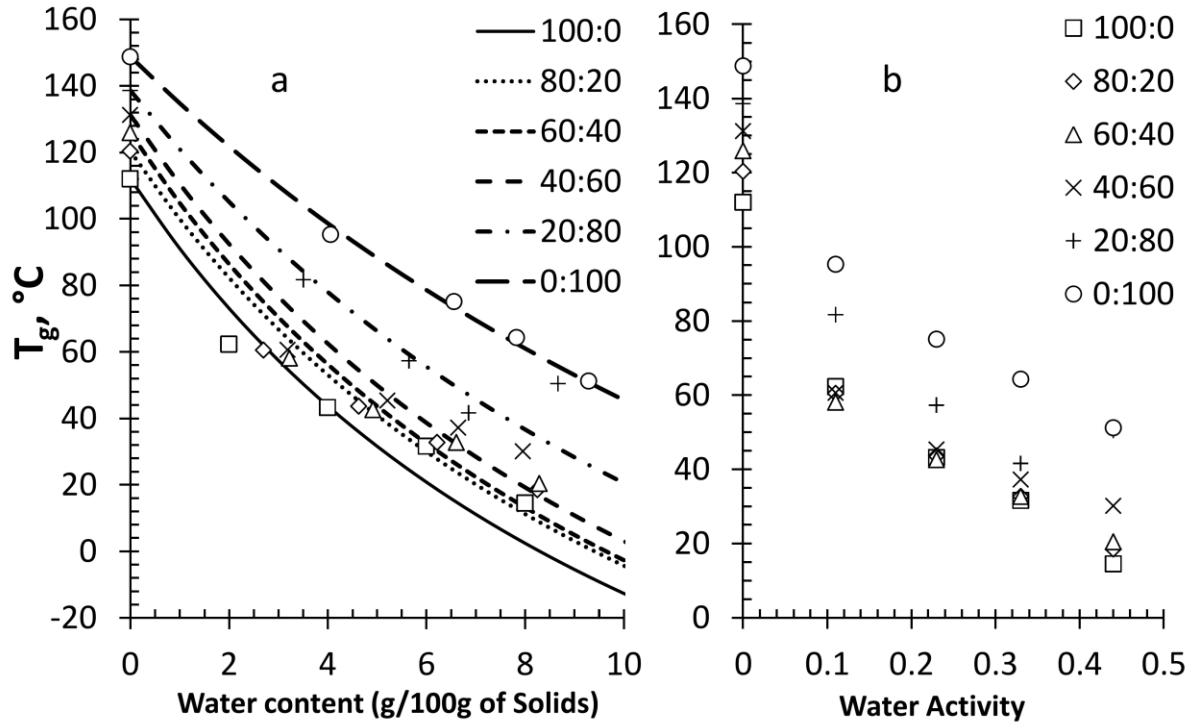

Figure 4.3. Dependence of the glass transition temperatures (T_g) on water content and water activity of freeze-dried trehalose-maltodextrin systems. Lines correspond to the T_g predicted by the Gordon-Taylor equation.

The presence of water often enhances miscibility by diluting polymer interactions (Krause, 1986; Silalai and Roos, 2011). Water sorption isotherms (Figure 4.2) showed that trehalose-maltodextrin systems with different ratios of components have different water contents and T_g at the same a_w (Figure 4.3, b). This indicated that trehalose-maltodextrin systems were plasticized by water resulting in the decrease of the T_g (Levine and Slade, 1986; Roos and Karel, 1991b; Silalai and Roos, 2011) (Figure 3). Water has similar effects on milk powders and other carbohydrates mixtures with maltodextrin (Jouppila et al., 1997; Haque and Roos, 2004; Silalai and Roos, 2011). Humidified systems with high amounts of maltodextrins showed significant increase in T_g due to high miscibility of the carbohydrates.

4.4.3 Rheology

Rheological behavior of aqueous trehalose-maltodextrin solutions (60, 70, 80 and 90% of water) over the temperature range 0-80°C was tested and results are presented in Figure 4.4. As expected, the apparent viscosity decreases with increasing temperature (Dokic et al., 1998; Longinotti and Corti, 2008). Maltodextrins have higher apparent viscosity than

trehalose due to longer linear maltodextrin chains. Therefore systems with high amounts of maltodextrins showed higher apparent viscosity values. For each trehalose-maltodextrin system, apparent viscosity increases with increasing solids concentration in water solutions.

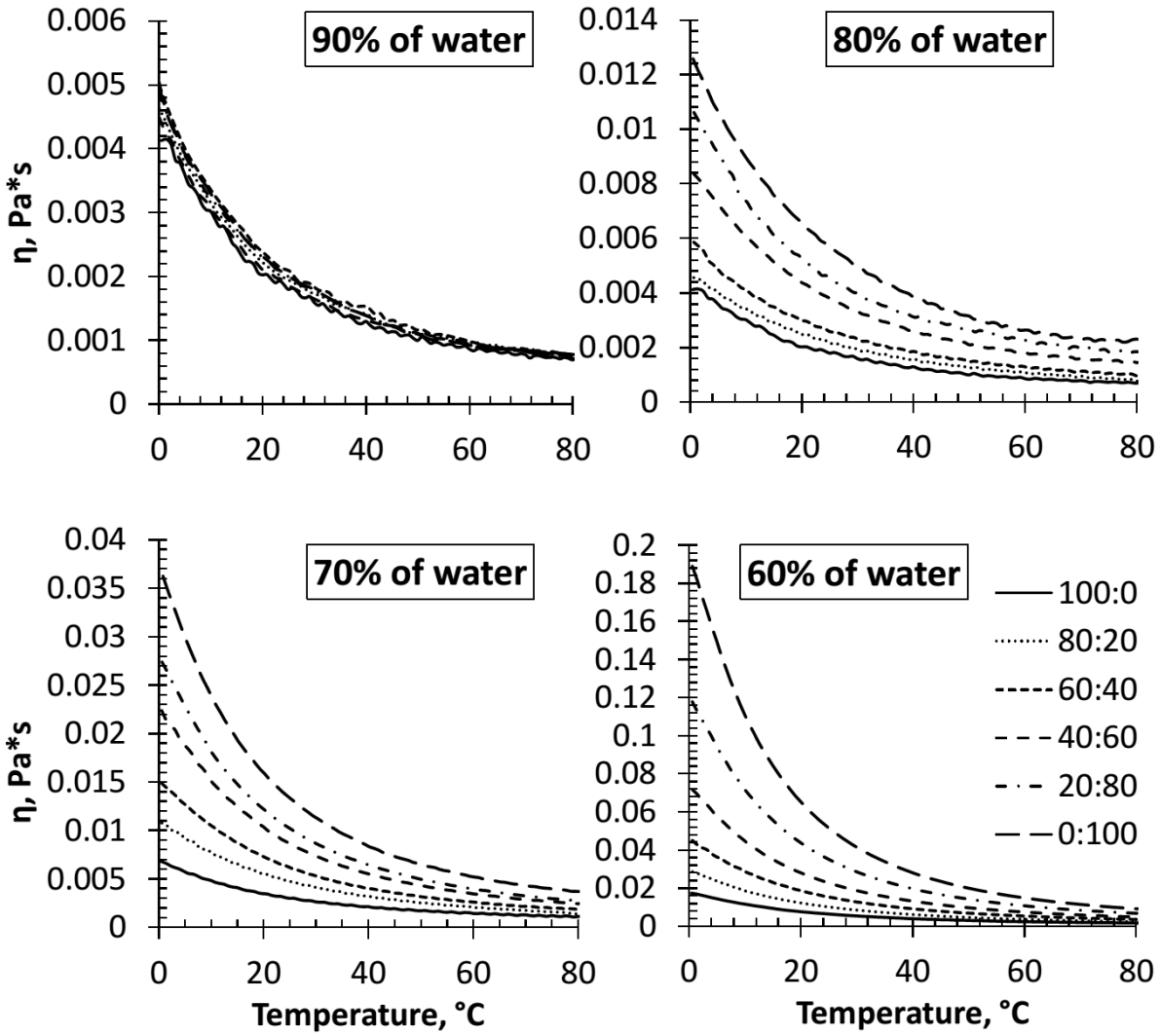

Figure 4.4. Temperature dependence of the apparent viscosity of aqueous (90, 80, 70 and 60% of water) trehalose-maltodextrin (100:0; 80:20; 60:40; 40:60; 20:80; 0:100) systems.

For aqueous solutions T_g was calculated using Gordon-Taylor equation (Eq. 4, Figure 4.3). The glass transition temperature of pure water (-135°C) (Angell, 2002) and experimental DSC data (Table 4.2) were used in calculations (Table 4.3). The Gordon-Taylor model was well fitted to experimental data, the constant *k* was 8.1±1.0 for 100:0 system, 8.5±0.8 for 80:20, 8.7±0.4 for 60:40, 8.4±0.6 for 40:60, 6.8±0.6 for 20:80 and 5.2±0.7 for 0:100 trehalose-maltodextrin system.

Table 4.3. Glass transition temperatures (T_g) calculated by Gordon-Taylor equation for 100:0, 80:20, 60:40, 40:60, 20:80 and 0:100 trehalose-maltodextrin systems with high water contents (60, 70, 80, 90% of water).

Water content, %	**Calculated glass transition temperature, (T_g) of trehalose-maltodextrin (w/w) systems, °C**					
	100:0	**80:20**	**60:40**	**40:60**	**20:80**	**0:100**
60	-118±1	-117±1	-117±2	-115±1	-111±1	-103±1
70	-124±2	-123±1	-123±1	-122±1	-119±1	-113±1
80	-128±1	-128±1	-128±1	-127±1	-125±1	-122±1
90	-132±1	-132±1	-132±1	-131±0	-130±2	-129±1

4.4.4 Dynamic-mechanical and dielectric properties

At temperatures around glass transition temperature significant changes in physical properties of materials occur, which also result in structural α-relaxations (Champion et al., 2000; Roudaut et al., 2004). This α-relaxation temperature T_α of amorphous anhydrous and humidified (0 – 0.44 a_w) trehalose-maltodextrin systems (100:0; 80:20; 60:40; 40:60; 20:80; 0:100) was obtained from the peak temperature of dielectric loss (ε'') and dynamic tan δ (tan δ = E''/E', where E'' – loss modulus (mechanical energy dissipation), E' – storage modulus (mechanical energy storage)) of dielectric and dynamic mechanical analyses (Fan and Roos, 2016a; Maidannyk and Roos, 2016; Potes et al., 2012; Silalai and Roos, 2011).

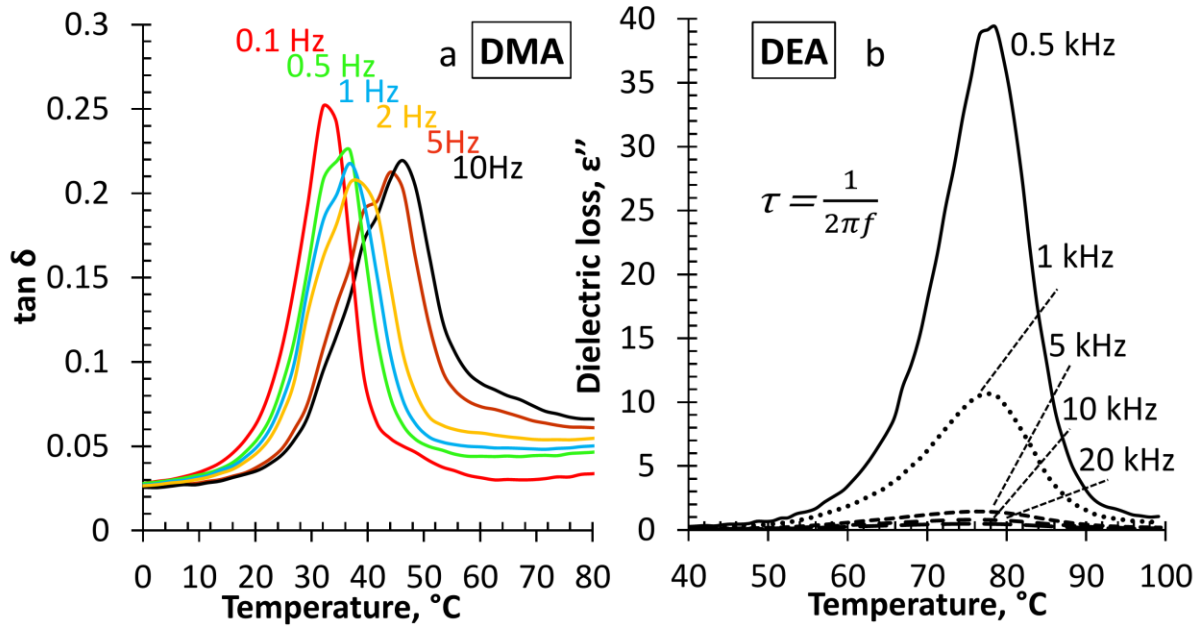

Figure. 4.5. (a) Temperature dependence of dynamic tangents δ for humidified (0.44 a_w) 80:20 trehalose-maltodextrin system determined by DMA in multi-frequency mode (0.1, 0.5, 1, 5, 10 Hz). (b) Temperature dependence of dielectric loss for humidified (0.44 a_w) 80:20 trehalose-maltodextrin system determined by DEA in multi-frequency (0.5, 1, 5, 10, 20 kHz).

Typical thermograms, obtained by DMA and DEA are presented in Fig. 4.5. Peak of α-relaxation occurred at ~20-30°C above the onset T_g and up to~60-70°C above the onset T_g for DEA measurements. High maltodextrin content systems showed broadened DMA and DEA peaks with less intensity. α-relaxation temperature for these systems was higher than for systems with low amounts of maltodextrins, probably because of complex composition of maltodextrin component molecules which can reduce molecular mobility of trehalose due to high degree of association (Silalai and Roos, 2011) (Table 4.4).

Both DMA and DEA spectra are frequency-dependent. Knowing frequency of each experiment and using equation 5, we obtained the relaxation time – temperature dependence for amorphous trehalose-maltodextrin systems.

Presence of water in the system significantly affects the value of T_α (Table 4.4), the similar result was observed before (Silalai and Roos, 2011; Potes et al., 2012; Fan and Roos, 2016a). For example, the T_α for 40:60 (at f = *100*Hz) trehalose-maltodextrin system decreased from 189.1°C at RH 0% to 72.1°C at RH 44%. Free-volume theory can explain these changes in the systems, by increasing of free volume and molecular mobility of

amorphous sugar in the system (Slade et al., 1991 ; Royall et al., 2005; Meinders and van Vliet, 2009).

Table 4.4. α-relaxation temperature (T_α) detected by DMA (0.1-10 Hz) and DEA (100.0-20000.0 Hz) for trehalose-maltodextrin mixtures equilibrated at different relative humidities (RH).

	RH 0%	**Trehalose-Maltodextrin systems**					
		100:0	**80:20**	**60:40**	**40:60**	**20:80**	**0:100**
f, Hz	**logτ, s**	**T_α, °C**	**T_α, °C**	**T_α, °C**	**T_α, °C**	**T_α, °C**	**T_α, °C**
0.1	**0.20**	123±3	131±1	143±3	158 ±2	181±1	208±3
0.5	**-0.49**	125±1	133±2	145±1	160±1	186±2	210±3
1.0	**-0.80**	127±2	135±2	149±2	163±2	188±2	215±3
2.0	**-1.10**	127±1	138±1	152±2	165±1	190±2	216±2
5.0	**-1.50**	128±1	140±2	154±2	169±2	193±2	217±2
10.0	**-1.80**	129±1	142±2	156±1	172±2	202±2	218±3
100.0	**-2.80**	-	-	-	189±2	206±2	220±2
500.0	**-3.50**	-	-	-	194±2	207±3	222±2
	RH 11%	**Trehalose-Maltodextrin systems**					
		100:0	**80:20**	**60:40**	**40:60**	**20:80**	**0:100**
f, Hz	**logτ, s**	**T_α, °C**	**T_α, °C**	**T_α, °C**	**T_α, °C**	**T_α, °C**	**T_α, °C**
0.1	**0.20**	71±1	73±1	76±3	88±1	108±2	127±1
0.5	**-0.49**	72±1	74±2	77±1	89±1	109±2	129±1
1.0	**-0.80**	72±2	76±2	79±2	89±1	113±2	129±1
2.0	**-1.10**	74±2	78±1	82±2	90±2	115±1	130±2
5.0	**-1.50**	77±2	79±2	82±2	93±2	116±1	131±2
10.0	**-1.80**	78±1	82±1	84±1	96±2	120±2	132±1
100.0	**-2.80**	80±1	84±1	85±1	97±1	120±2	134±2
500.0	**-3.50**	81±1	86±1	87±1	98±1	123±3	146±3
1000.0	**-3.80**	81±1	87±2	89±2	101±3	125±2	149±3
5000.0	**-4.50**	82±1	88±2	90±2	103±3	125±2	-
10000.0	**-4.80**	83±1	89±2	92±2	106±3	128±3	-
20000.0	**-5.10**	83±2	91±2	93±2	109±3	129±3	-
	RH 23%	**Trehalose-Maltodextrin systems**					
		100:0	**80:20**	**60:40**	**40:60**	**20:80**	**0:100**
f, Hz	**logτ, s**	**T_α, °C**	**T_α, °C**	**T_α, °C**	**T_α, °C**	**T_α, °C**	**T_α, °C**
0.1	**0.20**	50±1	53±2	51±2	58±1	78±1	96±2
0.5	**-0.49**	53±1	53±2	53±2	64±2	80±1	103±3
1.0	**-0.80**	53±1	56±2	56±2	65±2	82±2	110±2
2.0	**-1.10**	55±1	58±1	60±2	66±2	83±1	114±2
5.0	**-1.50**	55±1	59±2	62±2	69±2	86±2	116±2
10.0	**-1.80**	56±2	60±2	64±2	71±2	88±1	118±2
100.0	**-2.80**	57±2	61±2	69±2	78±1	90±2	122±3
500.0	**-3.50**	58±2	61±1	70±2	78±1	92±2	125±2
1000.0	**-3.80**	58±2	62±1	72±2	80±2	95±1	127±3
5000.0	**-4.50**	59±2	-	73±1	81±2	97±2	129±2
10000.0	**-4.80**	60±3	-	75±2	81±2	99±3	130±3
20000.0	**-5.10**	60±3	-	76±3	83±2	100±4	132±4

RH 33%		Trehalose-Maltodextrin systems					
		100:0	80:20	60:40	40:60	20:80	0:100
f, Hz	logτ, s	T_{α}, °C	T_{α}, °C	T_{α}, °C	T_{α}, °C	T_{α}, °C	T_{α}, °C
0.1	**0.20**	38±3	40±2	44±2	54±2	61±2	87±2
0.5	**-0.49**	40±2	41±1	45±2	56±2	63±1	90±2
1.0	**-0.80**	41±2	42±1	46±2	57±2	65±2	92±3
2.0	**-1.10**	42±1	45±1	46±2	58±2	66±3	94±2
5.0	**-1.50**	43±2	47±2	49±1	59±3	66±3	98±3
10.0	**-1.80**	44±1	49±2	50±2	61±3	67±2	101±2
100.0	**-2.80**	45±1	50±2	52±3	64±3	70±2	102±2
500.0	**-3.50**	46±2	50±3	53±3	66±3	72±3	103±2
1000.0	**-3.80**	46±2	51±3	56±3	69±3	73±3	105±2
5000.0	**-4.50**	47±3	52±2	58±2	69±2	74±3	107±2
10000.0	**-4.80**	47±3	53±3	59±2	70±3	74±3	108±4
20000.0	**-5.10**	48±3	55±3	59±2	70±3	76±3	110±3
RH 44%		**Trehalose-Maltodextrin systems**					
		100:0	**80:20**	**60:40**	**40:60**	**20:80**	**0:100**
f, Hz	**logτ, s**	**T_{α}, °C**	**T_{α}, °C**	**T_{α}, °C**	**T_{α}, °C**	**T_{α}, °C**	**T_{α}, °C**
0.1	**0.20**	18±1	23±1	26±1	47±2	62±2	62±1
0.5	**-0.49**	19±1	24±1	28±1	49±1	64±2	65±3
1.0	**-0.80**	20±2	26±2	29±1	51±1	64±2	67±1
2.0	**-1.10**	20±2	29±3	31±2	54±2	65±3	69±2
5.0	**-1.50**	22±2	33±3	35±2	55±2	65±2	71±2
10.0	**-1.80**	24±3	33±1	38±3	56±3	66±1	73±3
100.0	**-2.80**	25±2	36±1	39±3	72±1	75±2	75±3
500.0	**-3.50**	26±3	37±2	41±3	73±1	76±2	77±3
1000.0	**-3.80**	27±3	38±3	43±3	75±3	77±3	78±1
5000.0	**-4.50**	28±3	39±3	46±2	76±2	77±3	80±2
10000.0	**-4.80**	29±3	41±3	48±2	78±2	78±3	80±2
20000.0	**-5.10**	29±2	42±3	53±3	78±2	79±3	81±2

4.4.4 WLF modeling and Strength

The Williams-Landel-Ferry or WLF equation with "non-universal" constants C_1 and C_2 is a suitable model for describing relaxation time – temperature dependence of glass formers close to the onset T_g (Peleg, 1992; Harnkarnsujarit et al., 2012; Roos, 2013; Roos and Drusch, 2015). In calculations, the viscosity and relaxation time of supercooled liquid approached 10^{12} Pa s and 100 s respectively. Upon heating, values of viscosity and relaxation time are decreasing down to 10^{5} Pa s and 10^{-14} s (Angell, 1991; Angell et al., 2000; Roos, 2013; Roos and Drusch, 2015; Maidannyk and Roos, 2016). The Equation 11 was used to calculate the WLF constants C_1 and C_2 for amorphous (0 – 44% RH) and high water content systems (60, 70, 80 and 90% of water) (Table 5, 6).

Table 4.5. Calculated WLF constants C_1 and C_2 for amorphous trehalose-maltodextrin systems stored at various relative humidities (RH).

Trehalose-MD 100	RH 0%		RH 11%		RH 23%		RH 33%		RH 44%	
	$-C_1$, s	$-C_2$, °C	$-C_1$, s	$-C_2$, °C	$-C_1$, s	$-C_2$, °C	$-C_1$, s	$-C_2$, °C	$-C_1$, s	$-C_2$, °C
100:0	3.9±0.2	34.7±0.4	13.0±0.4	62.2±2.1	7.7±0.3	36.7±0.5	8.7±0.6	37.6±0.2	-16.2±0.3	-28.0±0.4
80:20	4.2±0.3	45.8±0.7	10.1±0.5	58.2±0.3	8.6±0.3	49.7±0.5	8.7±0.6	75.7±0.5	-19.8±0.3	-43.5±0.5
60:40	18.5±0.2	176.3±0.8	7.5±0.4	56.2±0.9	56.2±0.4	278.8±0.3	18.0±0.3	57.4±0.6	-16.0±0.2	-40.2±0.3
40:60	19.8±0.3	272.0±2.8	5.1±0.3	60.0±1.3	17.0±0.3	134.0±0.7	8.9±0.2	43.3±0.9	-11.3±0.3	-30.4±0.4
20:80	4.2±0.3	132.7±3.4	4.3±0.2	71.6±0.7	7.7±0.3	101.9±2.3	3.1±0.2	44.3±1.2	12.3±0.6	77.1±0.7
0:100	1.5±0.1	99.8±0.2	3.8±0.4	83.8±0.9	11.4±0.2	160.7±0.7	4.0±0.3	69.7±0.5	11.4±0.5	80.4±0.5

Table 4.6. Calculated WLF constants C_1 and C_2 for high water content (60, 70, 80 and 90% of water) trehalose-maltodextrin systems.

Trehalose-MD 100	90% of water		80% of water		70% of water		60% of water	
	C_1, s	C_2, °C	C_1, s	C_2, °C	C_1, s	C_2, °C	C_1, s	C_2, °C
100:0	16.5±0.6	20.0±0.7	16.7±0.3	20.2±0.5	16.6±0.3	22.2±0.4	16.6±0.4	26.3±0.5
80:20	16.5±0.8	19.4±0.9	16.8±0.6	22.3±0.7	16.5±0.8	21.9±0.9	16.6±0.4	27.4±0.5
60:40	16.5±0.8	19.6±0.8	16.8±0.5	22.9±0.7	16.5±0.5	23.3±0.6	16.6±0.9	28.0±0.9
40:60	16.3±0.3	20.3±0.6	17.0±0.3	23.7±0.4	16.4±0.5	24.8±0.6	16.3±0.5	28.6±0.5
20:80	16.3±0.4	20.6±0.5	17.0±0.6	24.2±0.6	16.4±0.4	25.0±0.5	16.5±0.6	29.5±0.6
0:100	15.3±0.7	20.8±0.8	16.0±0.5	24.2±0.6	16.4±0.4	25.1±0.5	16.4±0.7	30.0±0.8

The "fragility" concept presented by Angell classified glass-formers to "fragile" and "strong" materials and it may predict some properties only for materials with the same T_g (Angell, 2002). However, this model does not give suitable results for real complex food systems (Roos, 2013). The structural strength parameter, proposed by Roos and co-workers (Roos et al., 2015; Fan and Roos, 2016a; Maidannyk and Roos, 2016), describes solid flow characteristics of amorphous materials based on the temperature dependence of structural relaxation times in a food system. Figure 6 shows that for systems with differences in water contents, upon heating, critical and large variation in the structural relaxation time occurred between 100 s and 0.01 s (between 2 and -2 in logarithmic scale). The temperature difference, $T-T_g$, at which structural relaxation times exceed time factors critical to characteristics of the materials was defined as "strength" parameter (S) (Eq. 16).

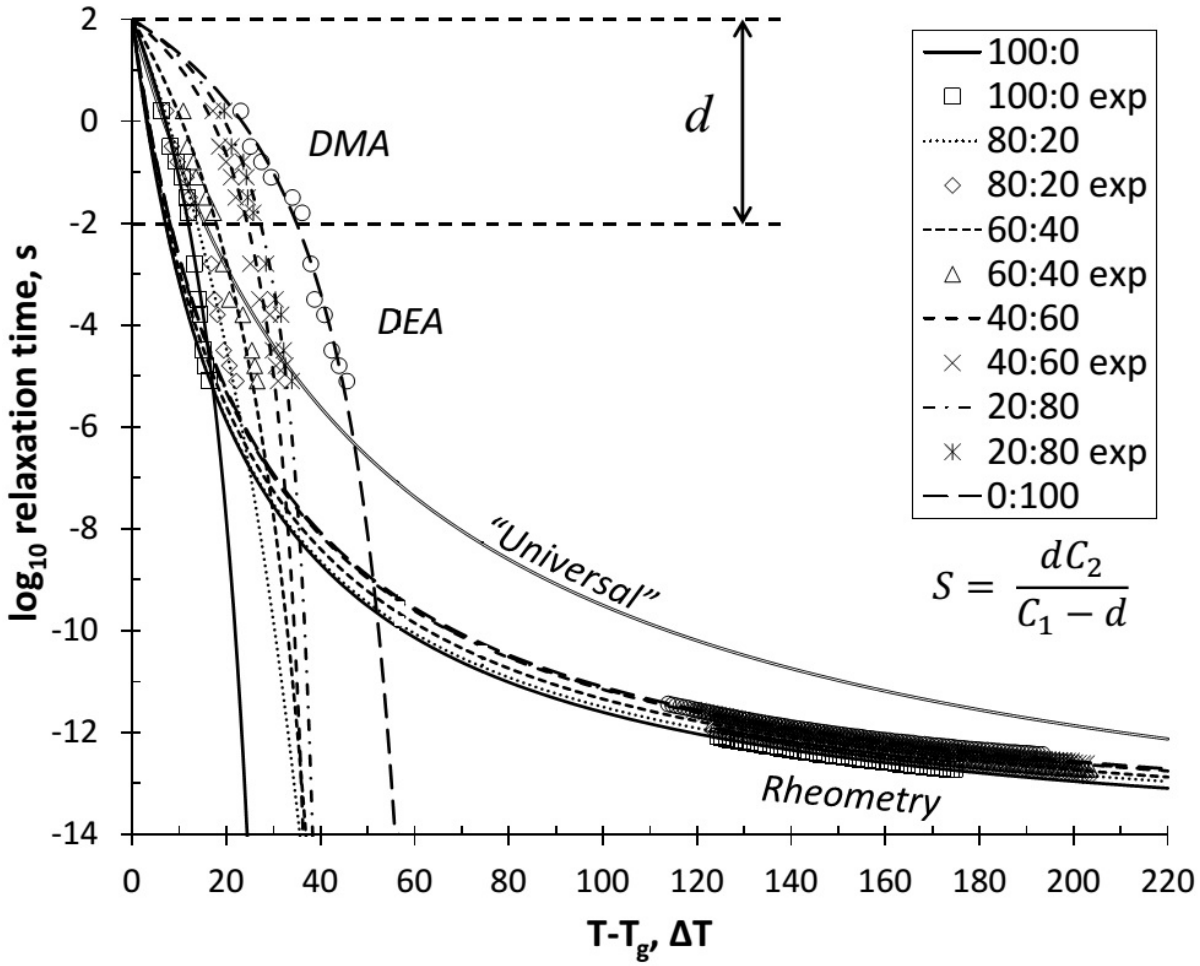

Figure 4.6. Modified WLF curves with calculated and "universal" constants (lines) and experimental data (symbols) for humidified (RH 33%) and high water content (70% of water) trehalose-maltodextrin systems.

At the same time, *rheological* measurements (Fig. 4.6, 4.7) showed that at high temperature difference (>100 °C) the structural relaxation time decreased very slowly compared to data obtained by DMA and DEA. For example for 80:20 trehalose-maltodextrin system structural relaxation time decreased from -11.9 to -12.4 s in logarithmic scale at temperature differences of 123 to 205 degree. These data provide a *physical limitation of change in structural relaxation time.*

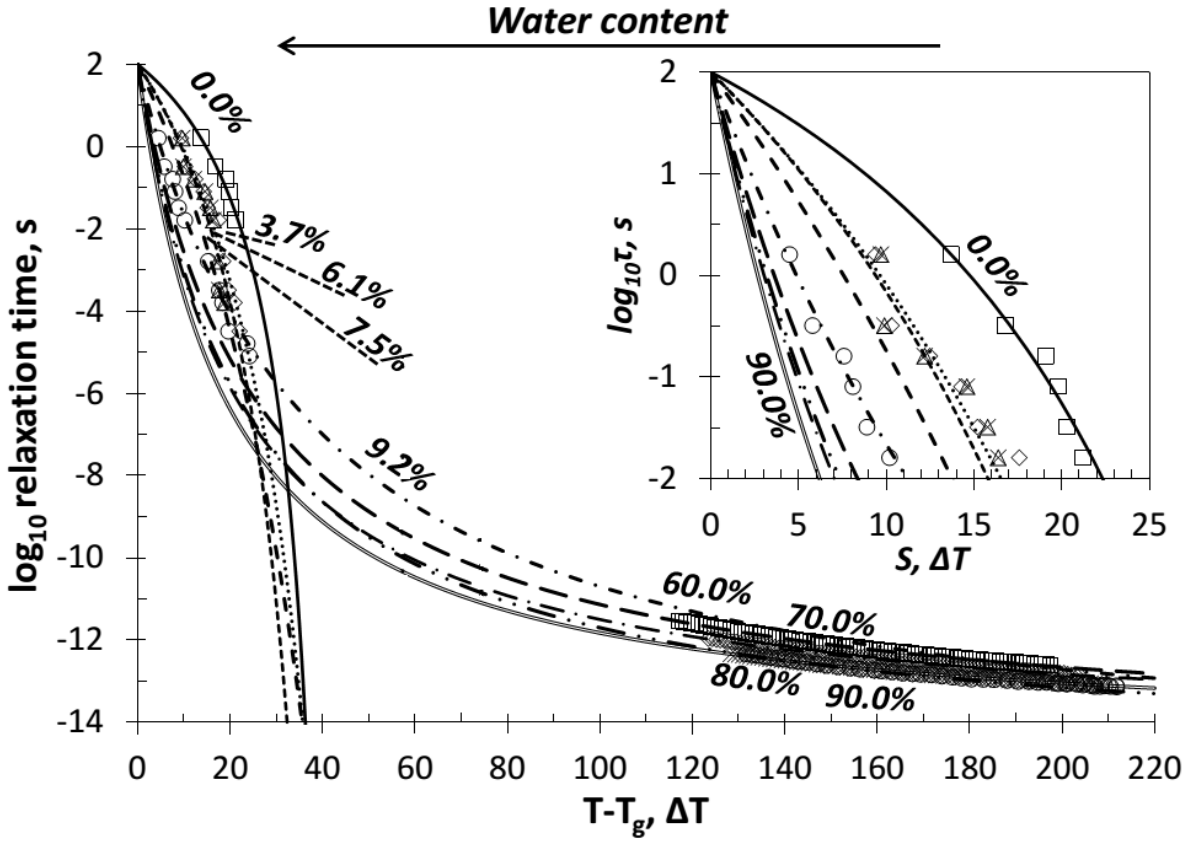

Figure 4.7. Modified WLF curves (lines), experimental data (symbols) and strength plot (inset) for 20:80 trehalose-maltodextrin system with different water contents (g/100 g of dry solids, %).

Table 4.7 summaries the strength data, which were determined for each trehalose-maltodextrin system at different water contents at *d = 4*.

Table 4.7. Strength S (at d = 4) for trehalose-maltodextrin systems at different relative humidities (RH) and water contents.

Trehalose-MD 100	RH 0%	RH11%	RH 23%	RH 33%	RH 44%	60% of water	70% of water	80% of water	90% of water
100:0	17.6±3.1	14.6±2.7	12.6±1.3	11.9±2.0	9.2±2.1	8.4±0.4	7.0±0.4	6.4±0.4	6.2±0.7
80:20	22.3±2.4	16.5±3.2	15.8±1.6	13.8±1.8	11.2±2.2	8.8±0.5	7.0±0.6	6.9±0.3	6.2±0.8
60:40	31.4±2.7	19.6±3.1	18.5±3.6	17.8±3.1	13.4±1.9	8.9±0.5	7.5±0.5	7.2±0.4	6.3±0.5
40:60	45.6±3.2	26.4±1.9	25.5±2.2	24.4±2.4	16.7±2.2	9.3±0.5	8.0±0.6	7.3±0.5	6.6±0.6
20:80	64.9±3.3	34.5±2.2	34.7±2.2	27.2±2.7	18.9±2.5	9.4±0.3	8.0±0.5	7.5±0.3	6.7±0.5
0:100	73.2±5.2	43.2±4.1	41.8±3.8	34.9±2.4	20.9±2.7	9.7±0.4	8.1±0.7	7.5±0.6	6.8±0.7

Figure 4.7 and Table 4.7 show that structural strength significantly depends on the water content in a system. Systems with a higher amount of water have a lower strength value. Very big difference (up to 30 degree) is observed between anhydrous and humidified

at RH 11% trehalose-maltodextrin systems. Fan and Roos (2016b) and Maidannyk and Roos (2017a) created and developed relationships (Equation 17) showing structural strength dependence on the water content.

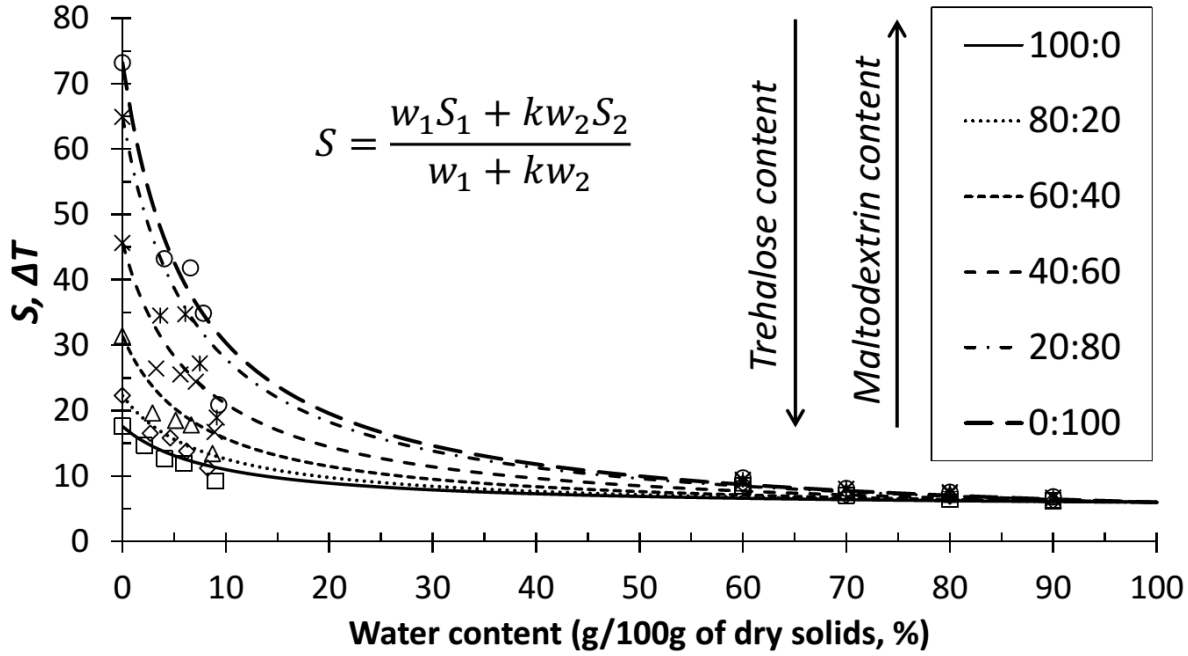

Figure 4.8. Modeled by equation 17 (lines) and experimental (symbols) S of trehalose-maltodextrin (100:0; 80:20; 60:40; 40:60; 20:80; 0:100) systems at different water contents.

Strength curves were obtained for each trehalose-maltodextrin system (Fig. 8). The k value was 11.9, 13.2, 14.5, 14.7, 15.2, 15.8 for 100:0, 80:20, 60:40, 40:60, 20:80, 0:100 trehalose-maltodextrin systems, respectively.

Structural strength was strongly dependent on the system composition. Systems with high amount of maltodextrin show more "strong" behaviour compare to "weak" high trehalose content systems (Table 4.7, Figure 4.9). For example, significant difference (> 50 degree) was observed between 100:0 and 0:100 anhydrous (RH 0%) trehalose-maltodextrin systems. It means that structural relaxation times achieved a critical level at higher temperature for systems with high amount of maltodextrin. Similar effects were observed in our previous studies of carbohydrate-protein systems (Fan and Roos, 2016a, b; Maidannyk and Roos, 2016).

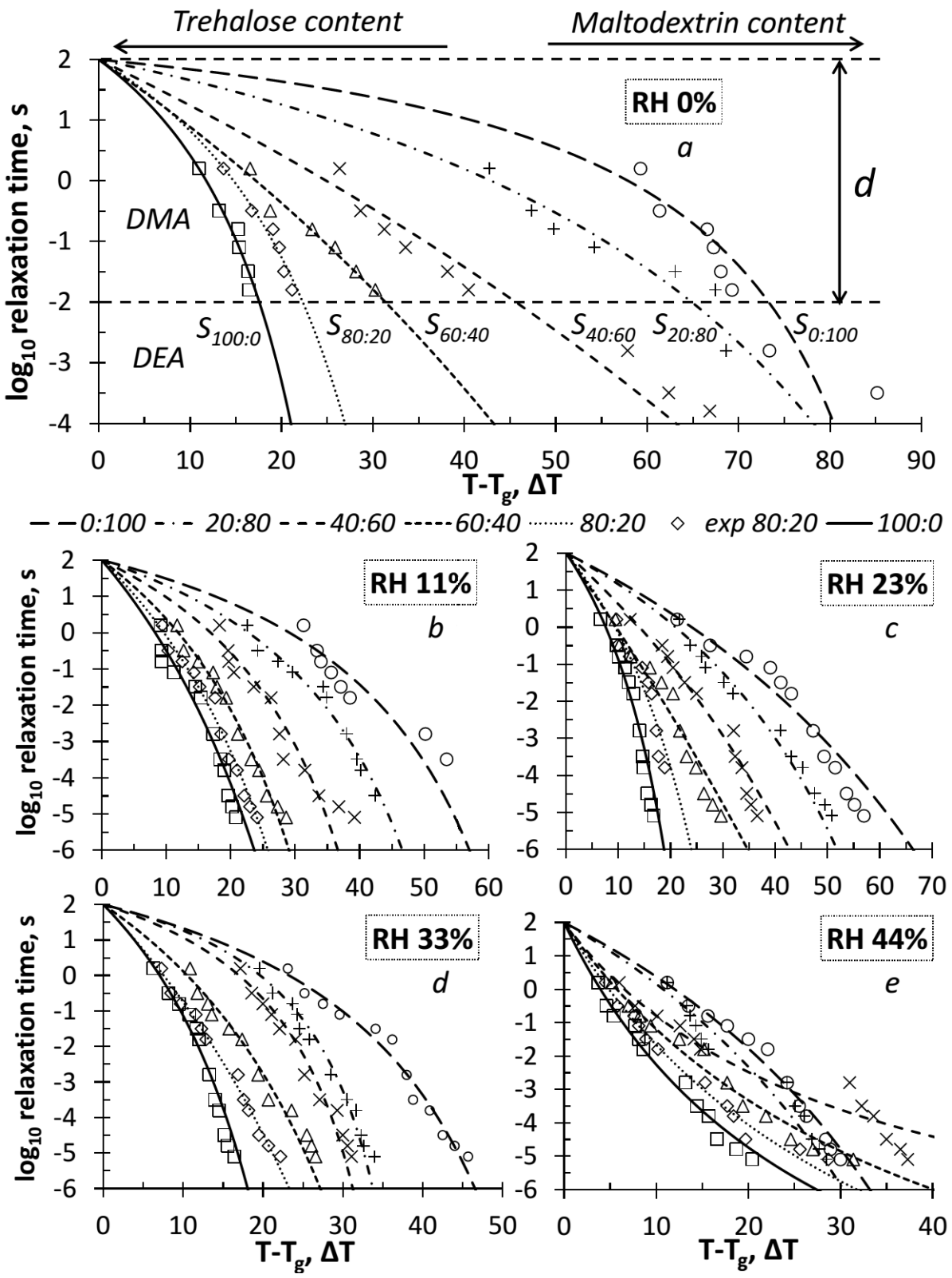

Figure 4.9. Modified WLF curves (lines) and experimental data (symbols) for trehalose-maltodextrin mixtures (100:0, 80:20, 60:40, 40:60, 20:80; 0:100) stored for 120 hours at various relative humidities (0 (a), 11 (b), 23 (c), 33 (d) and 44% (e)) at 25±1°C.

Analysing the experimental data and data obtained by equation 17 we found that structural strength depends on the maltodextrin content (Figure 4.10).

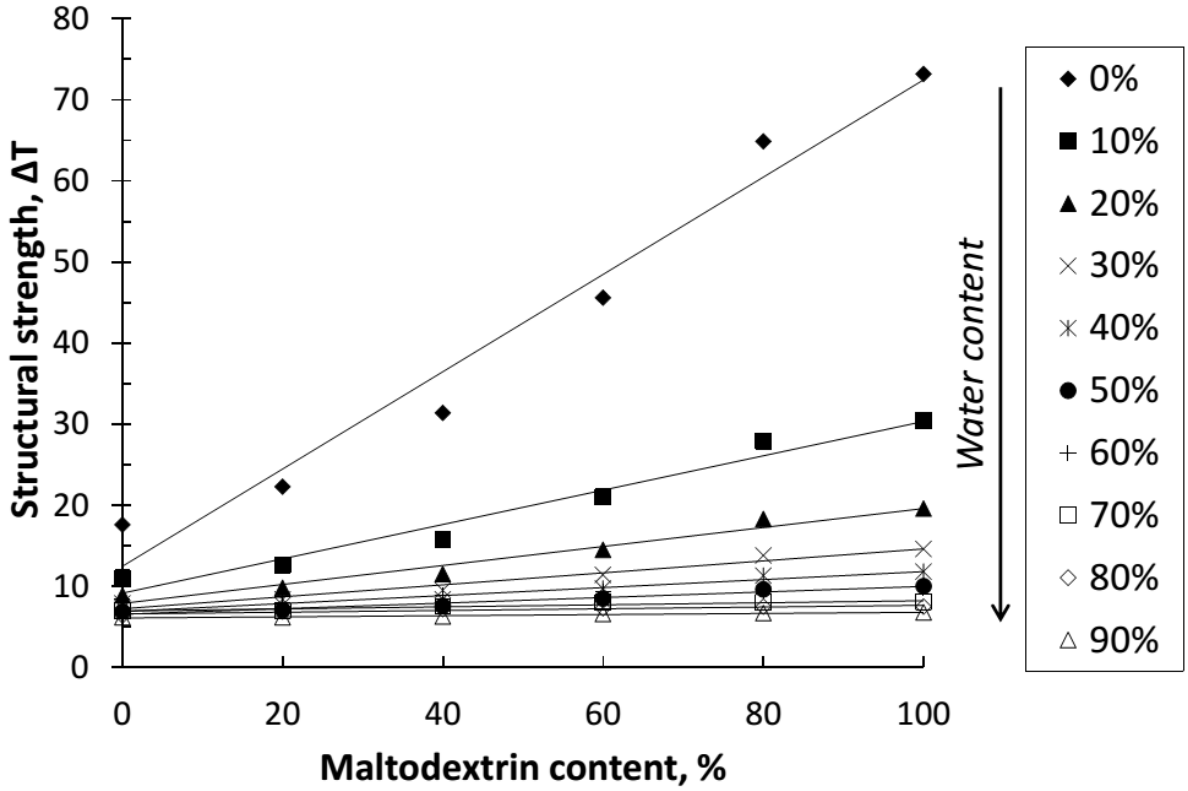

Figure 4.10. The dependence of S from maltodextrin content (%) for trehalose-maltodextrin system at different water contents (0%, 60%, 70%, 80%, 90% - experimental data; 10%, 20%, 30%, 40%, 50% - the data predicted by Eq. 9).

Structural strength was increasing linearly (with 0.9673; 0.9640; 0.9637; 0.9617; 0.9633; 0.9591; 0.9217; 0.8901; 0.8757 and 0.9315 R^2 for 0%; 10%; 20%; 30%; 40%; 50%; 60%; 70%; 80% and 90% of water respectively) with increasing maltodextrin concentration in the system. Our previous studies showed similar results for carbohydrate-protein systems. Thus, *strength is linearly dependant on the composition of a miscible system*. Knowing this dependence, equation 17 and strength values of pure components, we can predict structural strength for their mixture at any water content. Therefore, the present work showed that the strength model can be applied for miscible carbohydrates systems and allows controlling processability, performance as well as the quality and stability of food products.

4.5 Conclusions

In this study the effect of miscibility on structural strength was under investigation. For this, trehalose-maltodextrin systems were used as a miscible carbohydrate model. Fractional water sorption analysis gives water content in different amorphous mixtures at low and high water activities. The presence of maltodextrin prevents trehalose crystallization. Apparent viscosity significantly decreases with increasing temperature in systems. Glass transition and α-relaxation temperature increases with increasing maltodextrin content in a system. Structural strength shows the same trend. Strength shows linear dependence on component concentration in a mixture and significantly decreasing with increasing of water content in a system. Knowing strength values of pure components allows predicting strength for their mixtures at any water content. These results can be used in processing and characterisation of the miscible materials, as well as for stability and quality control during production and storage of food formulations.

CHAPTER V

Structural strength analysis of partially crystalline trehalose.

V.A. Maidannyk, Y.H. Roos

School of Food and Nutritional Sciences, University College Cork, Ireland.

Source: (Manuscript under review in the *"LWT – Food Science and Technology"* journal).

5 Structural strength analysis of partially crystalline trehalose

5.1 Abstract

Strength concept, which is based on the Williams-Landel-Ferry (WLF) model, was developed using mixed structured powders containing amorphous and crystalline components. At the present study, semi-crystalline trehalose powders with various (100:0; 80:20; 60:40; 40:60; 20:80) amorphous to crystalline ratios were analyzed. Amorphous components were prepared from 20% solids in water solution by freeze-drying. Strength analysis, which included water sorption, differential scanning calorimetry, dynamic mechanical analysis and microscopy, was applied. The results indicated that water content significantly affects glass transition and α-relaxation temperatures as well as structural strength parameter, while, the effect of crystalline component is less pronounced. This study can be used in processing and characterization of various partially crystalline food products including nutritional formulations and infant formulas.

Keywords: Structural relaxation, WLF, "Strength" parameter, partially crystalline trehalose.

2 Introduction

The improvement of processing and storage techniques requires a deep and fundamental knowledge of thermodynamics and kinetics. Food solids can exist in crystalline, amorphous or partially (e. g. semi) crystalline powders. Crystalline and amorphous materials show significantly different physicochemical properties (Bhandari et al., 2013), due to differences in microstructure. Crystalline structures have long range molecular order, while amorphous structures are more disordered (short range molecular alignment) (Nurhadi and Roos, 2016). To preserve the taste, flavor and color of food the materials should be maintained in the amorphous form (Roos and Drusch, 2015). Amorphous materials are thermodynamically unstable compared to crystalline structures, however they are fairly stable in the glassy state (e. g. glass) (Slade et al., 1991; Roos, 2008). At temperatures close to the calorimetric glass transition temperature (T_g), physical properties of solids, such as molecular mobility, viscosity, etc. significantly change and materials are converted to supercooled liquids (e. g. rubber) showing time-dependent flow (Angell et al., 2000; Roos, 2008). Hence, obtaining the time-dependent characteristics of thermal, electric and mechanical changes is practically important. Structural strength concept, proposed by Roos and co-workers combine

temperature differences ($T-T_g$) and a practically important time factor (critical change in structural relaxation time) (Roos et al., 2015).

Trehalose is a natural disaccharide of glucose with a high T_g (Green and Angell, 1989). Trehalose is widely used in food and biotechnology areas due to specific physicochemical properties such as prevention of biomolecules degradation (Crowe et al., 1985; Uritani et al., 1995); preservation of vaccines and medical proteins capabilities (Xie and Timasheff, 1997; Miller and de Pablo, 2000).

Amorphicity of materials can be detected gravimetrically from changing mass during water sorption (Buckton and Darcy, 1995; Mackin et al., 2002; Lehto et al., 2006; Nurhadi and Roos, 2016). Amorphous materials have larger porosity and more hydroscopic properties, hence amorphous structures show a higher sorption capacity than crystalline forms (Bhandari et al., 2013; Nurhadi and Roos, 2016).

Differential scanning calorimetry (DSC) has been used as a method for detection and quantification of the amorphous components in carbohydrate systems. For this, sample is heated to above the T_g to get dehydration (T_h) (endotherm peak in DSC thermogram) and recrystallization (exotherm peak in DSC thermogram). The areas of exothermal and endothermal peaks are proportional to the amorphous content in a partially crystalline sample. Another approach to detect amorphous component in material by DSC is to determine the change of specific heat capacity (C_p) over the glass transition (Saleki-Gerhardt et al., 1994; Sebhatu et al., 1994; Lehto et al., 2006). Optical (light) microscopy usually shows that the partially crystalline structure tends to increase in transparency while approaching the transition temperature of dehydration without losing their external morphology (Sussich et al., 1998). A dynamic mechanical analysis (DMA) in multi-frequency mode is a useful tool to characterize mechanical properties including α, β, γ-relaxations, which happen due to variation in molecular mobility below and around T_g (Moates et al., 2001; Silalai and Roos, 2011; Potes et al., 2012). Knowing the frequency of measurements allows obtaining the value of structural relaxation time of α-relaxation process (Noel et al., 2000), which may be related to particle structure, collapse and viscous flow. As the determination of viscous flow characteristics at temperatures close to the T_g is extremely difficult, strength concept provides an estimation of resistance to structural changes for amorphous materials above the calorimetry onset temperature during heating.

Strength analysis, which included water sorption, DSC and DMA, was successfully applied for various carbohydrate-protein, carbohydrate-carbohydrate and miscible models such as trehalose-whey protein isolate (WPI) (Fan and Roos, 2016a, b; Maidannyk and Roos, 2016), lactose-WPI (Fan and Roos, 2016a, b; Maidannyk and Roos, 2017), lactose-trehalose (Fan and Roos, 2016a) and trehalose-maltodextrin (Maidannyk et al., 2017). These studies showed that structural strength linearly depends on concentration of components and significantly decreases with increasing water content in a system. However, structural strength analysis of partially crystalline systems has not been addressed. The main aim of the present study was to develop the strength model using partially crystalline systems of trehalose. For this, effect of crystalline component on structural strength of amorphous trehalose was under investigation and effects of water content on structural strength of the partially crystalline systems were also studied.

5.3 Materials and Methods

5.3.1 Materials

D-(+)-Trehalose crystalline dihydrate (Hayashibara Co., Ltd., Okayama, Japan) and de-ionized water (KB scientific, Cork, Ireland) were used without purification.

5.3.1.1 Amorphous structure

Amorphous structure was obtained by freeze-drying (Lyovac GT2, Steris®, Hürth, Germany). For this, trehalose solution (total solid of 20%) in water was prepared. After that, 5 ml aliquots of solution were frozen in pre-weighted and semi-closed with septum in 10 ml glass vials (Schott, Mulheim, Germany) at -20°C for 24 h, then at -80°C for 3 h, followed by freeze-drying for 60 h at pressure $p < 0.1$ mbar. All vials were hermetically sealed under the vacuum conditions inside the freeze dryer at $p < 0.1$ mbar and stored over P_2O_5 in vacuum desiccators (Roos and Karel, 1990) at room temperature (25 ± 1°C) to protect samples from water uptake.

5.3.1.2 Crystalline structure

Crystalline trehalose powder was prepared by grinding and stored in a desiccator over P_2O_5 at 25±1°C for 3 days. The small amount of amorphous structure can be detected after grinding procedure (Willart et al., 2010; Nurhadi and Roos, 2016).

5.3.1.3 Partially crystalline structures

Partially crystalline trehalose systems were prepared by blending accurately weighted amount of 100% crystalline and 100% amorphous structures at 100:0; 80:20; 60:40; 40:60; 20:80 and 0:100 amorphous:crystalline ratios. Mixing was done by spatula and shaking the closed vials (Nurhadi and Roos, 2016).

5.3.2 Determination of the initial water content

Samples of trehalose powder with final weight 0.5-1.0 g were dried at 70°C with absolute pressure P_{abs}<10 mbar for 24 hours in a WTB Binder vacuum oven (Mason Technology®, Tuttingen, Germany) to measure the initial water content of the material. The difference in mass of samples before and after drying was defined as initial water content.

5.3.3 Water sorption analysis

Partially crystalline systems with various ratios of amorphous and crystalline structures (described above) were stored in desiccator over P_2O_5. Each system was stored at evacuated desiccator (25±1°C) for 10 days over the saturated solutions of LiCl, CH_3COOK, $MgCl_2$, K_2CO_3, $Mg(NO_3)_2$, $NaNO_2$, NaCl and KCl (Sigma Chemical Co., St. Louise, MO. U.S.A.), which at equilibrium provided 0.11, 0.23, 0.33, 0.44, 0.545, 0.66, 0.76 and 0.85 a_w, respectively. AQUALAB 4 (TE) (Decagon Devices Inc., NE) water activity meter was used to measure water activity for each material after storage. Samples were weighted at intervals of 0, 2, 4, 6, 8, 10, 24, 48, 72, 96 and 120 hours upon storage. Possible crystallization of amorphous trehalose was assessed from the loss of sorbed water. The water content in each mixture was plotted as a function of time, and the Guggenheim-Anderson-deBoer (GAB) relationship was fitted to data to know water activity-water content dependence of amorphous trehalose systems (Eq. 2).

Equation 18 was used to determine the combined effects of amorphous and crystalline components (Bronlund and Paterson, 2004):

$$W_{mixture} = n_1 W_{crystalline} + n_2 W_{amorphous} \quad (18)$$

where, $W_{mixture}$ is the total equilibrium water content in the mixture; n_1 and n_2 are multipliers of crystalline and amorphous components in the system ($n_1+n_2 = 1$); $W_{crystalline}$ and $W_{amorphous}$ are water contents in crystalline and amorphous component.

5.3.4 Differential Scanning Calorimetry (DSC)

Differential scanning calorimeter (DSC) (Mettler Toledo Schwerzenbach, Switzerland) was used to measure the glass transition temperature, dehydration and spontaneous recrystallization of partially crystalline trehalose mixtures with 0, 0.11, 0.23, 0.33 and 0.44 a_w. Samples of all mixtures were transferred to pre-weighted standard DSC aluminium pans (40 μL, Mettler Toledo Schwerzenbach, Switzerland) and hermetically sealed. An empty punctured pan was used as a reference. For anhydrous systems only, the lids of DSC aluminium pans were punctured to allow evaporation of residual water upon the measurement. All samples were scanned with 5°C/min heating rate. The onset of T_g, heat capacity of endotherm and exotherm were determined by the STAR^e software version 8.10 (Mettler Toledo Schwerzenbach, Switzerland).

5.3.5 Dynamical Mechanical Analyses (DMA)

Dynamic mechanical analyzer (DMA) (Tritec 2000 DMA, Triton Technology Ltd., UK) was used to measure mechanical properties (E'' – loss modulus, E' – storage modulus and tanδ = E''/E') of anhydrous and humidified partially crystalline trehalose systems (described above for the DSC experiments). The DMA instrument was balanced or set at zero to determine the zero displacement position before starting. Approximately 60 g of grinded samples were spread on a metal pocket-forming sheet (Triton Technology Ltd., UK). This sheet was fixed between the stationary and drive shaft clamps inside the measuring head of the DMA. Length, width and thickness were measured for each sample. All results were obtained using 1.43.00 DMA software version. To control temperature the DMA was connected to a liquid nitrogen tank (1l; Cryogun, Brymill Cryogenic Systems, Labquip Ltd., Dublin, Ireland). Samples were scanned from ~ 50°C below to over the α-relaxation region with cooling rate of 5°C/min and heating rate of 2°C/min using the single cantilever bending mode (Potes et al., 2012; Fan and Roos, 2016a, b; Maidannyk and Roos, 2016). The α-relaxation temperatures (T_α) were determined from peaks of tanδ above the glass transition.

Equation 5 was used to calculate the relaxation times (τ) of peak T_α, measured by DMA at various frequencies (f) (Noel et al., 2000; Potes et al., 2012).

5.3.6 Optical light microscopy

Microscope observation (OLYMPUS BX51, with magnification x20) was done on humidified (0, 0.11, 0.23 and 0.44 a_w) partially crystalline trehalose powders (described above for the DSC experiments) placed between cover glass and mounted Linkam 120 (TP 94) temperature controller stage. The samples were scanned from 5 to 150°C, with 2°C/min heating rate.

5.3.7 Calculation of WLF model constants and Structural Strength

The constants C_1 and C_2 from Williams Landel Ferry (WLF) equation were obtaining as described by Roos and Drusch (Roos and Drusch, 2015).

The WLF equation in the form of (Eq. 10) was used to fit DMA and DSC data (Williams et al., 1955). The WLF equation in the form of (Eq. 11) suggested that the plot of $1/lg(\tau/\tau_s)$ versus $1/(T-T_g)$ gives a linear correlation. The WLF constants C_1 and C_2 were derived from the slope and intercept of the straight line (Roos and Drusch, 2015).

Mathematically, structural strength parameter (S) is based on WLF relationship and can be calculated by Equation (16).

Equation 17 was used to predict structural strength at different water contents (Maidannyk and Roos, 2017).

5.3.8 Data analysis

All experiments were performed in triplicate. Mean data of the water sorption analyses, DSC, DMA were calculated from 3 replicates with standard deviations expressed in error bars.

5.4 Results and discussion

5.4.1 Water sorption analysis

Table 5.1 and Figure 5.1 shows experimental water content of partially crystalline trehalose systems, over the whole range of water activities at 25±1°C.

Table 5.1. Water content of partially crystalline trehalose systems (ratios of components 100:0, 80:20, 60:40, 40:60, 20:80, 0:100) stored at different water activities (0.11, 0.23, 0.33, 0.44, 0.55, 0.65, 0.76, 0.85, 0.99) for 120 hours at 25±1°C.

a_w	**Experimental water content for partially crystalline (amorphous:crystalline) trehalose systems (g/100 g of solids)**					
	100:0	**80:20**	**60:40**	**40:60**	**20:80**	**0:100**
0.11	2.2±0.1	1.7±0.1	1.3±0.1	0.9±0.1	0.4±0.1	0.010±0.0
0.23	4.1±0.4	3.3±0.1	2.5±0.3	1.7±0.2	0.8±0.2	0.014±0.0
0.33	5.9±0.4	4.7±0.2	3.7±0.1	2.4±0.2	1.2±0.2	0.019±0.0
0.44	9.0±0.2	6.9±0.2	5.3±0.1	3.4±0.3	1.8±0.2	0.023 ±0.0
0.55	9.5±0.1	7.6±0.1	5.6±0.3	3.8±0.3	1.9±0.3	0.029±0.0
0.65	9.4±0.3	7.6±0.2	5.7±0.1	3.8±0.1	1.9±0.3	0.037±0.0
0.76	8.8±0.4	7.2±0.3	5.5±0.2	3.6±0.2	1.8±0.2	0.049±0.0
0.85	9.5±0.4	7.6±0.1	5.5±0.2	3.7±0.2	1.9±0.3	0.066±0.0
0.99	9.7±0.3	7.8±0.3	5.7±0.3	3.8±0.3	2.3±0.2	0.598±0.0

Crystalline structures humidified at low water activities (0-0.76 a_w) adsorb very little amount of water while at high water activities (0.85-0.99 a_w) the amount of sorbed water increases exponentially (Table 5.1) due to capillary condensation and dissolution (Bronlund and Paterson, 2004).

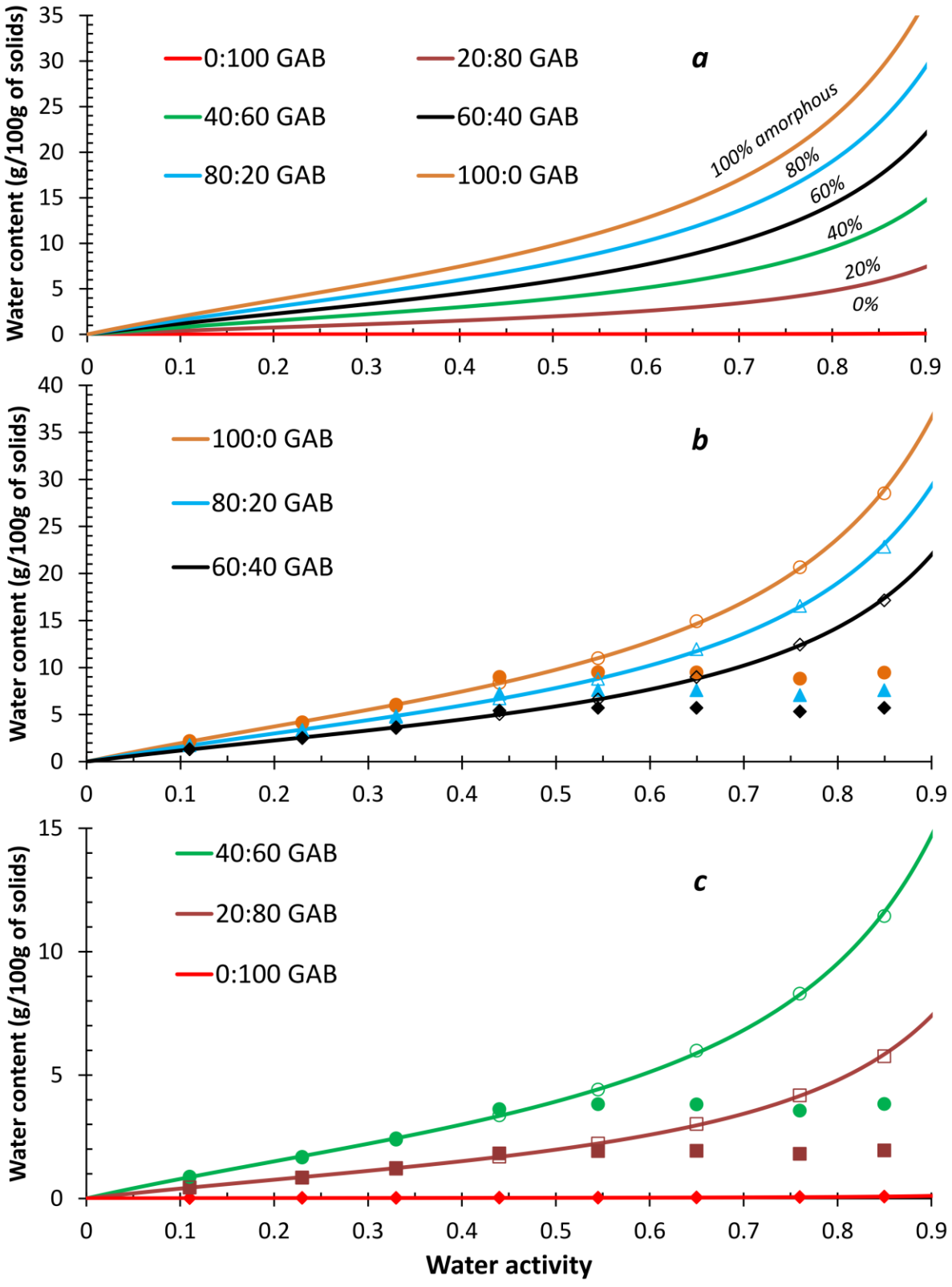

Figure 5. 1. The GAB sorption isotherms at 25±1°C (lines) (a), experimental data (solid symbols) and calculated water contents (Eq. 2) (clear symbols) for partially crystalline trehalose system with various ratios (amorphous:crystalline) 100:0 (b); 80:20 (b); 60:40 (b) and 40:60 (c); 20:80 (c) and 0:100 (c) systems.

Steady-state water contents of each mixture at 120 hours were used in GAB model. The GAB model was fitted to experimental data of 100:0 amorphous:crystalline systems below $0.55a_w$ (Labuza, 1984; Maidannyk and Roos, 2016). However, at higher water activities (≥0.55 a_w), the crystallization of trehalose occurred and extrapolated sorption data from GAB relationship give misleading results for sorbed water contents (Potes et al., 2012). Fractional isotherm approach (Eq. 18) allowed calculating water contents at high water activities and showed very good fit with experimental data at low water activities $0\text{-}0.44a_w$. Using previously published data for pure amorphous trehalose (Maidannyk and Roos, 2016; Maidannyk at el., 2017) and experimental data for pure crystalline trehalose, the GAB model was fitted to obtain sorption isotherms at high water activities (Figure 5.1). Amorphous structure adsorbs around 100 times more water than crystalline structure (Table 5.1). That's why the presence of a small amount of amorphous component in crystalline structure results in significant difference to the water sorption isotherm of material.

5.4.2 Differential Scanning Calorimetry and Microscopy

The onset of calorimetric glass transition temperature (T_g) was obtained by DSC for each anhydrous and humidified ($0\text{-}0.44a_w$) partially crystalline trehalose system (Table 5.2).

Table 5. 2. The onset of calorimetric glass transition temperatures (T_g) of anhydrous (0 a_w) and humidified (0.11-0.44 a_w) partially crystalline trehalose systems (amorphous:crystalline) stored for 120 hours at 25±1°C.

	Glass transition temperature (T_g) of partially crystalline (amorphous:crystalline) trehalose systems, ^oC				
a_w	**100:0**	**80:20**	**60:40**	**40:60**	**20:80**
0	112±3	112±2	111±3	111±2	111±2
0.11	62±1	61±3	60±2	59±2	59±2
0.23	43±2	43±1	42±3	42±1	41±1
0.33	32±2	32±1	32±2	31±3	31±2
0.44	15±2	15±3	15±2	15±1	14±3

Detected values of T_g belong to amorphous component in partially crystalline systems. The obtained data for pure anhydrous trehalose is in agreement with previous study

(Green and Angell, 1989; Roos 1993; Miller et al., 2000; Maidannyk and Roos, 2016; 2017a). As expected crystalline fraction has no effect on the T_g of the amorphous fraction in the partially crystalline systems (Table 5.2). Glass transition is that of the amorphous fraction which is shown by the proportional decrease of heat capacity (C_p) over the T_g region. A slight decrease of T_g value with increase of crystalline component content in the systems is in agreement with water sorption data (Table 5.1). Water as a good and strong plasticizer significantly increases mobility of molecules of the amorphous component, which results in the decrease of T_g values with increasing water content (Silalai and Roos, 2011). For example, in the present study T_g of 100:0 amorphous:crystalline system decreased from 112°C (at 0 a_w) to 15°C (at 0.44 a_w) due to water plasticization.

Microscope observation, carried out on the same samples placed between cover glasses, showed that crystalline and amorphous components of trehalose became more transparent during heating to above T_g. However, at the same time the external morphology of the structure was not changed until the temperature about 135°C, that the "solid" sample appears to change morphological shape ("edge roundness") with an increasing mobility of the phase, although still firm (sticky) (Sussich et al, 1998) (Figure 5.2). These observations were the same for anhydrous and humidified (0.11, 0.23, 0.33 and 0.44a_w) partially crystalline trehalose systems.

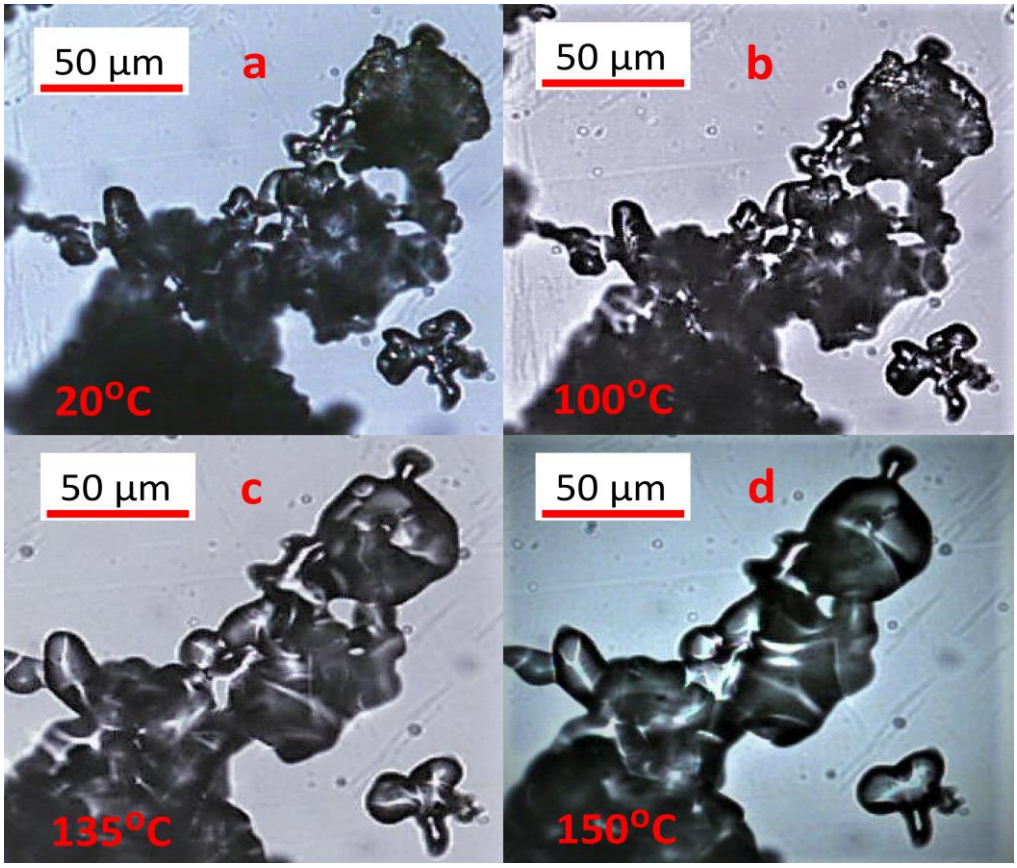

Figure 5.2. Microscope observation of 60:40 amorphous:crystalline trehalose, stored at 0.11 a_w, scanned at 2 K min^{-1} at the temperature of (a) 20°C; (b) 100°C; (c) 135°C and (d) 150°C.

5.4.3 Dynamical Mechanical Analyses (DMA)

Partially crystalline trehalose systems with different ratios of amorphous and crystalline components (described above for DSC experiments) were scanned by DMA in multi-frequency mode.

The rapid changes in mechanical properties, which related to the amount of energy converted to heat during relaxation can be detected by DMA, while DSC directly detects the difference in the amount of heat (Talja and Roos, 2001; Gonnet et al., 2002; Roos and Drusch, 2015). Figure 5.3 shows typical frequently-dependent thermogram obtained by DMA. The α-relaxation temperature values were determined from the temperature peak of tanδ, at ~ 20-30ºC above the onset of the T_g.

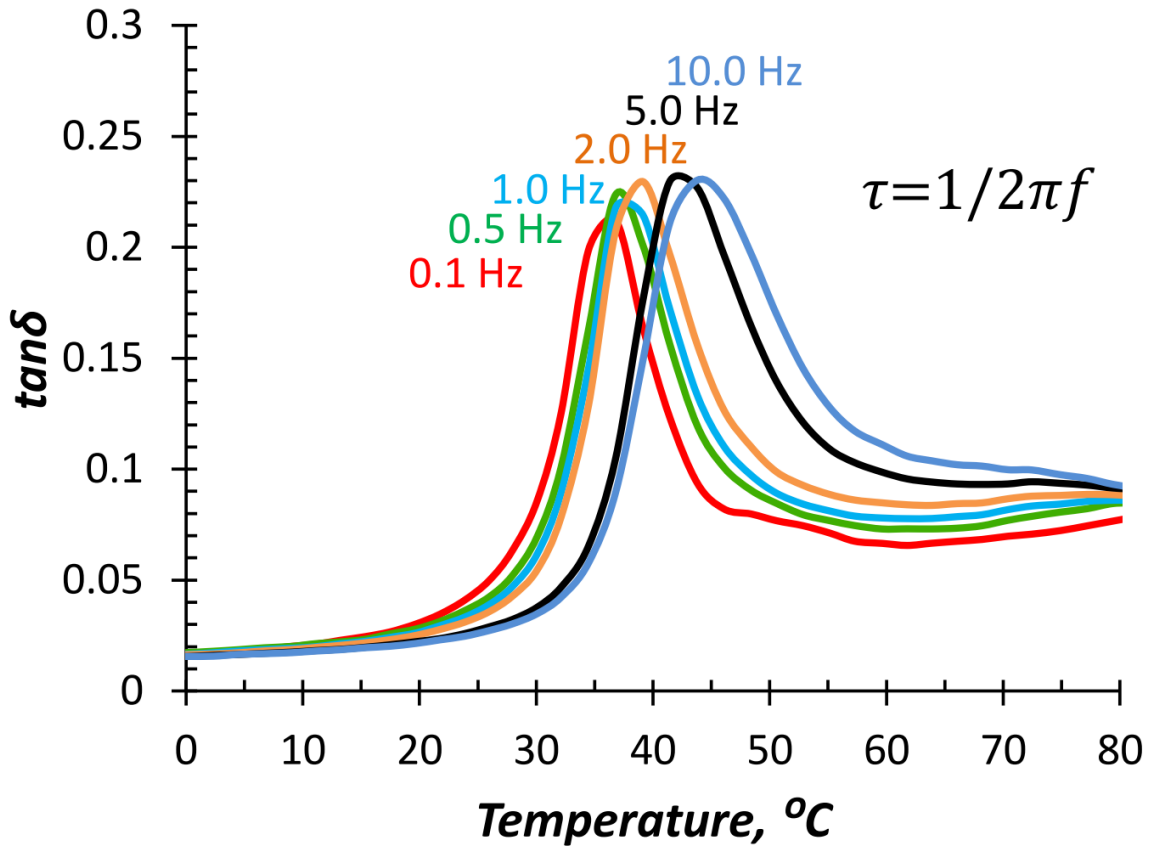

Figure 5.3. Temperature dependence of tangents δ for humidified (0.23 a_w) 80:20 amorphous:crystalline trehalose system determined by DMA in multi-frequency mode (0.1, 0.5, 1, 2, 5, 10 Hz).

Systems with high amount of crystalline component showed slightly lowered α-relaxation temperature peak with less intensity, due to significant difference between crystalline and amorphous particle sizes (crystalline particles needs less mechanical energy than amorphous and α-relaxations occurs at lower temperature). Also crystalline phase may slightly decreased α-relaxation temperature due to sliding effect inside the partially crystalline system (Cano-Chauca et al., 2005). The big differences (~6-10ºC) were observed for anhydrous partially crystalline trehalose systems, while for humidified systems (0.44 a_w) these differences were not significant (~2-5ºC) and α-relaxation occurred at similar temperatures at all amorphous and crystalline ratios (Table 5.3).

Table 5.3. α-Relaxation temperature (T_α) detected by DMA for partially crystalline trehalose systems with different amorphous:crystalline ratios, equilibrated at different relative humidities (RH).

RH 0%		**Amorphous:Crystalline trehalose**				
		100:0	**80:20**	**60:40**	**40:60**	**20:80**
f, Hz	**logτ, s**	**T_α, °C**	**T_α, °C**	**T_α, °C**	**T_α, °C**	**T_α, °C**
0.1	**0.20**	123±2	122±2	118±2	117±2	116±1
0.5	**-0.49**	125±1	123±1	119±1	118±1	116±2
1.0	**-0.80**	127±2	125±2	120±2	119±2	117±2
2.0	**-1.10**	128±2	126±3	121±1	120±2	118±1
5.0	**-1.50**	128±3	127±1	123±3	121±2	119±3
10.0	**-1.80**	130±1	128±2	124±2	122±1	120±2
RH 11%		**Amorphous:Crystalline trehalose**				
		100:0	**80:20**	**60:40**	**40:60**	**20:80**
f, Hz	**logτ, s**	**T_α, °C**	**T_α, °C**	**T_α, °C**	**T_α, °C**	**T_α, °C**
0.1	**0.20**	71±2	68±2	66±2	64±2	64±2
0.5	**-0.49**	73±2	69±2	67±2	65±2	65±2
1.0	**-0.80**	75±1	70±3	68±2	66±2	65±3
2.0	**-1.10**	77±2	71±2	69±1	67±2	66±1
5.0	**-1.50**	78±2	73±1	70±2	68±3	67±2
10.0	**-1.80**	79±3	75±2	72±2	69±3	68±2
RH 23%		**Amorphous:Crystalline trehalose**				
		100:0	**80:20**	**60:40**	**40:60**	**20:80**
f, Hz	**logτ, s**	**T_α, °C**	**T_α, °C**	**T_α, °C**	**T_α, °C**	**T_α, °C**
0.1	**0.20**	52±1	51±2	50±3	49±1	47±2
0.5	**-0.49**	53±1	52±3	50±2	50±2	47±1
1.0	**-0.80**	53±2	52±2	51±2	51±3	48±2
2.0	**-1.10**	54±2	53±2	52±3	51±1	48±2
5.0	**-1.50**	55±1	54±3	53±1	52±1	49±2
10.0	**-1.80**	57±2	55±3	53±2	52±2	50±2
RH 33%		**Amorphous:Crystalline trehalose**				
		100:0	**80:20**	**60:40**	**40:60**	**20:80**
f, Hz	**logτ, s**	**T_α, °C**	**T_α, °C**	**T_α, °C**	**T_α, °C**	**T_α, °C**
0.1	**0.20**	38±2	38±1	37±1	36±1	36±1
0.5	**-0.49**	40±2	39±2	39±1	37±2	36±1
1.0	**-0.80**	41±2	40±1	39±2	38±2	37±1
2.0	**-1.10**	42±3	41±2	41±1	39±1	38±2
5.0	**-1.50**	43±3	42±2	41±2	39±2	38±2
10.0	**-1.80**	44±2	43±1	41±2	40±2	39±2
RH 44%		**Amorphous:Crystalline trhalose**				
		100:0	**80:20**	**60:40**	**40:60**	**20:80**
f, Hz	**logτ, s**	**T_α, °C**	**T_α, °C**	**T_α, °C**	**T_α, °C**	**T_α, °C**
0.1	**0.20**	19±1	18±2	18±1	18±1	17±1
0.5	**-0.49**	19±1	19±2	19±1	19±1	18±2
1.0	**-0.80**	20±2	20±1	20±2	20±2	19±1
2.0	**-1.10**	21±1	21±1	21±2	21±2	20±1
5.0	**-1.50**	23±1	22±1	23±1	22±1	20±1
10.0	**-1.80**	25±1	24±2	23±2	23±1	22±2

Water as a good plasticizer, increases free volume in the systems as well as molecular mobility of amorphous components (Slade et al., 1991; Royall et al., 2005; Meinders and van Vliet, 2009) that result in significant decrease (~85ºC for 100:0 amorphous:crystalline) of the T_α for every partially crystalline system with increasing water content. These results are in agreement with previous studies (Silalai and Roos, 2011; Potes et al., 2012; Fan and Roos, 2016a,b; Maidannyk and Roos, 2016; 2017; Maidannyk et al., 2017;).

5.4.4 Applications of WLF equation and Strength

Williams-Landel-Ferry or WLF model (Eq. 10) is a popular equation, which can describe dependence of relaxation time and viscosity on the temperature close to onset T_g. Original relationship (Williams et al., 1955) showed that glass formers possessed similar decreases in relaxation times over the temperature range of T_g to T_g + 100 K. Because of that authors offered "universal" values for WLF constants: C_1 =17.44 and C_2 = 51.6 for many different materials (inorganic and organic). However, using WLF equation with "non-universal" constants C_1 and C_2 provides more realistic modeling with good fit to experimental data (Ferry, 1980; Peleg, 1992; Slade and Levine, 1995; Peleg and Chinachoti, 1996; Harnkarnsujarit, Charoenrein, Roos, 2012; Roos, 2013; Roos and Drusch, 2015;). In the present study, WLF constants C_1 and C_2 were calculated by Eq. 5 and summarized in table 5.4.

Table 5.4. Calculated WLF (τ_s = 100s; η_s = 10^{12} Pa s) constants C_1 and C_2 for partially crystalline trehalose systems, stored at various relative humidities (RH).

Amorphous: Crystalline Trehalose	***RH 0%***		***RH 11%***		***RH 23%***		***RH 33%***		***RH 44%***	
	-C_1, s	***-C_2, °C***	***-C_1, s***	***-C_2, °C***	***-C_1, s***	***-C_2, °C***	***-C_1, s***	***-C_2, °C***	***-C_1, s***	***-C_2, °C***
100:0	5.0±0.3	40.7±0.5	23.7±0.5	123.8±2.4	3.8±0.9	25.6±1.7	31.8±2.6	111.4±2.3	-10.0±0.7	-14.6±1.1
80:20	5.5±0.3	38.7±0.6	27.4±1.5	104.0±3.1	3.2±1.1	21.0±1.5	11.9±1.3	43.6±1.2	-9.6±0.5	-12.5±1.0
60:40	15.1±0.3	61.0±0.5	20.9±0.7	70.8±1.3	3.8±1.4	22.1±0.7	24.0±2.1	71.5±1.6	-9.5±0.9	-12.3±0.7
40:60	11.9±0.2	43.6±1.2	36.4±1.1	101.1±1.7	2.8±0.6	17.4±1.7	10.7±0.9	33.9±2.9	-11.1±1.3	-15.0±0.9
20:80	44.6±0.2	109.6±2.7	9.1±0.6	28.4±2.1	4.6±1.3	18.8±1.0	8.9±1.1	25.9±1.4	-13.4±1.6	-18.8±2.0

Using 10^{12} Pa s and 100s as reference values of viscosity and structural relaxation time respectively, Roos and co-workers (Roos et al., 2015; Fan and Roos, 2016a,b; Maidannyk and Roos, 2016; 2017; Maidannyk et al., 2017) adapted WLF equation in a

simple and convenient form, named "Strength" concept. Structural strength measures solid flow characteristics of amorphous materials above T_g and links the material state with a practically important time factor. As large and critical changes in structural relaxation time upon heating happened between 100 s and 0.01 s (between 2 and -2 in logarithmic scale) (Figure 5.4), the corresponding temperature difference, $T\text{-}T_g$, was defined as strength, S (Equation 16) (Roos et al., 2015; Fan and Roos, 2016a,b; Maidannyk and Roos, 2016; 2017; Maidannyk et al., 2017).

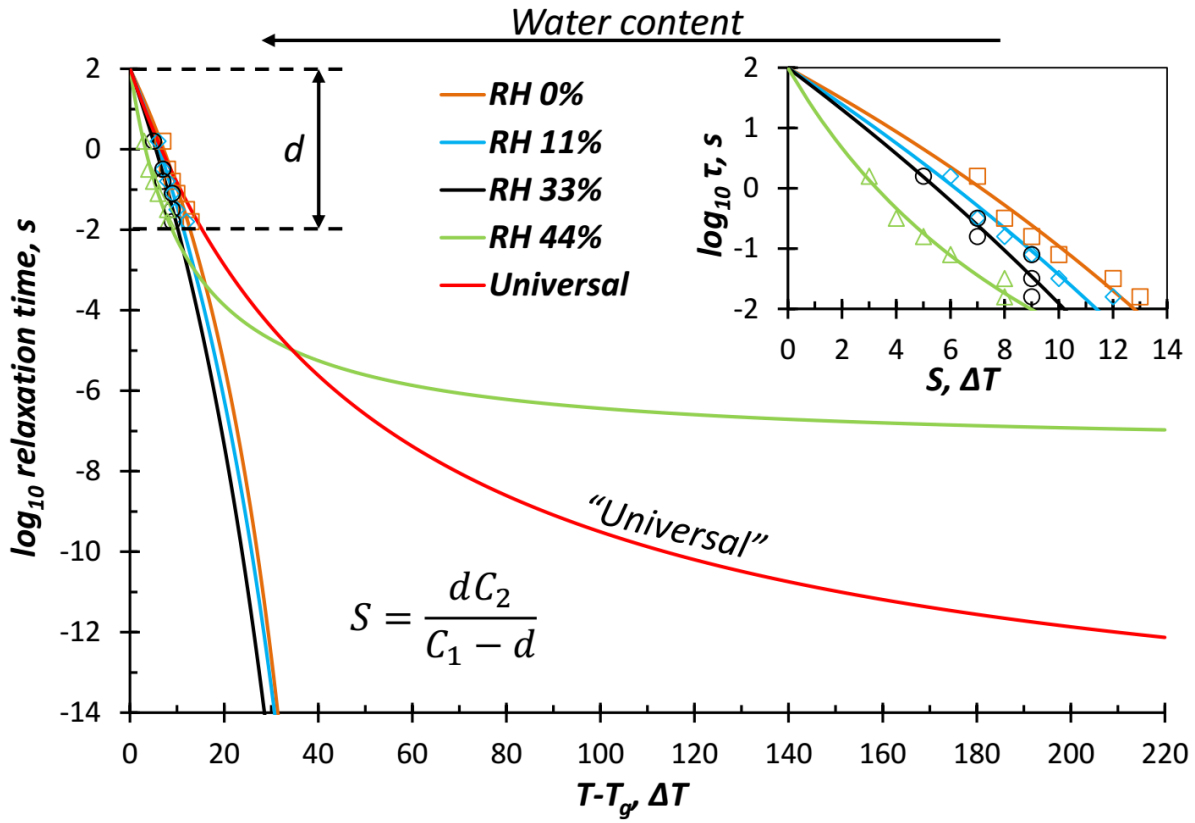

Figure 5.4. Modified WLF curves (lines), experimental data (symbols) and "strength" plot (inset) for 60:40 amorphous:crystalline trehalose system humidified at different relative humidities (0, 11, 33, 44% RH) with different water content (0, 1.3, 3.7, 5.3 g/100g of dry solids, respectively).

S was obtained (at d = 4) for partially crystalline trehalose systems at all ratios (Table 5.5). Strength curves, which show structural strength dependence on water content, were calculated by Equation 17 (Fig. 5.5). The k value was 15.2, 26.0, 17.1, 21.0 and 26.0 for 100:0, 80:20, 60:40, 40:60 and 20:80 amorphous:crystalline trehalose systems respectively.

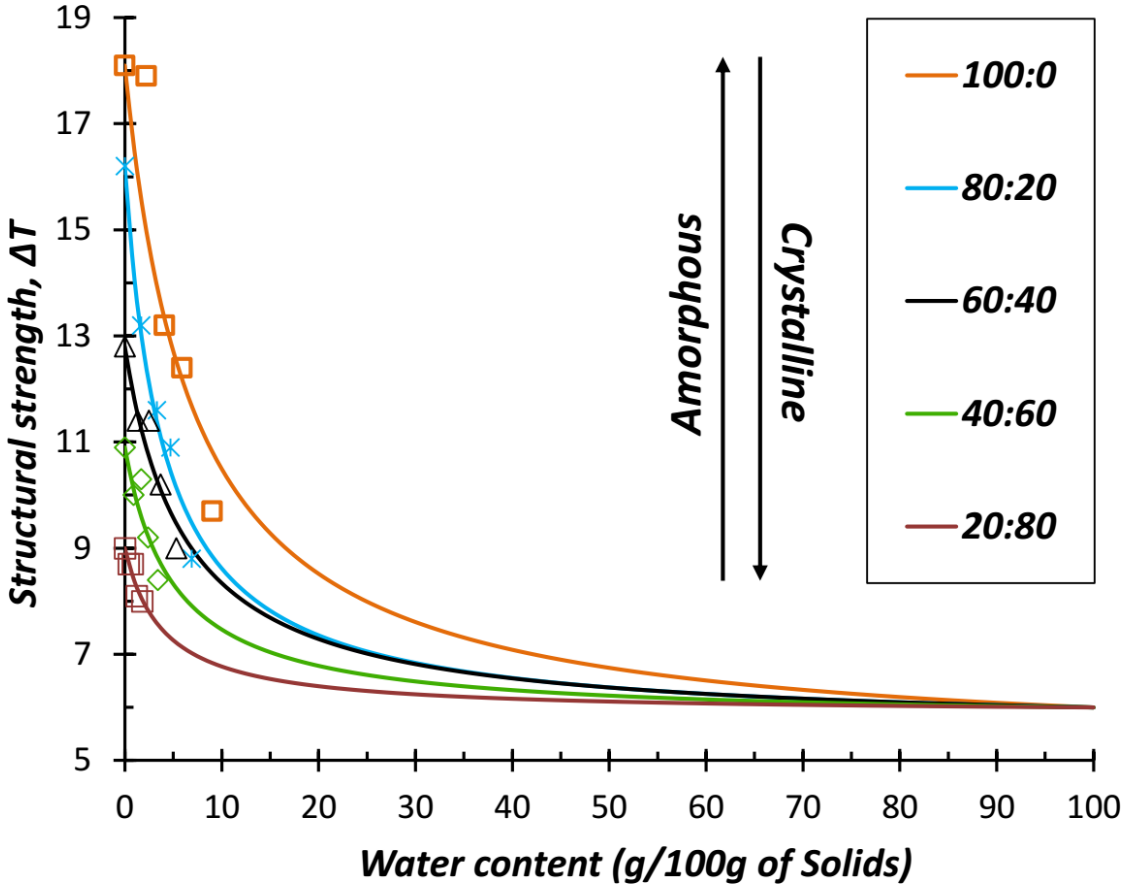

Figure 5.5. Strength curves, modeled by Eq. 7 (lines) and experimental (symbols) S of partially crystalline trehalose systems (100:0, 80:20, 60:40, 40:60 and 20:80 amorphous:crystalline ratios) at different water contents (g/100g of dry solids).

Table 5.5 and Figure 5.5 shows that for anhydrous systems (RH 0%) the S value significantly decreased (ΔS = 9.1ºC) with increasing crystalline component in a system, while for humidified systems (RH 44%) these differences were not so pronounced (ΔS = 1.7 ºC). This result is similar to our previous findings and can be explained by molecular mobility of amorphous component and by strong plasticization properties of water (Roos et al., 2015; Fan and Roos, 2016a,b; Maidannyk and Roos, 2016; 2017; Maidannyk et al., 2017).

Table 5.5. "Strength" S (calculated at d = 4) for partially crystalline trehalose systems at all ratios (amorphous:crystalline) stored at different relative humidities (RH).

Amorphous: Crystalline Trehalose	RH 0%	RH11%	RH 23%	RH 33%	RH 44%
100:0	18.1±2.9	17.9±2.1	13.2±1.8	12.5±1.2	9.7±1.1
80:20	16.2±2.5	13.2±1.9	11.6±1.3	10.9±1.1	8.9±1.4
60:40	12.8±2.3	11.4±1.1	11.4±1.1	10.2±2.1	9.0±0.4
40:60	10.9±1.7	10.0±1.2	10.3±0.9	9.2±1.3	8.4±0.5
20:80	9.0±0.9	8.7±0.4	8.7±0.5	8.1±0.7	8.0±0.7

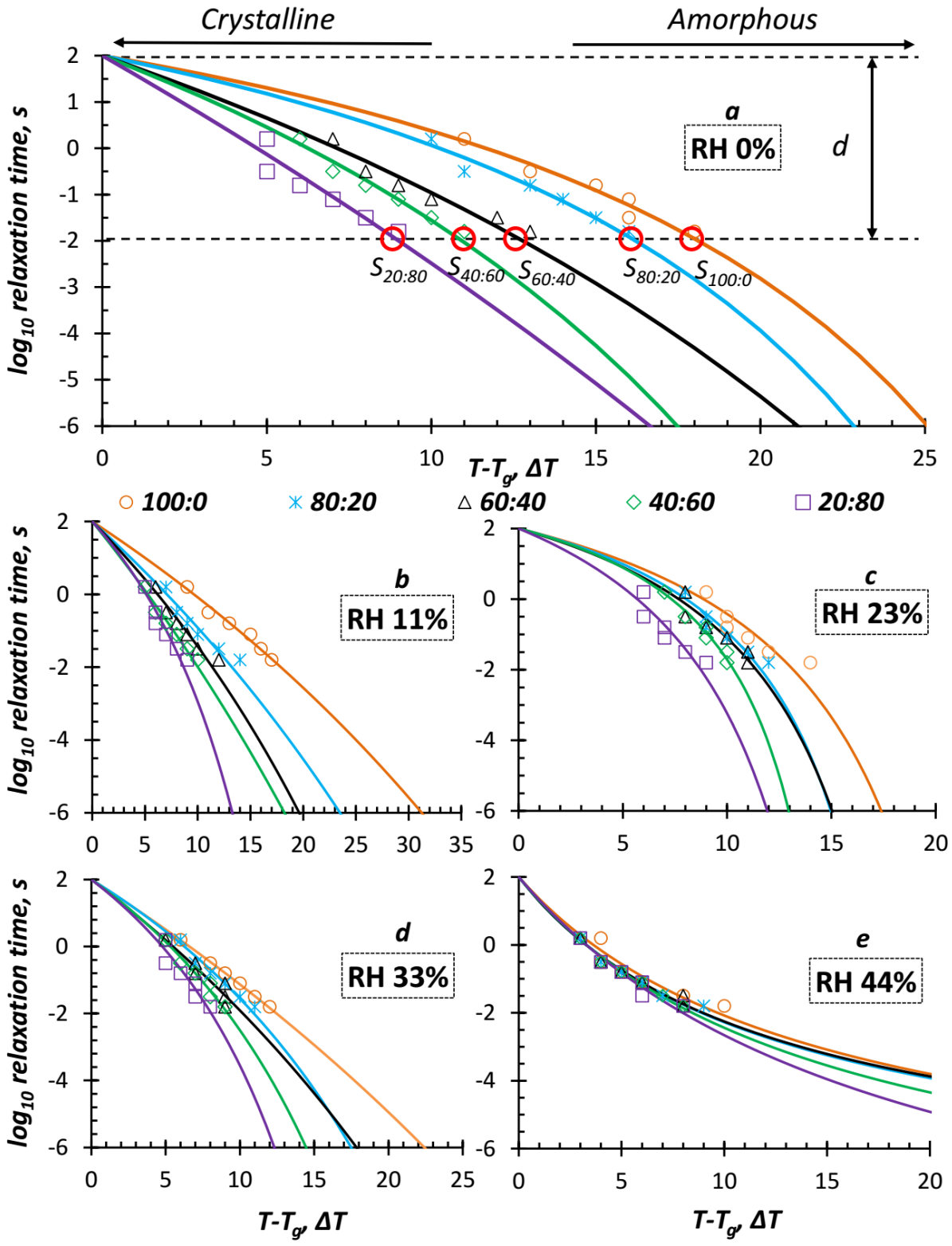

Figure 5.6. Modified WLF curves (lines) and experimental data (symbols) for partially crystalline trehalose (100:0, 80:20, 60:40, 40:60 and 20:80 amorphous:crystalline ratios) stored 120 h (at 25±1ºC) at different relative humidities (a (RH 0%), b (RH 11%), c (RH 23%), d (RH 33%) and e (RH 44%).

Even small variation in material structure significantly changes the structural strength in a system (Figure 5.6). Amorphous systems show more "strong" behavior compare to "weak" highly crystalline trehalose systems. However, this difference is significant only for anhydrous systems, while humidified systems shows very similar values of strength for all partially crystalline system. Hence, the presence of water is a very important factor, which significantly influences a structural strength and structure of food material. Despite the fact that for humidified systems, the values of S are similar, they are still decreasing linearly (with R^2 0.9879, 0.9310, 0.9045, 0.8860, 0.8816, 0.8789, 0.8767, 0.8750, 0.8743 and 0.8737 at 0%, 10%, 20%, 30%, 40%, 50%, 60%, 70%, 80% and 90% of water respectively) with increasing crystalline content in partially crystalline systems (Figure 5.7).

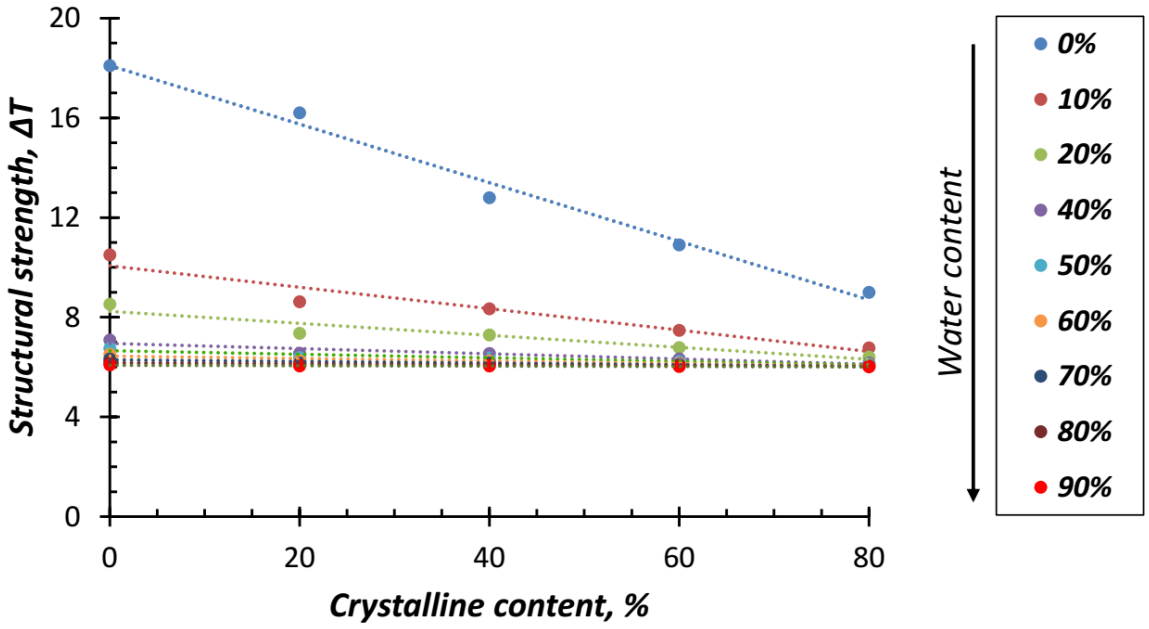

Figure 5.7. Structural strength versus crystalline component content of partially crystalline trehalose (%) at different water contents (%) (the data predicted by Eq.1 7).

Knowing structural strength of pure amorphous component and reference partially crystalline systems allows calculation of S value for systems at any crystalline content at any water content, as well as prediction of crystalline content in unknown partially crystalline system. Therefore, the present study showed that strength concept is a suitable model for determining crystalline content in partially crystalline system and allows controlling stability and quality in various food systems.

5.5 Conclusions

This study was focused on applying and further development of the structural strength concept. For this, strength analysis was used to determine crystalline content in partially crystalline trehalose. Water sorption analysis allows controlling water contents in different partially crystalline mixtures at low and high water activities. The glass transition and α-relaxation temperatures were detected by DSC and DMA respectively. The values of T_g and T_α as well as structural strength significantly decreasing with increasing water content in a system. Structural strength shows linear decreasing with increasing of crystalline content in a system. Strength analysis showed good consistency in predicting the crystalline content in unknown systems at any water content. Hence structural strength concept can be used in adaptation of processing and characterization of various food materials as well as in quality and stability control during production and storage.

CHAPTER VI

GENERAL DISCUSSION

6 General discussion

6.1 Structural Strength concept

Manufacturing of food and dairy ingredients is often based on dehydration of solids using empirical knowledge of drying process. The common problems include accumulation of solids on dryer surfaces, poor dehydration and low stability of products due to the water uptake, which leads to stickiness, caking and component crystallization (Langrish and Wang, 2009). To produce food materials with complex compositions and structure, a fundamental knowledge of process thermodynamics and kinetics is required. To predict the changes in physical properties of these systems a new simple kinetic "strength" concept was created (Equation 16). By definition, the structural strength parameter is the cross of non-universal WLF curve with the axis $\log_{10}\tau$ at $\log_{10}\tau = -2$ (at d = 4) (Figures 2.8, 3.7, 3.9, 4.9, 5.6). "Strength" characterisation is based on changes in relaxation times of structure-forming components in the system and interaction of dispersed and continuous phases.

6.2 Structural "Strength" versus "Fluidness"

The new strength parameter classifies materials on "strong" (high value of S) which are more resistant against flow and easier to process and store, and "weak" (low value of S), which are sensitive to glass transition and difficult to process and store. Our strength classification has similarities with "Fragility" model on "fragile" (high value of m) and "strong" (low value of m) materials. Structural "fluidness" is used here as term referring to the analysing of glass-forming materials above the T_g and characterised specific changes in structural relaxation times in their amorphous state, which is similar to "fragility". Mathematically "fluidness" could be quantifying by a "fluidness" index S_f, which is equal to steepness index m. High "fluidness" index S_f means low resistance to flow in a system, while low S_f means high resistance to flow. "Strength" was compared to "fragility" concept as a modern and widely employed model at the moment. As example, experimental data for lactose-WPI (chapter III) and trehalose-maltodextrin (chapter IV) systems at different ratios were compared as carbohydrate-protein and miscible system, respectively. The same C_1 and C_2 (Tables 3.5, 4.5) constants from WLF equation were used to calculate "fluidness" index (S_f) (Equation 14) and structural "strength" parameter (S) (Equation 16). However, the strength concept can show a simple temperature value allowed above T_g without significant changes and the C_1 and C_2 values can be used to compare how relaxation times change

around and above the glass transition, i.e., the concavity and steepness of the loss in stiffness (relaxation time).

6.2.1 Lactose-WPI systems

Tables 6.1 and Figures 6.1, 6.2 show the "fluidness" measured by (S_f) and "strength" (S), which were derived using the same experimental data of lactose-WPI powders at low water contents (RH 0 – RH 44%). Fluidness decreased irregularly (Figure 6.1 b) with increasing WPI content in the system. For example, fluidness decreased linearly for anhydrous system and systems humidified at RH 23% and RH 33%, while for system humidified at RH 44% fluidness dropped between 0% and 20% of WPI content. Humidified at RH 44% pure lactose system showed the highest (133.7) (Table 6.1) fluidness, while anhydrous system showed the lowest (26.9). However, this trend changed with increasing WPI content in the system. For example, the system with 60% of WPI at RH 23% had the highest (20.9) fluidness, while at RH 33% - the lowest (18.1), with overall much narrower range of values.

All lactose-WPI systems showed statistically the same ($P>0.05$) fluidness at different humidities and water contents except 0 and 60% WPI systems, which showed irregular and non-linear behaviour (Figure 6.2 c, d). Hence, the fluidness concept could not predict flow properties of carbohydrate-protein systems at different protein and water content with required accuracy.

Table 6.1. Structural strength (S) and "fluidness" (S_f) for lactose-WPI systems with different ratios of components and humidified at different relative humidities (RH).

Lactose: WPI	RH 0%		RH 23%		RH 33%		RH 44%	
	S, ΔT	***S_f***	***S, ΔT***	***S_f***	***S, ΔT***	***m***	***S, ΔT***	***S_f***
100:0	22.9±2.7	***26.9±3.1***	21.5±0.6	***45.9±1.1***	20.6±1.6	***40.1±3.3***	17.0±1.2	***133.7±9.1***
80:20	27.9±3.6	***26.5±2.9***	22.4±1.3	***28.8±4.3***	21.6±1.5	***25.5±3.4***	21.3±0.9	***26.8±5.5***
60:40	31.0±2.8	***20.3±1.7***	24.7±3.0	***20.9±3.5***	23.3±1.9	***18.1±2.7***	22.7±1.8	***19.1±3.5***
40:60	39.6±7.1	***13.6±1.3***	26.8±4.3	***21.5±2.9***	24.1±3.8	***9.6±1.5***	24.1±1.4	***10.3±2.2***
20:80	45.0±3.2	***8.9±0.9***	33.6±3.0	***9.8±1.8***	30.8±3.4	***6.0±0.6***	29.6±3.3	***6.9±0.9***

At the same time, structural "strength" increases linearly with increasing WPI content for anhydrous and all humidified systems (Figure 6.1 a). Therefore, adding WPI increases the strength of the system, while pure lactose shows "weak" behaviour.

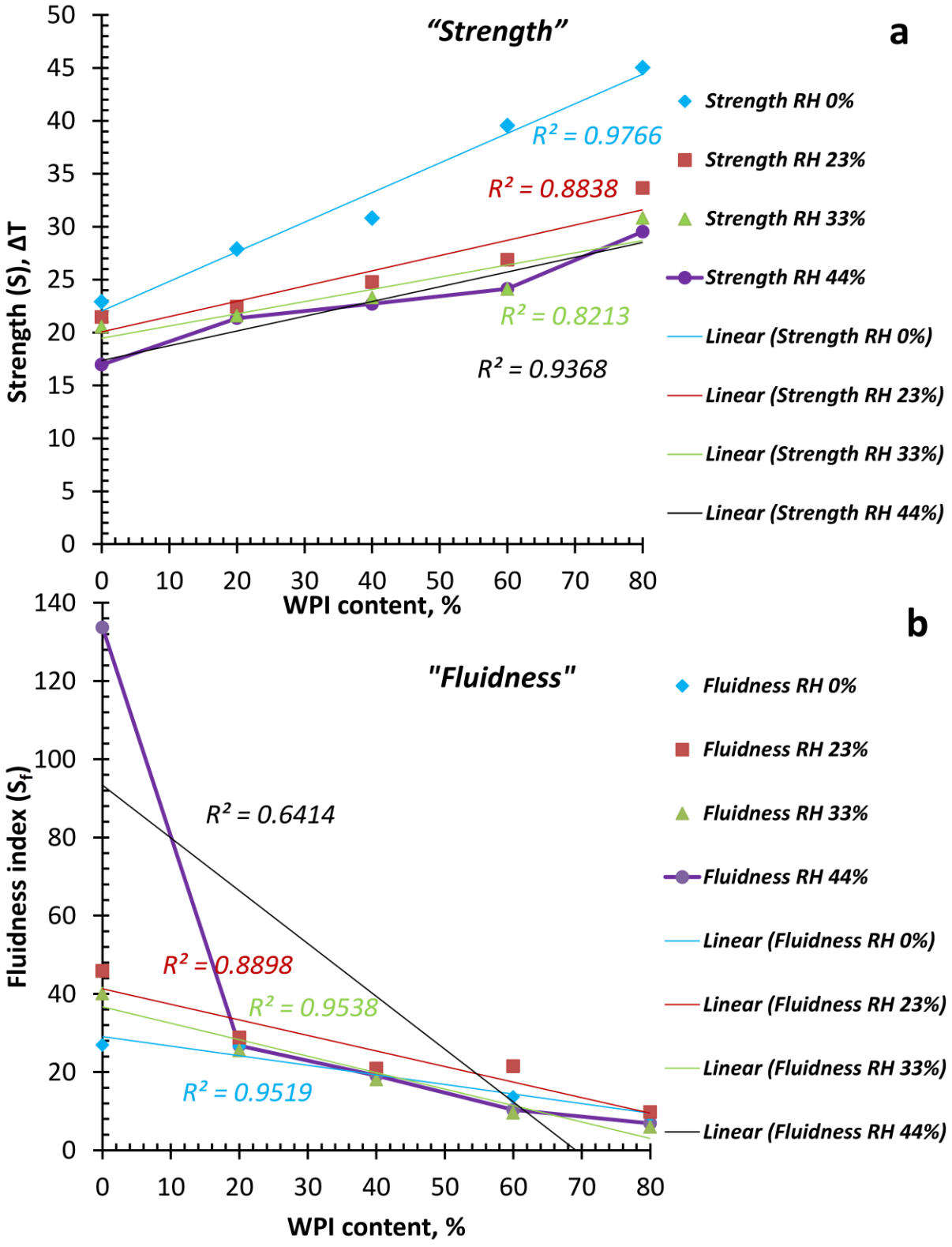

Figure 6.1. Structural strength (S) (a) and fluidness (S_f) (b) for lactose-WPI systems with different ratios of components and humidified at different relative humidities (RH).

Humidified at RH 44% pure lactose system showed the lowest (17.0) strength value while anhydrous 80% WPI system showed the highest (22.9). Overall increase in RH leads to decreasing strength of all lactose-WPI systems.

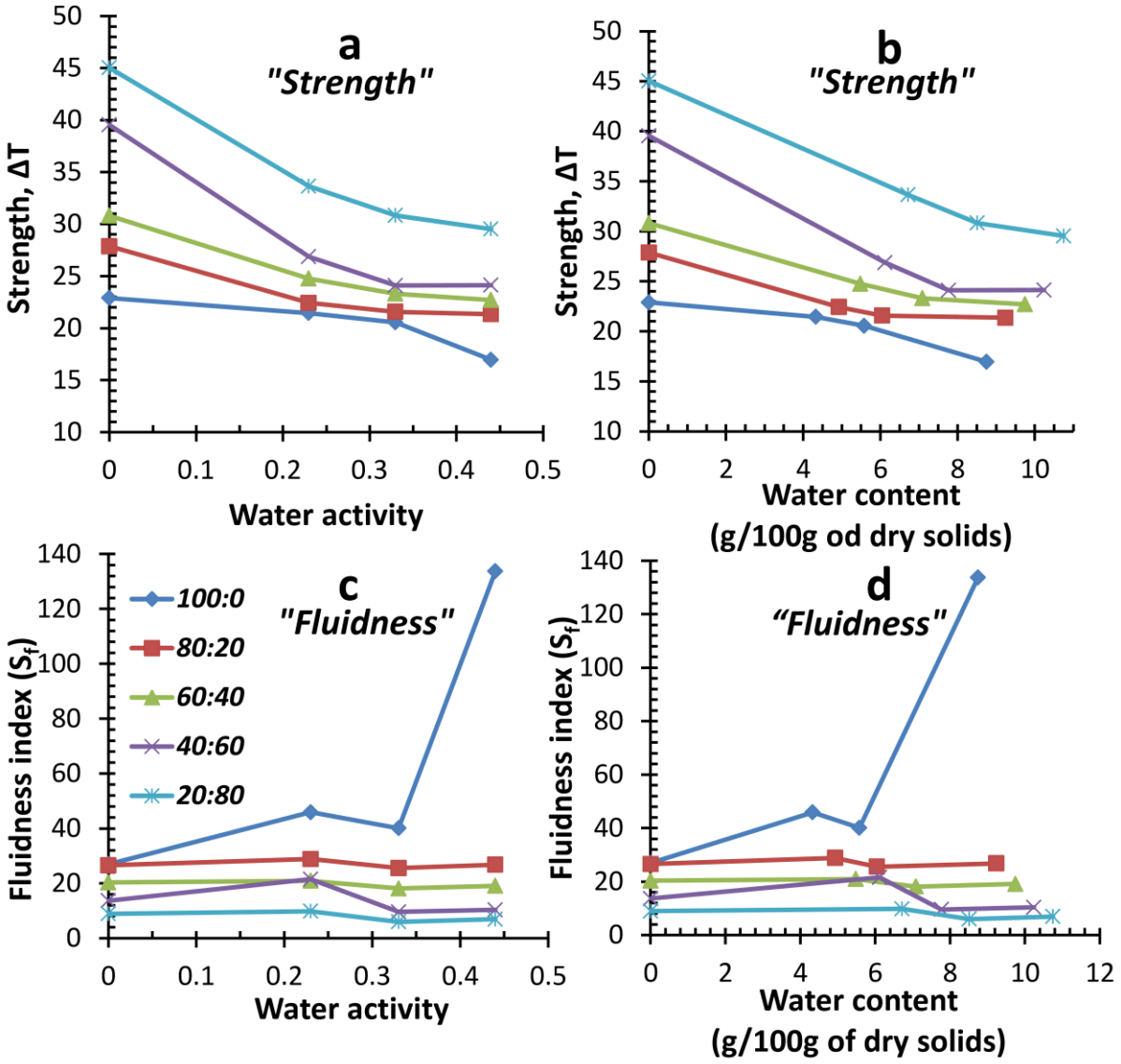

Figure 6.2. Structural strength (S)(a, b) and fluidness (S_f) (c, d) versus water activity and water content (g/100g of dry solids) for lactose-WPI systems at different component ratios (100:0; 80:20; 60:40; 40:60 and 20:80).

Structural strength was significantly decreasing ($P<0.01$) with increase of water activity and water content in the system (Figure 6.2 a, b). Moreover, strength can be calculated at any water content (Equation 17). This equation showed a good fit to experimental data (Figure 3.8). Hence structural strength concept allows predicting relaxation

behaviour for complex carbohydrate-protein systems at different component ratios and at any water content.

6.2.2 Trehalose-maltodextrin miscible systems

The comparison of "fluidness" and structural "strength" parameter of miscible trehalose-maltodextrin systems with various component ratios and at different relative humidities is presented in Table 6.2 and Figures 6.3, 6.4.

Table 6.2. Structural strength (S) and "fluidness" (S_t) for miscible trehalose-maltodextrin systems with different ratios of components and humidified at different relative humidities (RH).

Trehalose: Maltodextrin	RH 0%		RH 11%		RH 23%		RH 33%		RH 44%	
	S, ΔT	***m***	***S, ΔT***	***m***	***S, ΔT***	***m***	***S, ΔT***	***m***	***S, ΔT***	***m***
100:0	17.6±3.1	***43.2±3.9***	14.6±2.7	***70.3±5.2***	12.6±1.3	***66.2±5.1***	11.9±2.0	***70.2±7.6***	9.2±2.1	***166.0±12.4***
80:20	22.3±2.4	***36.1±3.2***	16.5±3.2	***58.3±3.3***	15.8±1.6	***54.7±4.2***	13.8±1.8	***72.8±7.3***	11.2±2.2	***135.2±11.3***
60:40	31.4±2.7	***41.8±3.5***	19.6±3.1	***44.9±3.7***	18.5±3.6	***63.8±5.3***	17.8±3.1	***47.5±5.5***	13.4±1.9	***117.2±9.5***
40:60	45.6±3.2	***29.5±3.8***	26.4±1.9	***29.1±2.1***	25.5±2.2	***40.6±3.6***	24.4±2.4	***22.1±2.9***	16.7±2.2	***112.7±9.7***
20:80	64.9±3.3	***13.0±2.3***	34.5±2.2	***21.5±2.3***	34.7±2.2	***25.1±2.8***	27.2±2.7	***17.8±2.1***	18.9±2.5	***49.7±3.6***
0:100	73.2±5.2	***6.1±1.5***	43.2±4.1	***16.5±2.4***	41.8±3.8	***24.6±3.3***	34.9±2.4	***19.3±2.2***	20.9±2.7	***45.9±4.1***

Fluidness decreased linearly (Figure 6.3 a) with increasing maltodextrin content in the systems humidified at RH 11% and RH 44%, while for anhydrous and humidified at RH 23% and RH 33% systems, fluidness index decreased irregularly. For example, system humidified at RH 33% showed the highest fluidness (72.8) at 20% of maltodextrin content and the lowest (17.8) at 80% of maltodextrin content. Systems humidified at RH 11%, RH 23% and RH 33% showed statistically the same ($P>0.05$) fluidness for 100:0, 20:80 and 0:100 trehalose-maltodextrin systems (Figure 6.4 a, b), while fluidness in 40:60, 60:40 and 80:20 systems decreased irregularly with increasing water activity and water content. Hence fluidness model

provides only qualitative results for the miscible system and cannot be used as an analytical tool.

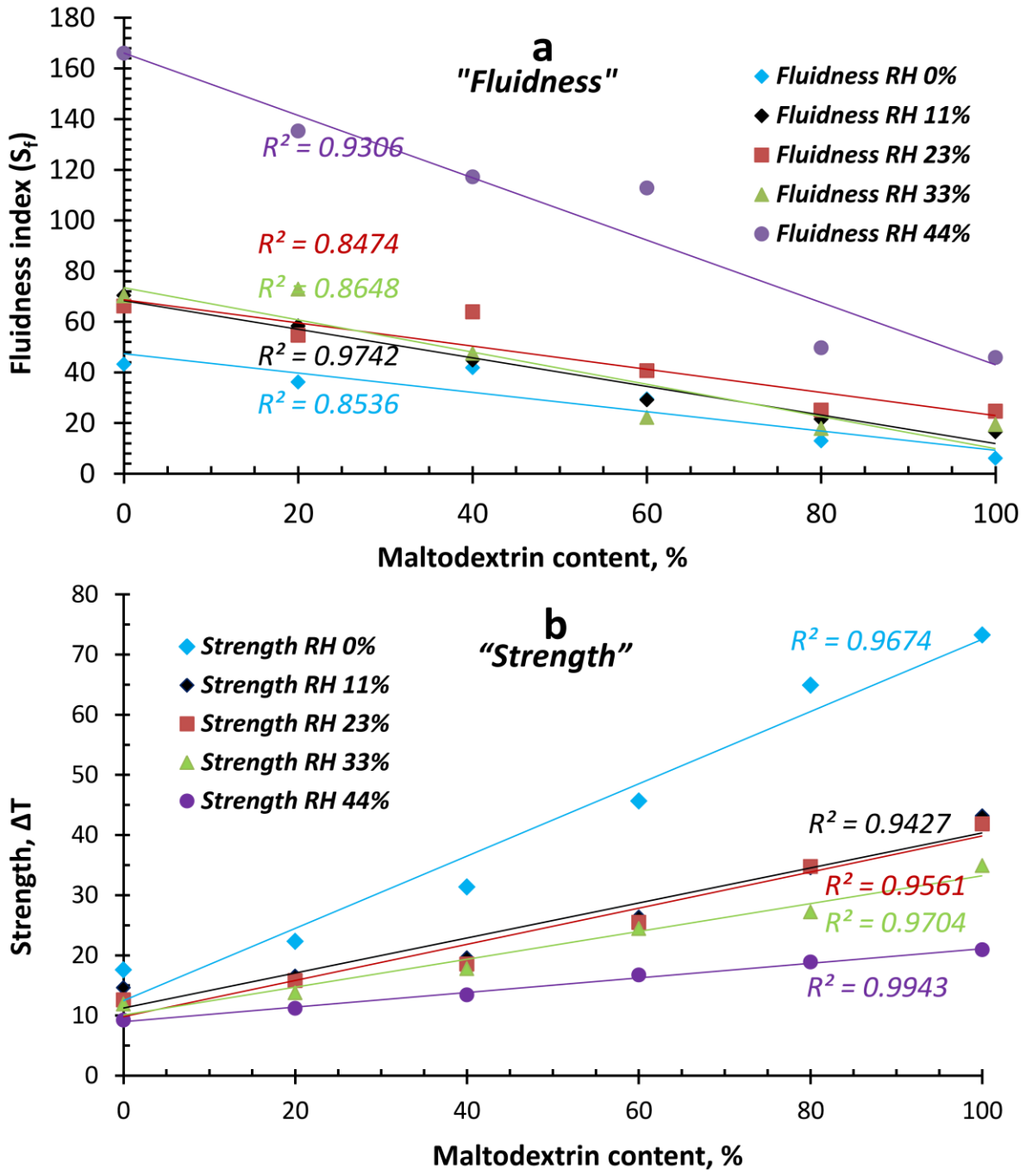

Figure 6.3. Structural strength (S)(b) and Fluidness (S_f)(a) versus maltodextrin content (%) in trehalose-maltodextrin systems at different relative humidities (RH).

At the same time structural strength increases linearly (Figure 6.3 b) with increasing maltodextrin content in humidified and anhydrous systems. Humidified at RH 44% pure

trehalose system showed the lowest (9.2) strength value while anhydrous pure maltodextrin system showed the highest (73.2). Maltodextrin has higher strength as compared to trehalose at any water activity and water content. Strength shows a linear behaviour and can be calculated at any maltodextrin content with a high accuracy.

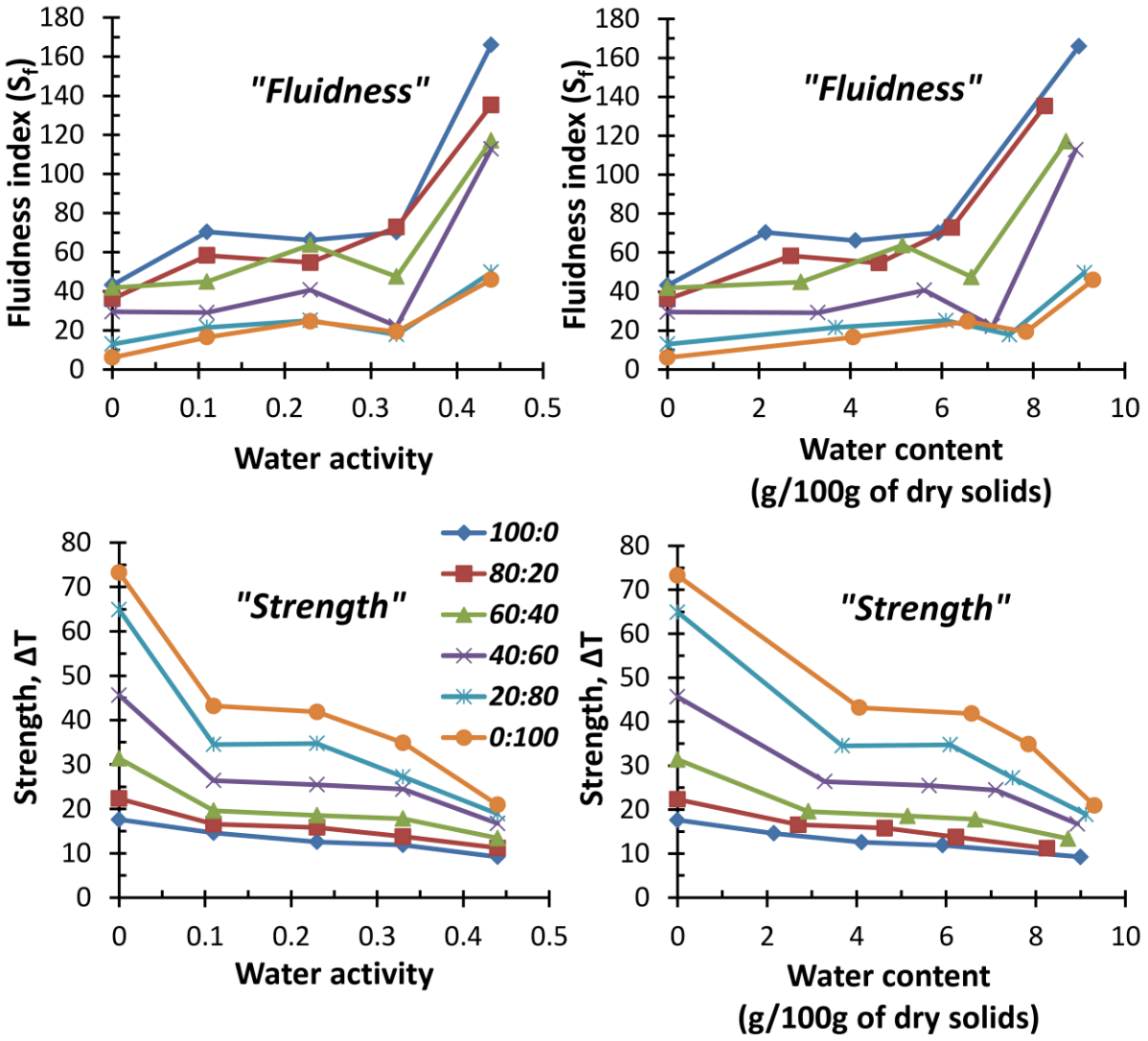

Figure 6.4. Structural strength (S)(c, d) and "fluidness" (S_f) (a, b) versus water activity and water content (g/100g of dry solids) for trehalose-maltodextrin systems at different component ratios (100:0; 80:20; 60:40; 40:60; 20:80 and 0:100).

Structural strength consistently decreased with increasing water activity and water content in all miscible trehalose-maltodextrin systems. Equation 17 allowed calculating S at any water content (including pure water) and showed good fit for to trehalose-maltodextrin experimental data (Figure 4.8).

Trehalose-WPI (chapter II) and partially crystalline (chapter V) systems showed similar trends. Thereby structural strength approach allows means to estimate critical relaxation properties, Different complex systems with various components and different water content are described by a high accuracy, which gives an advantage in comparison to "fluidness" model.

6.3 Structural strength analysis of various food system

At the present study carbohydrate-protein (trehalose-WPI (chapter II), lactose-WPI (chapter III), miscible trehalose-maltodextrin (chapter IV)) and partially crystalline (partially crystalline trehalose (chapter V)) systems were chosen as models of complex food systems. Structural strength analysis which included fractional water sorption, rheology, DSC, DMA, DEA and light microscopy was carried out for all types of model systems.

6.3.1 Fractional water sorption analysis

A fractional water sorption analysis (Potes et al., 2012, Potes, 2014) has been done for trehalose-WPI, lactose-WPI, trehalose-maltodextrin and partially crystalline trehalose systems. This method allows calculating real water content for complex systems at very high water activities (Figures 2.2, 3.2, 4.2, 5.1). Experimental water sorption analysis also showed crystallisation in amorphous system, which can occur at high water activities. Knowing the real water sorption isotherm allows controlling water content and guids to avoid crystallisation of amorphous components in carbohydrate-protein, miscible and partially crystalline systems.

6.3.2 Thermal properties

The calorimetric glass transition temperature was detected for all systems at various ratios of components and at different water contents. Water, as strong plasticizer significantly increases mobility of molecules of the amorphous component, which results in the decrease of T_g values with increasing water content in all systems (Figures 2.3, 3.3, 4.3) (Roos and Karel, 1991a; Silalai and Roos, 2011).

Carbohydrate-protein systems showed almost protein-independent glass transition temperature. The little increasing of the T_g values occurs due to the high molecular weight of WPI molecules, which can interact with carbohydrates (lactose, trehalose) to some extent

(López-Dıez and Bone, 2004; Haque and Roos, 2004). The T_g increases with increasing maltodextrin content in miscible trehalose-maltodextrin systems due to the high molecular weight of maltodextrin molecules (Roos and Karel, 1991a; Buera et al., 1992; Bhandari et al., 1997; Bhandari and Howes, 1999; Avaltroni et al., 2004; Silalai and Roos, 2011). This increase in the T_g values can be an evidence of trehalose-maltodextrin system miscibility (Krause, 1986; Silalai and Roos, 2011).

Partially crystalline trehalose showed crystals-independent glass transition temperature values (Table 5.2). However, the heat capacity (C_p) over the T_g region proportionally decreases with increasing crystals content.

6.3.3 Structural relaxations

Dynamic mechanical measurements were done for all systems while dielectric analysis was used only for miscible trehalose-maltodextrin systems. Both DMA and DEA spectra showed frequency-dependent behavior, and were used in multi-frequency mode, which allowed determination of α-relaxation temperatures. For all systems, the value of T_α was highly dependent on water content and decreased with increasing water content in the system, which can be explained by the free-volume theory (Slade et al., 1991; Royall et al., 2005; Meinders and van Vliet, 2009). Probably, water increases the free volume in the system and molecular mobility of amorphous material consequently.

For anhydrous and humidified (0.11, 0.23, 0.33, 0.44 a_w) *carbohydrate-protein systems* the T_α of amorphous trehalose, lactose and trehalose-WPI, lactose-WPI systems occurred at ~20-30°C above the onset T_g. The presence of WPI in the system significantly increased the T_α values (Figures 2.4, 3.5; Tables 2.4, 3.4). The amorphous trehalose and lactose showed the lowest T_α, while 20:80 trehalose-WPI and lactose-WPI systems - the highest T_α for all humidities, respectively. This dependence demonstrated that the WPI could affect the molecular mobility of amorphous component. WPI is macromolecular component and probably reduces diffusion process in the system (Silalai and Roos, 2011, Potes et al., 2012). In this study, we showed that presence of water or protein is important for the changes of molecular mobility, which could be detected by DMA.

For *miscible trehalose-maltodextrin system*, the peak of α-relaxation occurred at ~20-30°C above the onset T_g and up to ~60-70°C above the onset T_g for DEA measurements (Figure 4.5, Table 4.4). High maltodextrin content systems showed broadened DMA and

DEA peaks with less intensity. Temperature of α-relaxation for these systems was higher than for systems with low amounts of maltodextrins, probably because of complex composition of maltodextrin component molecules, which can reduce molecular mobility of trehalose due to high degree of association (Silalai and Roos, 2011).

For *partially-crystalline systems*, high amount of crystalline component led to lowering of α-relaxation temperature peak (Figure 5.3, Table 5.3), due to significant difference between crystalline and amorphous particle sizes (crystalline particles need less mechanical energy than amorphous and α-relaxations occurs at lower temperature). Also crystalline phase may slightly decrease α-relaxation temperature due to sliding or sanding effect inside the partially crystalline system (Cano-Chauca et al., 2005). The big differences in structural strength values were observed for anhydrous partially crystalline trehalose systems, while for humidified systems (0.44 a_w) these differences were not significant and α-relaxation occurred at similar temperatures for all amorphous and crystalline ratios.

6.3.4 Rheology

Rheological measurements were done for high water content (60, 70, 80 and 90%) carbohydrate-protein and miscible systems with various ratios of components. For all systems apparent viscosity significantly decreases upon heating (Figures 2.5, 3.4, 4.4). Original WLF (Equation 10) and Equation 15 allow calculating structural relaxation time for these systems. The Gordon-Taylor equation (Equation 4) was used for prediction of T_g values for high water content carbohydrate-protein and miscible systems. These data allow intrapolation of glass transition temperature and strength values at any water content.

6.3.5 Morphology observations

Microscope observation of *partially crystalline trehalose system* with different ratios of components and at different relative humidities showed that crystalline and amorphous components of trehalose became more transparent during heating to above T_g. However, at the same time the external morphology of the structure was not changed until the temperature about 135°C, where the "solid" sample started changing morphological shape ("edge roundness") with an increasing mobility of the phase, although stays firm (sticky) (Sussich et al, 1998) (Figure 5.2). These observations were the same for anhydrous and humidified (0.11, 0.23, 0.33 and 0.44a_w) partially crystalline trehalose systems.

6.3.6 WLF constants and structural strength

In chapter II, based on WLF equation with "non-universal" constant, the structural strength parameter was defined (Equation 16). WLF equation is a simple empirical model (Figure 2.6), but at the same time it shows the best fit to experimental data at low and high water contents (Figure 2.7). Structural strength analysis uses WLF equation in a simple and convenient form, describing the structural relaxation time – temperature dependence over a wide temperature range, including the glass transition temperature region. Strength significantly increases with increasing WPI content in the system, which indicates that WPI shows more "strong" behaviour compare to "weak" trehalose.

Similar results were demonstrated for lactose-WPI carbohydrate-protein system (chapter III). This system was used to create a relationship (Equation 17), which allowed determination of strength values over a range of water contents (from anhydrous system to pure water) (Figures 3.8, 3.10). Structural strength of pure water (6.0 °C) and WPI at different water contents were also predicted and determined.

The miscible carbohydrate (trehalose-maltodextrin) systems (chapter IV) showed that the strength concept could explain and predict variation of structural relaxation times at different ratios of miscible components and at various water contents (Figures 4.8, 4.10).

Moreover, structural strength analysis has a good consistency in calculating amorphous or crystalline content in *partially crystalline systems* (chapter V). The strength linearly decreased with increasing content of crystals in partially crystalline systems (Figures 5.5, 5.7).

6.4 Application of the research outcomes and future work

The results from the current study are useful in understanding and predicting thermodynamic and kinetic behaviour of complex food systems in a wide temperature range including the T_g region, that important in food stability and safety. For all systems, a known strength value for pure substances allows calculation of a strength estimate for mixtures of such components at various water contents. These possibilities make structural strength concept a powerful tool in analyses and prediction of properties of amorphous carbohydrates, carbohydrate-protein, miscible, precrystallise and carbohydrate-protein-lipid systems in food, such as dairy powders, infant formulae, confectionary products, cheese products,

supplements, high protein foods, etc. The outcomes of current research can be applied in different areas such as food, nutritional, pharmaceutical, polymer and material science to develop stability and quality control during processing and storage of amorphous materials. The strength concept has a wide range of aplications, therefore in the future strength analysis can be applied to study kinetics of diffusion phenomena, browning and Maillard reactions and oxidations in various food materials.

6.5 Overall conclusions

In the present study, a new approach describing structural relaxation time – temperature dependence have defined and developed, using carbohydrate-protein (trehalose-WPI, lactose-WPI), miscible (trehalose-maltodextrin) and precrystallise (partially crystalline trehalose) systems. The effect of components and water content on a strength parameter was also investigated.

The overall conclusions could be stated as follow:

- Based on the modified WLF equation a new simple and convenient structural strength concept was created. Strength allows describing the relaxation time – temperature dependence over a wide temperature range, including region around T_g.
- Structural strength concept was developed in terms of component and water contents influence on a parameter.
- Fractional water sorption analysis of amorphous and partially crystalline systems allows controlling water content and crystallization at different water activities (up to 0.85 a_w) and different ratios of components.
- DSC, DMA, DEA, rheology: the glass transition temperature, alpha relaxation temperature and structural strength parameter significantly decreased with increasing water content in the system.
- The relationship, which allows predicting values of new parameter for pure components and their mixtures at various water contents was created and experimentally verified. The values of strength parameter for pure water and pure food components were detected and predicted.
- Structural strength concept showed advantages in comparison with “fragility” model.
- Strength model can explain and predict variations of structural relaxation times at different ratios of miscible components at different water contents.

- Structural strength analysis has a good consistency in calculating the content of amorphous or crystalline components in partially crystalline systems.

BIBLIOGRAPHY

Adam, G. and Gibbs, J. H. (1965). On the temperature dependence of cooperative relaxation properties in glass-forming liquids. The Journal of Chemical Physics 43: 139-146.

Adhikari, B., Howes, T., Shrestha, A. and Bhandari, B. (2007). Effect of surface tension and viscosity on the surface stickiness of carbohydrate and protein solutions. Journal of Food Engineering 79 (4): 1136-1143.

Aguilera, J.M., Levi, G. and Karel, M. (1993). Effect of water content on the glass transition and caking of fish protein hydrolyzates. Biotechnology Progress 9(6): 651-654.

Alves, N. M., Mano, J. F., Ribelles, J. G. and Tejedor, J. G. (2004). Departure from the Vogel behaviour in the glass transition—thermally stimulated recovery, creep and dynamic mechanical analysis studies. Polymer, 45 (3): 1007-1017.

Angell, C. (2002). Liquid fragility and the glass transition in water and aqueous solutions. Chemical Reviews 102(8): 2627-2650.

Angell, C. and Smith, D. (1982). Test of the entropy basis of the Vogel-Tammann-Fulcher equation. Dielectric relaxation of polyalcohols near Tg. The Journal of Physical Chemistry 86 (19): 3845-3852.

Angell, C. A. (1991a). Thermodynamic aspects of the glass transition in liquids and plastic crystals. Pure and Applied Chemistry 63 (10): 1387-1392.

Angell, C. A. (1991b). Relaxation in liquids, polymers and plastic crystals-strong/fragile patterns and problems. Journal of Non-Crystalline Solids 131: 13-31.

Angell, C. A., Ngai, K. L., McKenna, G. B., McMillan, P. F. and Martin, S. W. (2000). Relaxation in glassforming liquids and amorphous solids. Journal of Applied Physics (88): 3113-3157.

Arvanitoyannis, I., Blanshard, J., Izzard, M., Lillford, P. and Ablett, S. (1993). Calorimetric study of the glass transition occurring in aqueous glucose: fructose solutions. Journal of the Science of Food and Agriculture 63: 177-188.

Avaltroni, F., Bouquerand, P. and Normand, V., (2004). Maltodextrin molecular weight distribution influence on the glass transition temperature and viscosity in aqueous solutions. Carbohydrate Polymers 58 (3): 323-334.

Bhandari, B., Bansal, N., Zhang, M. and Schuck, P. (2013). Handbook of food powders: processes and properties. Elsevier. Woodhead Publishing. Limited. Oxford. pp. 1-12.

Bhandari, B. and Howes, T., (1999). Implication of glass transition for the drying and stability of dried foods. Journal of Food Engineering 40 (1): 71-79.

Bhandari, B.R., Datta, N., Crooks, R., Howes, T. and Rigby, S. (1997). A semi-empirical approach to optimise the quantity of drying aids required to spray dry sugar-rich foods. Drying Technology 15 (10): 2509-2525.

Bell, L.N. and Labuza, T.P. (2000). Moisture sorption: practical aspects of isotherm measurement and use. St. Paul, MN: American Association of Cereal Chemists. Inc. pp. 1-6.

Bellows, R. and King, C.J. (1973). Product collapse during freeze drying of liquid foods. AICHE Symposium Series, 69 (1973), pp. 33-41.

Biliaderis, C., Lazaridou, A., Mavropoulos, A. and Barbayiannis, N. (2002). Water plasticization effects on crystallization behavior of lactose in a co-lyophilized amorphous polysaccharide matrix and its relevance to the glass transition. International Journal of Food Properties 5 (2): 463-482.

Blahovec, J. and Yanniotis, S. (2009). Modified classification of sorption isotherms. Journal of Food Engineering 91 (1): 72-77.

Böhmer, R., Ngai, K. L., Angell, C. A., and Plazek, D. J. (1993). "Nonexponential relaxations in strong and fragile glass formers." The Journal of chemical physics, 99(5), 4201-4209.

Boonyai, P., Bhandari, B., Howes, T. (2004). "Stickiness measurement techniques for food powders: a review." Powder Technology 145(1): 34-46.

Boonyai, P., Bhandari, B., & Howes, T. (2005). "Measurement of glass–rubber transition temperature of skim milk powder by static mechanical test." Drying Technology, 23(7), 1499-1514.

Britannica, E. (2015). The Editors of Encyclopaedia Britannica. Encyclopædia Britannica. https://www.britannica.com/science/activation-energy.

Bronlund, J., and Paterson, T. (2004). Moisture sorption isotherms for crystalline, amorphous and predominantly crystalline lactose powders. International Dairy Journal, 14 (3): 247-254.

Buckton, G. and Darcy, P., (1995). The use of gravimetric studies to assess the degree of crystallinity of predominantly crystalline powders. International Journal of Pharmaceutics 123: 265-271.

Buera, M.D.P., Levi, G. and Karel, M., (1992). Glass transition in poly (vinylpyrrolidone): effect of molecular weight and diluents. Biotechnology Progress 8 (2): 144-148.

Cano-Chauca, M., Stringheta, P. C., Ramos, A. M. and Cal-Vidal, J. (2005). Effect of the carriers on the microstructure of mango powder obtained by spray drying and its functional characterization. Innovative Food Science & Emerging Technologies, 6 (4): 420-428.

Casalini, R. and C. Roland (2007). An equation for the description of volume and temperature dependences of the dynamics of supercooled liquids and polymer melts. Journal of Non-Crystalline Solids 353 (41): 3936-3939.

Clegg, J., (1965). The origin of threhalose and its significance during the formation of encysted dormant embryos of Artmia salina. Comparative Biochemistry and Physiology 14(1): 135-143.

Champion, D., Le Meste and M., Simatos, D., (2000). Towards an improved understanding of glass transition and relaxations in foods: molecular mobility in the glass transition range. Trends in Food Science and Technology 11(2): 41-55.

Chirife, J. and A. J. Fontana (2007). Introduction: Historical highlights of water activity research. Water Activity in Foods: Fundamentals and Applications (G.V. Barbosa-Cánovas, A.J. Fontana, S.J. Schmidt and T.P. Labuza, eds.) Blackwell Publishing, Iowa., pp. 3–13.

Chung, H.J. and Lim, S.T., (2003). Physical aging of glassy normal and waxy rice starches. Carbohydrate Polymers 53 (2): 205-211.

Crowe, L.M., Crowe, J.H., Rudolph, A., Womersley, C. and Appel, L., (1985). Preservation of freeze-dried liposomes by trehalose. Archives of Biochemistry and Biophysics 242 (1): 240-247.

Cruz, I. B., Oliveira, J. C., and MacInnes, W. M. (2001). Dynamic mechanical thermal analysis of aqueous sugar solutions containing fructose, glucose, sucrose, maltose and lactose. International journal of food science & technology, 36 (5): 539-550.

Darby, R. (1976). Viscoelastic Fluids: An Introduction to Their Properties and Behavior, Marcel Dekker, Inc, New York.

Dokic, P., Jakovljevic, J. and Dokic-Baucal, L., (1998). Molecular characteristics of maltodextrins and rheological behaviour of diluted and concentrated solutions. Colloids and Surfaces A: Physicochemical and Engineering Aspects 141(3): 435-440.

Downton, G. E., Flores-Luna, J. L., and King, C. J. (1982). Mechanism of stickiness in hygroscopic, amorphous powders. Industrial & Engineering Chemistry Fundamentals, 21 (4): 447-451.

Ediger, M. D., Inoue, T., Cicerone, M. T., and Blackburn, F. R. (1996). Probe rotation near and below the glass transition temperature: Relationship to viscoelasticity and physical aging. In Macromolecular Symposia (Vol. 101, No. 1, pp. 139-146). Hüthig & Wepf Verlag.

Elbein, A.D., Pan, Y., Pastuszak, I. and Carroll, D., (2003). New insights on trehalose: a multifunctional molecule. Glycobiology 13 (4): 17R-27R.

Ehrenfest, P. (1933). Phase changes classified according to the singularities of the thermodynamic potential. Proceedings of the Academy of Science, Amsterdam 36, 153; Suppl. 75b, Mitt. Kammerlingh Onnes Inst., Leiden.

Ermolina, I., Polygalov, E., Bland, C., and Smith, G. (2007). Dielectric spectroscopy of low-loss sugar lyophiles: II. Relaxation mechanisms in freeze-dried lactose and lactose monohydrate. Journal of Non-Crystalline Solids, 353 (47): 4485-4491.

Fan, F. and Roos, Y.H., (2016a). Structural relaxations of amorphous lactose and lactose-whey protein mixtures. Journal of Food Engineering 173, 106-115.

Fan, F.,Roos and Y. H. (2016b). Crystallization and structural relaxation times in structural strength analysis of amorphous sugar/whey protein systems. Food Hydrocolloids (60): 85-97.

Ferry, J. D. (1980). Viscoelastic properties of polymers. John Wiley & Sons. New York.

Foster, K.D., Bronlund, J.E. and Paterson, A.T., (2005). The prediction of moisture sorption isotherms for dairy powders. International Dairy Journal 15(4): 411-418.

Fulcher, G. (1925). Analysis of recent measurements of the viscosity of glasses.—ii1. Journal of the American Ceramic Society 8 (12): 789-794.

Gaisford, S., Kett, V., and Haines, P. (Eds.). (2016). Principles of thermal analysis and calorimetry. Royal society of chemistry. Cambridge, UK.

Gearing, J., Malik, K.P. and Matejtschuk, P., (2010). Use of dynamic mechanical analysis (DMA) to determine critical transition temperatures in frozen biomaterials intended for lyophilization. Cryobiology 61 (1): 27-32.

Gibbs, J. H. and E. A. DiMarzio (1958). Nature of the glass transition and the glassy state. The journal of chemical physics 28 (3): 373-383.

Gonnet, J.M., Guillet, J., Sirakov, I., Fulchiron, R. and Seytre, G., (2002). "In-situ" monitoring of the non-isothermal crystallization of polymers by dielectric spectroscopy. Polymer Engineering Science 42 (6): 1159-1170.

Gordon, M. and J. S. Taylor (1952). Ideal copolymers and the second-order transitions of synthetic rubbers. I. Non-crystalline copolymers. Journal of Chemical Technology and Biotechnology 2 (9): 493-500.

Green, J.L. and Angell, C.A., (1989). Phase relations and vitrification in saccharide-water solutions and the trehalose anomaly. The Journal of Physical Chemistry 93 (8): 2880-2882.

Halle, B., (2004). Protein hydration dynamics in solution: a critical survey. Philosophical Transactions of the Royal Society B: Biological Sciences 359(1448), 1207-1224.

Haque, M. and Roos, Y., **(2004a).** Water Sorption and Plasticization Behavior of Spray-dried Lactose/Protein Mixtures. Journal of food science 69 (8), E384-E391.

Haque, M.K., Kawai, K. and Suzuki, T., (2006). Glass transition and enthalpy relaxation of amorphous lactose glass. Carbohydrate research 341 (11): 1884-1889.

Haque, M.K. and Roos, Y., (2004b). Water Plasticization and Crystallization of Lactose in Spray-dried Lactose/Protein Mixtures. Journal of Food Science 69 (1): FEP23-FEP29.

Hardy, L., Stevenson, I., Boiteux, G., Seytre, G. and Schönhals, A., (2001). Dielectric and dynamic mechanical relaxation behaviour of poly (ethylene 2, 6 naphthalene dicarboxylate). I. Amorphous films. Polymer 42 (13): 5679-5687.

Harnkarnsujarit, N., Charoenrein, S. and Roos, Y.H., (2012). Porosity and Water Activity Effects on Stability of Crystalline β-Carotene in Freeze-Dried Solids. Journal of food science 77(11), E313-E320.

Herrington, B., (1934). Some physico-chemical properties of lactose: I. The spontaneous crystallization of supersaturated solutions of lactose. Journal of Dairy Science 17(7), 501-518.

Jay, J. M. (2012). Modern food microbiology. Springer Science & Business Media. Berlin.

Jouppila, K. and Roos, Y., (1994). Glass transitions and crystallization in milk powders. Journal of Dairy Science 77 (10): 2907-2915.

Jouppila, K., Kansikas, J., and Roos, Y. H. (1997). Glass transition, water plasticization, and lactose crystallization in skim milk powder. Journal of Dairy Science 80 (12): 3152-3160.

Kalichevsky, M., Blanshard, J., (1992). A study of the effect of water on the glass transition of 1: 1 mixtures of amylopectin, casein and gluten using DSC and DMTA. Carbohydrate Polymers 19 (4): 271-278.

Kalichevsky, M. T., Jaroszkiewicz, E. M., Ablett, S., Blanshard, J. M. V., and Lillford, P. J. (1992). The glass transition of amylopectin measured by DSC, DMTA and NMR. Carbohydrate Polymers 18 (2): 77-88.

Kalichevsky, M.T. and Blanshard, J.M., (1993). The effect of fructose and water on the glass transition of amylopectin. Carbohydrate Polymers 20 (2): 107-113.

Kedward, C. J., MacNaughtan, W., and Mitchell, J. R. (2000). Crystallization kinetics of amorphous lactose as a function of moisture content using isothermal differential scanning calorimetry. Journal of food science, 65 (2): 324-328.

Kestin, J., Sokolov, M. and Wakeham, W.A., (1978). Viscosity of liquid water in the range− 8 C to 150 C. Journal of Physical and Chemical Reference Data 7 (3): 941-948.

Kilmartin, P.A., Reid, D.S. and Samson, I., (2004). Dielectric properties of frozen maltodextrin solutions with added NaCl across the glass transition. Journal of the Science of Food and Agriculture 84 (11), 1277-1284.

Kittel, C. and D. F. Holcomb (1967). Introduction to solid state physics. American Journal of Physics 35 (6): 547-548.

Kokini, J., Cocero, A., Madeka, H., De Graaf, E., (1994). The development of state diagrams for cereal proteins. Trends in Food Science & Technology 5 (9): 281-288.

Krause, S., (1986). Polymer-polymer miscibility. Pure and applied chemistry 58 (12), 1553-1560.

Labuza, T.P., (1984). Moisture sorption: practical aspects of isotherm measurement and use. American Association of Cereal Chemists.

Pitaevskii, L. P., E. M. Lifshitz, and J. B. Sykes. (2013). Course of Theoretical Physics: Physical Kinetics. Vol. 10. Elsevier. Amsterdam.

Landau, L. D. and E. M. Lifshitz (1984). Physique statistique. Editions Mir, Moscow. pp. 583.

Landel, R. F. and L. E. Nielsen (1993). Mechanical properties of polymers and composites. CRC Press. Florida.

Lehto, V.-P., Tenho, M., Vähä-Heikkilä, K., Harjunen, P., Päällysaho, M., Välisaari, J., Niemelä, P. and Järvinen, K., (2006). The comparison of seven different methods to quantify the amorphous content of spray dried lactose. Powder Technology 167 (2): 85-93.

Levine, H. and L. Slade (1986). A polymer physico-chemical approach to the study of commercial starch hydrolysis products (SHPs). Carbohydrate Polymers 6 (3): 213-244.

Levine, H. and Slade, L., (1988). Thermomechanical properties of small-carbohydrate–water glasses and ‘rubbers’. Kinetically metastable systems at sub-zero temperatures. Journal of the Chemical Society, Faraday Transactions 1: Physical Chemistry in Condensed Phases 84 (8): 2619-2633.

Lillie, M. and Gosline, J., (1990). The effects of hydration on the dynamic mechanical properties of elastin. Biopolymers 29 (8-9): 1147-1160.

Linden, G. and Lorient, D., (1999). New ingredients in food processing: biochemistry and agriculture. CRC Press. Florida.

Liu, Y., Bhandari, B., and Zhou, W. (2006). Glass transition and enthalpy relaxation of amorphous food saccharides: a review. Journal of Agricultural and Food Chemistry 54 (16): 5701-5717.

Longinotti, M.P. and Corti, H.R., (2008). Viscosity of concentrated sucrose and trehalose aqueous solutions including the supercooled regime. Journal of Physical and Chemical Reference Data 37 (3): 1503-1515.

López-Dıez, E. and Bone, S., (2004). The interaction of trypsin with trehalose: an investigation of protein preservation mechanisms. Biochimica et Biophysica Acta (BBA)-General Subjects 1673 (3): 139-148.

Luyben, W. L. (1989). Process modeling, simulation and control for chemical engineers. McGraw-Hill Higher Education. New-York.

Mackin, L., Zanon, R., Park, J.M., Foster, K., Opalenik, H. and Demonte, M., (2002). Quantification of low levels (< 10%) of amorphous content in micronised active batches using dynamic vapour sorption and isothermal microcalorimetry. International journal of pharmaceutics 231 (2): 227-236.

Maidannyk, V. A. and Roos, Y. H. (2016). Modification of the WLF model for characterization of the relaxation time-temperature relationship in trehalose-whey protein isolate systems. Journal of Food Engineering, 188: 21-31.

Maidannyk, V. A., and Roos, Y. H. (2017). Water sorption, glass transition and "strength" of lactose–Whey protein systems. Food Hydrocolloids (70): 76-87.

Maidannyk, V. A., and Roos, Y. H. (2017b). . Structural strength analysis of partially crystalline trehalose. LWT – Food Science and Technology. In press.

Maidannyk, V. A., Nurhadi, B., and Roos, Y. H. (2017). Structural strength analysis of amorphous trehalose-maltodextrin systems. Food Research International (96): 121-131.

Matsuoka, S. (1992). Relaxation phenomena in polymers. Hanser Munich etc. Munich.

Meinders, M. B. and T. van Vliet (2009). Modeling water sorption dynamics of cellular solid food systems using free volume theory. Food Hydrocolloids 23 (8): 2234-2242.

Miller, D.P., de Pablo, J.J. and Corti, H.R., (1999). Viscosity and glass transition temperature of aqueous mixtures of trehalose with borax and sodium chloride. The Journal of Physical Chemistry B 103 (46): 10243-10249.

Miller, D.P. and de Pablo, J.J., (2000). Calorimetric solution properties of simple saccharides and their significance for the stabilization of biological structure and function. The Journal of Physical Chemistry B 104 (37): 8876-8883.

Moates, G. K., Noel, T. R., Parker, R., and Ring, S. G. (2001). Dynamic mechanical and dielectric characterisation of amylose–glycerol films. Carbohydrate Polymers 44 (3): 247-253.

Morison, K.R., Mackay, F.M., (2001). Viscosity of lactose and whey protein solutions. International Journal of Food Properties 4 (3): 441-454.

Netto, F., Desobry, S., Labuza, T., (1998). Effect of water content on the glass transition, caking and stickiness of protein hydrolysates. International Journal of Food Properties 1(2): 141-161.

Noel, T.R., Parker, R., Ring, S.G., (2000). Effect of molecular structure and water content on the dielectric relaxation behaviour of amorphous low molecular weight carbohydrates above and below their glass transition. Carbohydrate research 329 (4): 839-845.

Nurhadi, B. (2016). Maltodextrin-incorporated-vacuum-dried honey powder: processing and stability. PhD Thesis, University College Cork.

Nurhadi, B., Roos, Y.H. and Maidannyk, V., (2016). Physical properties of maltodextrin DE 10: Water sorption, water plasticization and enthalpy relaxation. Journal of Food Engineering 174: 68-74.

Ojovan, M. I. and W. E. Lee (2006). Topologically disordered systems at the glass transition. Journal of Physics: Condensed Matter 18 (50): 11507.

Okos, M. R., Campanella, O., Narsimhan, G., Singh, R. K., & Weitnauer, A. C. (2006). Food dehydration. Handbook of Food Engineering, Second Edition. CRC Press: 601-744.

Ollett, A.L., Parker, R., (1990). The viscosity of supercooled fructose and its glass transition temperature. Journal of texture studies 21 (3), 355-362.

Parks, G. S., Huffman, H. M., & Cattoir, F. R. (1928). Studies on glass. II. The transition between the glassy and liquid states in the case of glucose. The Journal of Physical Chemistry 32 (9): 1366-1379.

Parks, G., Gilkey, W., (1929). Studies on glass. IV. Some viscosity data on liquid glucose and glucose-glycerol solutions. The Journal of Physical Chemistry 33 (9), 1428-1437.

Parks, G. S. and H. Huffman (1927). Studies on Glass. I. The Journal of Physical Chemistry 31 (12): 1842-1855.

Parks, G. S. and S. B. Thomas (1934). The heat capacities of crystalline, glassy and undercooled liquid glucose. Journal of the American Chemical society 56 (6): 1423-1423.

Peleg, M. (1992). On the use of the WLF model in polymers and foods. Critical Reviews in Food Science & Nutrition 32 (1): 59-66.

Peleg, M. and P. Chinachoti (1996). On modeling changes in food and biosolids at and around their glass transition temperature range. Critical Reviews in Food Science & Nutrition 36 (1-2): 49-67.

Peleg, M., Engel, R., Gonzalez-Martinez, C., and Corradini, M. G. (2002). Non-Arrhenius and non-WLF kinetics in food systems. Journal of the Science of Food and Agriculture 82(12): 1346-1355.

Perez, J. (1990). Quasi-punctual defects in vitreous solids and liquid-glass transition. Solid State Ionics 39(1-2): 69-79.

Perez, J. (1994). Theories of liquid-glass transition. Journal of Food Engineering 22 (1-4): 89-114.

Potes, N. (2014). Physico-chemical properties and component interactions in high solids food systems. PhD Thesis, University College Cork.

Potes, N., Kerry, J. P., and Roos, Y. H. (2012). Additivity of water sorption, alpha-relaxations and crystallization inhibition in lactose–maltodextrin systems. Carbohydrate polymers, 89 (4): 1050-1059.

Priestley, R.D., Ellison, C.J., Broadbelt, L.J. and Torkelson, J.M., (2005). Structural relaxation of polymer glasses at surfaces, interfaces, and in between. Science 309 (5733): 456-459.

Rahman, M. S., Senadeera, W., Al-Alawi, A., Truong, T., Bhandari, B., and Al-Saidi, G. (2011). Thermal transition properties of spaghetti measured by differential scanning calorimetry (DSC) and thermal mechanical compression test (TMCT). Food and bioprocess technology 4(8): 1422-1431.

Rault, J. (2000). Origin of the Vogel–Fulcher–Tammann law in glass-forming materials: the α–β bifurcation. Journal of Non-Crystalline Solids 271 (3): 177-217.

Rizvi, S. (2005). Thermodynamic properties of foods in dehydration. Di dalam: Rao MA, Rizvi SSH, Datta AK, (Eds). Engineering Properties of Foods. CRC Press, Singapore.

Roos, Y. (1993). Melting and glass transitions of low molecular weight carbohydrates. Carbohydrate research 238: 39-48.

Roos, Y. and Karel, M., (1990). Differential scanning calorimetry study of phase transitions affecting the quality of dehydrated materials. Biotechnology Progress 6(2), 159-163.

Roos, Y. and M. Karel (1991). Applying state diagrams to food processing and development." Food Technology 45(12): 66, 68-71, 107.

Roos, Y. and Karel, M., (1991b). Nonequilibrium ice formation in carbohydrate solutions. Cryo-letters 12 (6): 367-376.

Roos, Y. and Karel, M.A., **(1992).** Crystallization of amorphous lactose. Journal of food science 57 (3), 775-777.

Roos, Y. H., and Potes, N. (2015). Quantification of protein hydration, glass transitions, and structural relaxations of aqueous protein and carbohydrate–protein systems. The Journal of Physical Chemistry B, 119 (23): 7077-7086.

Roos, Y.H., Fryer, P.J., Knorr, D., Schuchmann, H.P., Schroën, K., Schutyser, M.A., Trystram, G. and Windhab, E.J., **(2015).** Food engineering at multiple scales: case studies, challenges and the future—a European perspective. Food Engineering Reviews, 1-25.

Roos, Y.H. (1995). Phase transitions in foods. Academic Press. San-Diego.

Roos, Y. H. (2008). The glassy state. Food Materials Science. Springer: 67-81.

Roos, Y. H. (2013). Relaxations, glass transition and engineering properties of food solids. Advances in Food Process Engineering Research and Applications. Springer: 79-90. New York.

Roos, Y. H. and S. Drusch (2015). Phase transitions in foods. Academic Press.

Roudaut, G., Simatos, D., Champion, D., Contreras-Lopez, E., and Le Meste, M. (2004). Molecular mobility around the glass transition temperature: a mini review. Innovative Food Science & Emerging Technologies 5 (2): 127-134.

Royall, P.G., Huang, C.-y., Tang, S.-w.J., Duncan, J., Van-de-Velde, G. and Brown, M.B., (2005). The development of DMA for the detection of amorphous content in pharmaceutical powdered materials. International journal of pharmaceutics 301 (1): 181-191.

Ruiz-Cabrera, M. and S. Schmidt (2015). Determination of glass transition temperatures during cooling and heating of low-moisture amorphous sugar mixtures. Journal of Food Engineering 146: 36-43.

Sakka, S. and J. Mackenzie (1971). Relation between apparent glass transition temperature and liquids temperature for inorganic glasses. Journal of Non-Crystalline Solids 6 (2): 145-162.

Saleki-Gerhardt, A., Ahlneck, C. and Zografi, G., (1994). Assessment of disorder in crystalline solids. International journal of pharmaceutics 101 (3), 237-247.

Sanford, W. and R. McCullough (1990). A free-volume-based approach to modeling thermoset cure behavior. Journal of Polymer Science Part B: Polymer Physics 28 (7): 973-1000.

Sebhatu, T., Angberg, M. and Ahlneck, C., (1994). Assessment of the degree of disorder in crystalline solids by isothermal microcalorimetry. International journal of pharmaceutics 104 (2), 135-144.

Shamblin, S.L., Huang, E.Y. and Zografi, G., **(1996).** The effects of co-lyophilized polymeric additives on the glass transition temperature and crystallization of amorphous sucrose. Journal of thermal analysis 47 (5): 1567-1579.

Shrestha, A.K., Howes, T., Adhikari, B.P. and Bhandari, B.R., **(2007).** Water sorption and glass transition properties of spray dried lactose hydrolysed skim milk powder. LWT-Food Science and Technology 40 (9): 1593-1600.

Silalai, N. and Y. H. Roos (2011). Mechanical relaxation times as indicators of stickiness in skim milk–maltodextrin solids systems. Journal of Food Engineering 106 (4): 306-317.

Slade, L. and H. Levine (1995). Glass transitions and water-food structure interactions. Advances in food and nutrition research 38: 103-269.

Slade, L., Levine, H., and Reid, D. S. (1991). Beyond water activity: recent advances based on an alternative approach to the assessment of food quality and safety. Critical Reviews in Food Science & Nutrition 30 (2-3): 115-360.

Sperling, L., (1991). Introduction to physical polymer science. John Wiley & Sons.

Sperling, L. H. (2005). Introduction to physical polymer science. John Wiley & Sons.

Stillinger, F. H. and J. A. Hodgdon (1994). Translation-rotation paradox for diffusion in fragile glass-forming liquids. Physical review E 50(3): 2064.

Supplee, G. (1926). Humidity equilibria of milk powders. Journal of Dairy Science 9 (1): 50-61.

Surana, R., Pyne, A., Rani, M. and Suryanarayanan, R., **(2005).** Measurement of enthalpic relaxation by differential scanning calorimetry—effect of experimental conditions. Thermochimica acta 433 (1): 173-182.

Sussich, F., Urbani, R., Princivalle, F. and Cesàro, A., (1998). Polymorphic amorphous and crystalline forms of trehalose. Journal of the American Chemical society 120 (31), 7893-7899.

Swenson, J. and Cerveny, S., (2015). Dynamics of deeply supercooled interfacial water. Journal of Physics: Condensed Matter 27 (3), 033102.

Talja, R.A. and Roos, Y.H., (2001). Phase and state transition effects on dielectric, mechanical, and thermal properties of polyols. Thermochimica Acta 380 (2), 109-121.

Tammann, G. and W. Hesse (1926). Die Abhängigkeit der Viscosität von der Temperatur bie unterkühlten Flüssigkeiten. Zeitschrift für anorganische und allgemeine Chemie 156(1): 245-257.

Thuc, T. T., Fukai, S., Truong, V., and Bhandari, B. (2010). Measurement of glass-rubber transition temperature of rice by thermal mechanical compression test (TMCT). International Journal of Food Properties 13 (1): 176-183.

Timmermann, E. O., Chirife, J., & Iglesias, H. A. (2001). Water sorption isotherms of foods and foodstuffs: BET or GAB parameters? Journal of Food Engineering 48 (1): 19-31.

Troy, H.C. and Sharp, P.F., (1930). α and β lactose in some milk products. Journal of Dairy Science 13(2): 140-157.

Uritani, M., Takai, M. and Yoshinaga, K., (1995). Protective effect of disaccharides on restriction endonucleases during drying under vacuum. Journal of biochemistry 117(4), 774-779.

Vega, C., Kim, E. H. J., Chen, X. D., and Roos, Y. H. (2005). Solid-state characterization of spray-dried ice cream mixes. Colloids and Surfaces B: Biointerfaces 45 (2): 66-75.

Vogel, H. (1921). The law of the relation between the viscosity of liquids and the temperature. Vogel, Hans Physikalische Zeitschrift 22: 645-646.

Weng, L. and G. D. Elliott (2015). Local Minimum in Fragility for Trehalose/Glycerol Mixtures: Implications for Biopharmaceutical Stabilization. The Journal of Physical Chemistry B 119 (22): 6820-6827.

White, G. and S. Cakebread (1966). The glassy state in certain sugar-containing food products. International Journal of Food Science and Technology 1(1): 73-82.

Willart, J., Dujardin, N., Dudognon, E., Danède, F. and Descamps, M., (2010). Amorphization of sugar hydrates upon milling. Carbohydrate research 345 (11): 1613-1616.

Williams, M. L., Landel, R. F., and Ferry, J. D. (1955). The temperature dependence of relaxation mechanisms in amorphous polymers and other glass-forming liquids. Journal of the American Chemical society 77 (14): 3701-3707.

Wolf, W., Spiess, W. E. L., anf Jung, G. (1985). Standardization of isotherm measurements (COST-project 90 and 90 bis). In Properties of water in foods (pp. 661-679). Springer Netherlands.

Xie, G. and Timasheff, S.N., (1997). The thermodynamic mechanism of protein stabilization by trehalose. Biophysical chemistry 64 (1): 25-43.

Zarzycki, J. (1991). Glasses and the vitreous state. Cambridge University Press.

Zhou, P., Labuza, T.P., (2007). Effect of water content on glass transition and protein aggregation of whey protein powders during short-term storage. Food Biophysics 2(2-3): 108-116.

APPENDIX

LIST OF PUBLICATIONS

- **Maidannyk, V. A., Roos, Y. H. (2016).** *Modification of the WLF model for characterization of the relaxation time-temperature relationship in trehalose-whey protein isolate systems.* Journal of Food Engineering, 188, 21-31.
- **Nurhadi, B., Roos, Y.H., Maidannyk, V. (2016).** *Physical properties of maltodextrin DE 10: Water sorption, water plasticization and enthalpy relaxation.* Journal of Food Engineering 174, 68-74.
- **Maidannyk, V. A., & Roos, Y. H. (2017).** *Water sorption, glass transition and "strength" of lactose–Whey protein systems.* Food Hydrocolloids, 70, 76-87.
- **Maidannyk, V. A., Nurhadi, B., & Roos, Y. H. (2017).** *Structural strength analysis of amorphous trehalose-maltodextrin systems.* Food Research International, 96, 121-131.
- **Maidannyk, V. A., Roos, Y. H. (2017b).** *Structural strength analysis of partially crystalline trehalose.* LWT-Food Science and Technology, In Press.
- **Maidannyk, V. A., A.S.L. Lim, M.A.E. Auty, Y. H. Roos. (2017c).** *Effects of lipids on the structural strength of carbohydrate-protein systems.* Manuscript to be submitted.

APPENDIX

LIST OF CONFERENCES

- **V.A. Maidannyk and Y.H. Roos.**
  ""Strength" Modeling of Structural Relaxation Times of Miscible Carbohydrates". *Conference of Food Engineering 2016, Columbus, USA, September 12-14, 2016.*
- **V.A. Maidannyk and Y.H. Roos.**
  "The temperature, water and time-dependence of noncrystalline solids as described using a "strength" parameter."
  Participant in the"ECCE10+ECAB3+EPIC5 congress, Symposium of the European Academy of Food Engineering", Nice, France, September 27th - October 1st 2015.
- **V. A. Maidannyk and Y. H. Roos.**
  "Structural relaxation times in amorphous states: the trehalose-whey protein system". *Amorph 2014 – The Felix Franks Symposium: A Celebration. 14-16 July 2014, Girton College, Cambridge, U.K.*
- **V. A. Maidannyk and Y. H. Roos.**
  "The influence of pH on rheological behavior of layer by layer emulsions".
  42rd Annual Food Research Conference, 22-28 June 2013, Teagasc, Dublin, Ireland.